

University of Memphis

University of Memphis Digital Commons

Electronic Theses and Dissertations

2020

Walks and games on graphs

Rebekah Herrman

Follow this and additional works at: <https://digitalcommons.memphis.edu/etd>

Recommended Citation

Herrman, Rebekah, "Walks and games on graphs" (2020). *Electronic Theses and Dissertations*. 2585.
<https://digitalcommons.memphis.edu/etd/2585>

This Dissertation is brought to you for free and open access by University of Memphis Digital Commons. It has been accepted for inclusion in Electronic Theses and Dissertations by an authorized administrator of University of Memphis Digital Commons. For more information, please contact khhgerty@memphis.edu.

WALKS AND GAMES ON GRAPHS

by

Rebekah Herrman

A Dissertation

Submitted in Partial Fulfillment of the

Requirements for the Degree of

Doctor of Philosophy

Major: Mathematical Sciences

The University of Memphis

May 2020

ACKNOWLEDGMENTS

I wish to thank my advisor, Dr. Béla Bollobás for his patience, encouragement, and advice. His love of mathematics is truly inspirational.

I also wish to thank my other committee members, Professors Paul Balister, James Campbell, David Gryniewicz, and Alistair Windsor for their time and feedback.

I want to express my gratitude to my collaborators, Andrew Carlotti, Vojtěch Dvořák, Peter van Hintum, Dr. Travis Humble, and Dr. Stephen Smith for many interesting questions and conversations.

I am grateful to Tricia Simmons for her help. She always finds time to answer questions and point me in the right direction.

The work in this dissertation would not have been possible without funding from the NSF grants Applications of Probabilistic Combinatorial Methods, DMS-1855745, and Probabilistic and Extremal Combinatorics, DMS-1600742.

Thanks for my family and friends who encouraged me throughout my graduate studies.

Finally, I wish to thank my husband, Steven Menezes, for his patience, understanding, love, and support. This would not have been possible without him.

ABSTRACT

Herrman, Rebekah Ph.D. The University of Memphis, May 2020. Walks and Games on Graphs. Major Professor: Béla Bollobás, Ph.D.

Chapter 1 is joint work with Dr. Travis Humble and appears in the journal *Physical Review A*. In this work, we consider continuous-time quantum walks on dynamic graphs. Continuous-time quantum walks have been well studied on graphs that do not change as a function of time. We offer a mathematical formulation for how to express continuous-time quantum walks on graphs that can change in time, find a universal set of walks that can perform any operation, and use them to simulate basic quantum circuits. This work was supported in part by the Department of Energy Student Undergraduate Laboratory Internship and the National Science Foundation Mathematical Sciences Graduate Internship programs.

The (t, r) broadcast domination number of a graph G , $\gamma_{t,r}(G)$, is a generalization of the domination number of a graph. In Chapter 2, we consider the (t, r) broadcast domination number on graphs, specifically powers of cycles, powers of paths, and infinite grids. This work is joint with Peter van Hintum and has been submitted to the journal *Discrete Applied Mathematics*.

Bridge-burning cops and robbers is a variant of the cops and robbers game on graphs in which the robber removes an edge from the graph once it is traversed. In Chapter 3, we study the maximum time it takes the cops to capture the robber in this variant. This is joint with Peter van Hintum and Dr. Stephen Smith.

In Chapter 4, we study a variant of the chip-firing game called the *diffusion game*. In the diffusion game, we begin with some integer labelling of the vertices of a graph, interpreted as a number of chips on each vertex, and for each subsequent step every vertex simultaneously fires a chip to each neighbour with fewer chips. In general, this could result in negative vertex labels. Long and Narayanan asked

whether there exists an $f(n)$ for each n , such that whenever we have a graph on n vertices and an initial allocation with at least $f(n)$ chips on each vertex, then the number of chips on each vertex will remain non-negative. We answer their question in the affirmative, showing further that $f(n) = n - 2$ is the best possible bound. We also consider the existence of a similar bound $g(d)$ for each d , where d is the maximum degree of the graph. This work is joint with Andrew Carlotti and has been submitted to the journal *Discrete Mathematics*.

In Chapter 5, we consider the eternal game chromatic number of random graphs. The eternal graph colouring problem, recently introduced by Klostermeyer and Mendoza [45], is a version of the graph colouring game, where two players take turns properly colouring a graph. In this chapter, we show that with high probability $\chi_g^\infty(G_{n,p}) = (\frac{p}{2} + o(1))n$ for odd n , and also for even n when $p = \frac{1}{k}$ for some $k \in \mathbb{N}$. This work is joint with Vojtěch Dvořák and Peter van Hintum, and has been submitted to the *European Journal of Combinatorics*.

CONTENTS

List of Figures	vii
1 Continuous-Time Quantum Walks on Dynamic Graphs	1
1.1 Introduction	1
1.2 Continuous-time Quantum Walks	3
1.3 Quantum walks on Disconnected Graphs	7
1.4 Quantum Walks on Dynamic Graphs	10
1.5 Quantum Walks for Elementary Gates	12
1.5.1 Single-qubit Gates	14
1.5.2 Multi-qubit gates	19
1.5.3 Measurement and Initialization	21
1.6 Quantum Walks For Quantum Circuits	22
1.6.1 Quantum Teleportation Circuit	23
1.6.2 Quantum Adder	25
1.7 Discussion	28
1.8 Appendix	30
2 Broadcast Domination Number of Some Regular Graphs	38
2.1 Introduction	38
2.2 Proof of Theorem 1	39
2.3 Generalizations of the (t, r) broadcast number for grids	47
2.4 Proof of Theorem 2	50
2.5 Proof of Theorem 3	52
2.6 Concluding Remarks	53
3 Capture Times in Bridge-Burning Cops and Robbers	55
3.1 Introduction	55

3.2	Capture times	56
3.3	Proof of Theorem 6	58
3.4	Appendix	68
4	Uniform Bounds for Non-negativity of the Diffusion Game	71
4.1	Introduction	71
4.2	Order-based Bounds	73
4.2.1	The Weak Diffusion Game	73
4.2.2	Proof of Theorem 4.1.1	75
4.2.3	Remarks	78
4.3	Bounds using the Maximum Degree	78
4.4	Concluding Remarks	82
5	Eternal Game Chromatic Number	83
5.1	Introduction	83
5.2	Upper bound	86
5.3	Lower bound for odd n	90
5.4	Generalization of the lower bound for odd n	95
5.5	Even n	100
5.6	Answer to a question of Klostermeyer and Mendoza	102
5.7	Appendix	104

LIST OF FIGURES

1.1	The K_2 graph supports perfect state transfer between the two vertices labeled by the single-qubit computational basis states $ 0\rangle$ and $ 1\rangle$. . .	5
1.2	The C_4 graph supports perfect state transfer between vertices labeled by the two-qubit computational states.	7
1.3	The time-dependent probability densities of two vertices, 0 and 1, as the state propagates under $K_1 + K_1$ for $t = \frac{\pi}{2}$ units of time before switching to K_2 and propagating for an additional time $t = \frac{3\pi}{2}$. In this example, the initial state $\sqrt{\frac{1}{3}} 0\rangle + \sqrt{\frac{2}{3}} 1\rangle$	12
1.4	The time-dependent probability density of four vertices, 0, 1, 2, and 3, as the state propagates under $K_2 + K_2$ for time $t = \frac{\pi}{2}$ followed by C_4 for time $t = \frac{3\pi}{2}$. In this example, the initial state is $\sqrt{\frac{1}{3}} 00\rangle + \sqrt{\frac{2}{3}} 10\rangle$.	13
1.5	A dynamic graph representation of the X gate consists of two graphs and the associated propagation times. This sequence of CTQW executes the logical bit flip operation on the graph state.	15
1.6	A graphical representation of the Z gate using CTQW on \mathcal{G}_Z	16
1.7	A graphical representation of the Y gate using CTQW on \mathcal{G}_Y	17
1.8	A graphical representation of the H gate using CTQW on \mathcal{G}_H	18
1.9	A graphical representation of the T gate using \mathcal{G}_T	19
1.10	A graphical representation of the CNOT gate using CTQW on $\mathcal{G}_{\text{CNOT}}$.	20
1.11	A graphical representation of the CCNOT (Toffoli) gate using CTQW on $\mathcal{G}_{\text{CCNOT}}$	21
1.12	The circuit model representation of quantum teleportation uses three qubits and a series of elementary gates.	23

1.13	In this graphical representation of quantum teleportation, each graph is labeled as (G_ℓ, τ_ℓ) with τ_ℓ the propagation time in the ℓ -th graph. The time $f(a) = \arcsin(\sqrt{a})$ is the state specific time required to rotate $ 000\rangle$ to $\sqrt{1-a} 000\rangle + \sqrt{a} 001\rangle$. From left to right, the first four graphs rotate the state while the next five graphs correspond to the H gate on the second qubit. The following four graphs represent a pair of CNOT gates. The next five graphs correspond with an H gate on the first qubit. Assuming a measurement outcome $(b_1 = 1, b_2 = 1)$, the remaining graphs implement the X and Z gates needed to complete teleportation.	24
1.14	The population dynamics for state preparation and quantum teleportation using CTQW on the dynamic graph shown in Fig. 1.13. This examples corresponds to the case of measurement outcomes $b_1 = 1$ and $b_2 = 1$ for qubits 1 and 2, respectively, and completes the protocol by applying the necessary recovery operations, X and Z	25
1.15	A quantum circuit for addition of two 1-bit numbers, where the carry circuit \mathcal{C} and the sum circuit \mathcal{S} are defined in Figs. 1.16 and 1.17. Note that since we only have one carry operation, it is our last carry, and thus is not reversed.	25
1.16	The carry subcircuit \mathcal{C} used in Fig. 1.15	26
1.17	The sum subcircuit \mathcal{S} used in Fig. 1.15	26
1.18	In this graphical representation of a one-bit quantum adder circuit, each graph is labeled as (G_ℓ, τ_ℓ) with τ_ℓ the propagation time in the ℓ -th graph.	27

1.19	The population dynamics of the CTQW for quantum addition of inputs $ a\rangle = 1\rangle$ and $ b\rangle = \frac{1}{\sqrt{2}} 0, 0\rangle + \frac{1}{\sqrt{2}} 0, 1\rangle$. Numerical simulations of the CTQW on the dynamic graph shown in Fig. 1.18 calculates exactly the amplitudes of each vertex and the final state is $ b_1, b_0, a_0, c_0\rangle = \frac{1}{\sqrt{2}}(0, 1, 1, 0\rangle + 1, 0, 1, 0\rangle)$, which corresponds to a uniform superposition of the vertices 6 and 10.	28
2.1	An example of a $(5, 1)$ broadcasting set. When considered as a $(6, 3)$ broadcasting set, the four large vertices in the middle receive excess signal.	40
2.2	The signal received from T and T' in Subcase 2.2.1.2, where second tower T' is located at $(t - 3, 1)$. The line (dashed line resp.) denote the boundary of those vertices receiving at least 2 signal from T (T'' resp.). For a minimal $(t - 1, 1)$ broadcasting set, these regions partition the plane. The $*$ marks the origin.	41
2.3	The signal received from T and T' in Subcase 2.2.1.3, where second tower $T' = (t - 3, 0)$	42
2.4	The signal received from T and T' in Subcase 2.2.1.4, where the second tower is at $T' = (t - 2, 0)$	42
2.5	The signal received from T and T' in Case 2.2.1.5 for the specific example $t = 5$ where second tower $T' = (2, 4)$	43
2.6	The signal received from T and T' in Case 4.3, where second tower $T' = (1, t - 2)$	44
3.1	The graph G described in the proof of Theorem 6. Most of the doors and holes are omitted though all the other vertices and edges are displayed.	61

3.2	The graph described in the proof of Lemma 3.3.2. The central vertices are doors, and the other vertices form cycles $\{a_i\}_i$ and $\{p_i, q_i, x_i\}$ patrolled by Alex and Charlie respectively which watch the doors. . .	63
3.3	The graph described in Lemma 3.3.5, where v is a vertex in $X \cup Y$. . .	65
4.1	An example of an infinite 3 regular tree. This figure shows $d(3) \geq 3$. . .	81

CHAPTER 1

CONTINUOUS-TIME QUANTUM WALKS ON DYNAMIC GRAPHS

1.1 Introduction

Quantum walks offer a unique paradigm for using quantum mechanics to perform computation [2], where a walk may represent either the discrete or continuous-time propagation of a quantum state over a graph [41, 60]. In a continuous-time quantum walk (CTQW), free evolution of an N -dimensional quantum state under a Hamiltonian is represented by probability amplitudes assigned to each vertex in a graph on N vertices. The CTQW was originally envisioned as a method for sampling decision trees [30] and later applied to a variety of search and sampling problems on d -dimensional lattices, searches on balanced trees, as well as quantum navigation of networks [1, 17, 33, 53, 49, 46]. Moreover, Childs has shown that CTQWs on time-independent graphs offer a novel model for universal quantum computation [16, 18], while Qiang et al. have described how efficient implementations of CTQWs may be useful for comparing the broader computational power of quantum computing to conventional computing models [51].

In a typical CTQW, the Hamiltonian is interpreted as the connectivity of the underlying graph on which the quantum state evolves. The graph connectivity determines the evolution of the quantum state and specific graphs have been found to demonstrate well-defined quantum walk behaviors. For example, perfect state transfer occurs in a quantum walk when the amplitude assigned to a subset of vertices transfers with unit probability to a distinct vertex set within a well-defined period of evolution [40]. Kendon and Tamon have surveyed perfect state transfer for a number of several specific graphs including the singleton graph, K_1 , the complete graph on two vertices, K_2 , the path graph on three vertices, and the cycle on four vertices, C_4 [42]. Perfect state transfer has also been shown to exist for graphs on

more vertices, including certain graph products, weighted join graphs, and quotient graphs [22, 4, 5].

The versatility of CTQWs across many known types of graphs motivates our consideration for how quantum walks may behave on dynamic graphs. We define a dynamic graph as a well-defined sequence of static graphs in which the CTQW evolution changes at specific transition times. In the dynamic graphs discussed below, we use perfect state transfer under the component static graphs to demonstrate how more complex unitary processes can be realized. We provide explicit realizations of quantum walks on dynamic graphs for realizing a complete set of computational gates, and we then illustrate how compositions of multiple walks correspond to examples of quantum circuits. This formalism establishes a connection between CTQWs on dynamic graphs and the gates found in the conventional quantum circuit model. We also provide a connection between this model of computation and the development of tunable optical waveguides for performing continuous-time quantum walks.

Our approach to quantum walks on dynamic graphs shares similarities with Childs' model for universal quantum computation [16, 18]. Both approaches draw on the use of unweighted and relatively sparse graphs to formalize state transfer as well as the composition of such graphs to describe more complex operations. However, the models differ in the types of underlying graphs as Childs relies on strictly static graphs while we employ dynamic graphs. Another closely related model is the hybrid quantum walk proposed by Underwood and Feder, which combines concepts from both continuous and discrete walk models [58]. In that work, a series of weighted adjacency matrices corresponding to distinct graphs are used to propagate a quantum state. They refer to this model as a discontinuous quantum walk, where free evolution is again based on widgets that control propagation dynamics.

Underwood and Feder emphasize the use of a dual-railing encoding to represent

individual qubits and the interleaving of continuous and discrete quantum walks to perform computation. By comparison, we design quantum walks on dynamic graphs to implement a sequence of continuous-time evolutions that perform quantum logic using perfect state transfer in the native vertex space. Du et al. considered the task of designing a quantum walk to implement a single-qubit X gate by walking on a single static, weighted graph [27], whereas our work develops implementations for a complete gate set using dynamics graphs. Chakraborty et al. have explored spatial search using CTQW on time-ordered sequences of random graphs, for which they demonstrated a threshold for the optimal run time using Grover’s algorithm [14], while our work uses deterministic, time-ordered sequences to carry out discrete logic gates.

The paper is organized as follows. Following a review of CTQWs on static graphs in Sec. 1.2, we describe quantum walks on disconnected graphs in Sec. 1.3 and dynamic graphs in Sec. 1.4. Using this formalism, we design a series of quantum walks that implement elementary logic gates in Sec. 1.5, and we demonstrate how the sparsely connected dynamic graphs on may be composed to correspond with gate-based circuits in Sec. 1.6. We offer a discussion on these results in Sec. 1.7, where we establish a connection between dynamic quantum walks and current approaches to designing quantum computing hardware based on optical waveguides and ion trap technologies.

1.2 Continuous-time Quantum Walks

Consider an undirected graph $G = (V, E)$ with a canonically labeled vertex set $V = \{0, 1, \dots, N - 1\}$ of N vertices and an edge set $E = \{(i, j) : i \sim j\}$. We allow no multi-edges in the graph, i.e., there can be at most one edge incident with any pair of vertices. However, we do allow for a self loop on a vertex $v \in V$ if and only if there does not exist $u \in V$ such that $u \neq v$ and $u \sim v$. Additionally, the edges of G

are undirected. Let $B_G = \{|j\rangle : \forall j \in V\}$ be a linearly independent basis for the complex vector space \mathbb{C}^N with the inner product $\langle j|k\rangle = \delta_{jk}$. Graphs G and $G' = (V', E')$ have the same basis if $V = V'$. The Hamiltonian for the graph G is denoted as H_G and is defined as the adjacency matrix of the graph as given by the edge set E . The adjacency matrix A of G is a 0-1 valued $N \times N$ matrix such that for $u, v \in V(G)$, if $u \sim v$, $A_{u,v} = A_{v,u} = 1$, and 0 otherwise. We will use the convention that if a vertex v is not adjacent to any other vertices then $A_{v,v} = 1$, a convention also used in studies of classical random walks. The resulting real-valued adjacency matrix A is symmetric about the main diagonal.

We define the quantum state of a graph G , or graph state for short, as a normalized vector $|\psi_G\rangle \in B_G$ such that

$$|\psi_G\rangle = \sum_{j \in V} c_j |j\rangle \quad (1.2.1)$$

with $c_j \in \mathbb{C}$ and

$$\langle \psi_G | \psi_G \rangle = \sum_{j \in V} |c_j|^2 = 1 \quad (1.2.2)$$

For a continuous-time quantum walk, the graph state transforms with respect to time τ under the Schrödinger equation

$$i\hbar \frac{\partial |\psi_G(\tau)\rangle}{\partial \tau} = H_G |\psi_G(\tau)\rangle \quad (1.2.3)$$

where \hbar is Planck's constant divided by 2π . When the Hamiltonian is constant over the interval $[t_0, t]$, the formal solution to Eq. (1.2.3) is given by the propagation operator

$$U_G(t, t_0) = e^{-iH_G(t-t_0)/\hbar} \quad (1.2.4)$$

such that

$$|\psi_G(t)\rangle = U_G(t, t_0) |\psi_G(t_0)\rangle \quad (1.2.5)$$

where the boundary condition $|\psi_G(t_0)\rangle$ is the state at time t_0 . The propagation

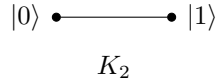


Figure 1.1: The K_2 graph supports perfect state transfer between the two vertices labeled by the single-qubit computational basis states $|0\rangle$ and $|1\rangle$.

operator U_G is unitary since H_G is Hermitian. We say that a graph G admits perfect state transfer between unique vertices $u, v \in V(G)$ at time t if

$$U_G(t, 0)|u\rangle = a|v\rangle \tag{1.2.6}$$

where $a \in \mathcal{C}$ such that $|a| = 1$.

There are several well-known examples that illustrate perfect state transfer using CTQW on static graphs. The singleton graph K_1 has vertex set $V = \{0\}$ and an empty edge set $E = \emptyset$. As the lone vertex $|0\rangle$ is adjacent to no other vertices during the CTQW, we represent the unitary dynamics by a self-loop. The K_1 Hamiltonian is then represented in its eigenbasis as

$$H_{K_1} = \lambda_1|0\rangle\langle 0|, \tag{1.2.7}$$

where λ_1 is the real-valued energy eigenvalue, and the normalized state

$$|\psi_{K_1}(t_0)\rangle = c_0(t_0)|0\rangle \tag{1.2.8}$$

has $|c_0| = 1$ for all time such that

$$|\psi_{K_1}(t)\rangle = e^{-i\nu_1 t}|0\rangle \tag{1.2.9}$$

where $\nu_1 = \lambda_1/\hbar$ is the frequency.

As a second example, the complete graph on two vertices K_2 shown in Fig. 1.1 has

vertex set $V = \{0, 1\}$ and edge set $E = \{(0, 1)\}$. We specify the Hamiltonian for K_2 as $\langle 0|H_{K_2}|0\rangle = \langle 1|H_{K_2}|1\rangle$, which offers a natural representation of a qubit in a degenerate eigenbasis. Setting this eigenenergy to zero, the Hamiltonian is represented as

$$H_{K_2} = \lambda_2 (|0\rangle\langle 1| + |1\rangle\langle 0|) \quad (1.2.10)$$

where the eigenvalue λ_2 defines the energy scale and the characteristic frequency $\nu_2 = \lambda_2/\hbar$. The time propagator for K_2 may be decomposed by series expansion as

$$U_{K_2}(t, t_0) = \cos[\nu_2(t - t_0)]\mathbb{I}_2 - i \sin[\nu_2(t - t_0)]H_{K_2} \quad (1.2.11)$$

where \mathbb{I}_N is the N -dimensional identity matrix. The K_2 -graph state evolves as

$$\begin{aligned} |\psi_{K_2}(t)\rangle &= (c_0 \cos[\nu_2(t - t_0)] - ic_1 \sin[\nu_2(t - t_0)]) |0\rangle \\ &+ (c_1 \cos[\nu_2(t - t_0)] - ic_0 \sin[\nu_2(t - t_0)]) |1\rangle \end{aligned} \quad (1.2.12)$$

which is capable of perfect state transfer up to a trivial phase factor for propagation time $t = \frac{\pi}{2\nu_2}$ [42].

As a final example, the cycle graph C_4 shown in Fig. 1.2 has a vertex set $V = \{0, 1, 2, 3\}$, edge set $E = \{(0, 1), (0, 2), (1, 3), (2, 3)\}$ and Hamiltonian

$$H_{C_4} = \lambda_4 (|0\rangle\langle 1| + |1\rangle\langle 2| + |2\rangle\langle 3| + |3\rangle\langle 0| + \text{H.C.}) \quad (1.2.13)$$

where H.C. denotes the Hermitian conjugate, λ_4 is the energy scale, and $\nu_4 = \lambda_4/\hbar$ defines the characteristic frequency. The propagation operator may be decomposed as

$$U_{C_4}(t, t_0) = \mathbb{I}_4 + \frac{1}{2} \cos(2\nu_4(t - t_0))H_{C_4}^2 - \frac{i}{2} \sin(2\nu_4(t - t_0))H_{C_4} \quad (1.2.14)$$

to yield the state $|\psi_{C_4}(t)\rangle$ with coefficients in the nodal basis as

$$c_0(t) = \frac{1}{2} [c_0 (1 + \cos(2t)) - i \sin(2t) (c_1 + c_2) + c_3 (-1 + \cos(2t))] \quad (1.2.15)$$

$$c_1(t) = \frac{1}{2} [-i \sin(2t) (c_0 + c_3) + c_1 (1 + \cos(2t)) + c_2 (-1 + \cos(2t))] \quad (1.2.16)$$

$$c_2(t) = \frac{1}{2} [-i \sin(2t) (c_0 + c_3) + c_1 (-1 + \cos(2t)) + c_2 (1 + \cos(2t))] \quad (1.2.17)$$

and

$$c_3(t) = \frac{1}{2} [c_0 (-1 + \cos(2t)) - i \sin(2t) (c_1 + c_2) + c_3 (1 + \cos(2t))] \quad (1.2.18)$$

Perfect state transfer in C_4 is a special instance of the case of an N -dimensional hypercube [42], which has been shown by Christandl et al. to be capable of perfect state transfer for all N at time $t = \frac{\pi}{2\nu_N}$ [20, 19]. For the remainder of our presentation, we will simplify the analysis to the case that $\nu_N = 1$ for $N = 1, 2, 4$ and we will set $\hbar = 1$ for convenience.

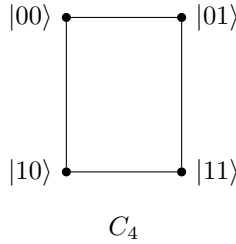


Figure 1.2: The C_4 graph supports perfect state transfer between vertices labeled by the two-qubit computational states.

1.3 Quantum walks on Disconnected Graphs

We now consider quantum walks on disjoint graphs G_1 and G_2 with $G_j = (V_j, E_j)$, where the disjoint union $G = G_1 + G_2$ has vertex set $V = V_1 \cup V_2$ and edge set $E = E_1 \cup E_2$. We require that G_1 and G_2 are connected graphs, termed components

of the graph G , and that $V_1 \cap V_2 = \emptyset$. The basis for the disjoint union G is $B_G = B_{G_1} \oplus B_{G_2}$ and a composite quantum state for G takes the form

$$|\psi_G\rangle = |\psi_{G_1}\rangle \otimes |\psi_{G_2}\rangle \quad (1.3.1)$$

with \oplus the direct sum and \otimes the Kronecker product. The corresponding Hamiltonian is defined as $H(G) = H_{G_1} \oplus H_{G_2}$, which yields decoupled equations of motion

$$i \frac{\partial |\psi_{G_j}(t)\rangle}{\partial t} = H_{G_j} |\psi_{G_j}(t)\rangle \quad j = 1, 2 \quad (1.3.2)$$

and a composite time propagator

$$U_{G_1+G_2}(t, t_0) = e^{-iH_{G_1}(t-t_0)} \otimes e^{-iH_{G_2}(t-t_0)} \quad (1.3.3)$$

The graph state of G is modeled by two disconnected states $|\psi_{G_1}\rangle \in B_{G_1}$ and $|\psi_{G_2}\rangle \in B_{G_2}$ and

$$|\psi_G(t)\rangle = U_{G_1}(t, t_0) |\psi_{G_1}(t_0)\rangle \otimes U_{G_2}(t, t_0) |\psi_{G_2}(t_0)\rangle \quad (1.3.4)$$

As an example, consider the empty graph on N vertices \bar{K}_N , which is the complement of the complete graph K_N and expressed as the union

$$\bar{K}_n = \bigcup_{j=0}^{N-1} K_1^{(j)} \quad (1.3.5)$$

where $K_1^{(j)}$ is the singleton graph with vertex label j . The composite Hamiltonian is the direct sum of N singleton Hamiltonians,

$$H_{\bar{K}_n} = \bigoplus_{j=0}^{N-1} H_{K_1^{(j)}}, \quad (1.3.6)$$

and the quantum state is defined as the Kronecker product of the individual states.

$$|\psi_{\bar{K}_N}\rangle = \bigotimes_{j=0}^{N-1} |\psi_{K_1^{(j)}}\rangle \quad (1.3.7)$$

in the basis formed from the union of these graphs

$$B_{\bar{K}_N} = \bigcup_{j=0}^{N-1} B_{K_1^{(j)}} \quad (1.3.8)$$

The graph state for the j -th singleton graph is now given as

$$U_{K_1^{(j)}}(t, t_0)|j\rangle = e^{-i\nu_1^{(j)}t}|j\rangle, \quad (1.3.9)$$

with $\nu_1^{(j)}$ the energy eigenvalue of the j -th vertex. We will assume that the vertices are indistinguishable and therefore $\nu_1^{(j)} = \nu_1$ for all j . Thus, the Hamiltonian of these N disjoint identical vertices

$$H_{\bar{K}_N} = \bigoplus_{j=0}^{N-1} \lambda_1 |j\rangle\langle j| = \lambda_1 \mathbb{I}_N \quad (1.3.10)$$

is proportional to the N -dimensional identity operator \mathbb{I}_N over the basis $B_{\bar{K}_N}$. This yields an N -fold Kronecker sum of K_1 states with the form of Eq. (1.2.9).

As a second example, consider the disjoint union $K_2 + K_1$ with Hamiltonian

$$H_{K_2+K_1} = H_{K_2} \oplus H_{K_1} \quad (1.3.11)$$

represented as

$$H_{K_2+K_1} = \begin{pmatrix} 0 & \lambda_2 & 0 \\ \lambda_2 & 0 & 0 \\ 0 & 0 & \lambda_1 \end{pmatrix} \quad (1.3.12)$$

The composite state of this disjoint graph propagates as

$$U_{K_2+K_1}(t, t_0)|\psi_{K_2+K_1}\rangle = U_{K_2}(t, t_0)|\psi_{K_2}(t_0)\rangle \oplus U_{K_1}(t, t_0)|\psi_{K_1}(t_0)\rangle \quad (1.3.13)$$

and may be recast as

$$\begin{aligned} U_{K_2+K_1}(t, t_0)|\psi_{K_2+K_1}\rangle &= [c_1 \cos(\nu_2(t - t_0)) - ic_1 \sin(\nu_2(t - t_0))] |0\rangle \\ &+ [c_1 \cos(\nu_2(t - t_0)) - ic_0 \sin(\nu_2(t - t_0))] |1\rangle \\ &+ c_2 e^{-i\nu_1 t} |2\rangle \end{aligned} \quad (1.3.14)$$

1.4 Quantum Walks on Dynamic Graphs

We next consider quantum walks on dynamic graphs, in which a dynamic graph $\mathcal{G} = \{(G_\ell, t_\ell)\}$ is a set of graphs $G_\ell = (V_\ell, E_\ell)$ with associated propagation times $t_\ell < t_{\ell+1}$ for $\ell \in \mathbb{Z}$. In subsequent discussion, we will consider the case that only the edge sets change while the vertex sets stay constant, i.e., $V_\ell = V$, such that the bases for all G_ℓ are the same. However, the case of changing vertex sets is equally valid as this represents the growth and reduction of the underlying Hilbert space, for example, through the addition or removal of ancillary vertices.

The Hamiltonian of a dynamic graph \mathcal{G} is expressed as the weighted sum

$$H_{\mathcal{G}} = \sum_{\ell=0}^{L-1} H_{G_\ell} \Pi_\ell(t), \quad (1.4.1)$$

where transitions between graphs are modulated by the functions $\Pi_\ell(t)$. We consider the explicit case that the ℓ -th transition function takes the form of the ℓ -th

rectangle function:

$$\Pi_\ell(t) = \begin{cases} 1 & t_\ell < t < t_{\ell+1} \\ 0 & \text{otherwise} \end{cases} \quad (1.4.2)$$

with $[t_0, t_L]$ the interval over which the entire walk is defined. The dynamics is then expressed as a sequence of propagations through the series of Schrödinger equations

$$i \frac{\partial |\psi_{G_\ell}(\tau)\rangle}{\partial \tau} = H_{G_\ell} |\psi_{G_\ell}(\tau)\rangle, \quad t_\ell < \tau < t_{\ell+1}. \quad (1.4.3)$$

As the set of discontinuities is countable, the function is still Riemann integrable, and this system of equations yields the composite propagation operator

$$U_{\mathcal{G}}(t_L, t_0) = \prod_{\ell=0}^{L-1} e^{-iH_{G_\ell}(t_{\ell+1}-t_\ell)} \quad (1.4.4)$$

which is understood to be a product ordered from right to left with increasing index. The quantum state of the dynamic graph \mathcal{G} is then defined under this operator transform as

$$|\psi_{\mathcal{G}}(t)\rangle = U_{\mathcal{G}}(t_L, t_0) |\psi_{\mathcal{G}}(t_0)\rangle \quad (1.4.5)$$

with initial condition $|\psi_{\mathcal{G}}(t_0)\rangle \in B_{\mathcal{G}}$ and $\langle \psi_{\mathcal{G}}(t_0) | \psi_{\mathcal{G}}(t_0) \rangle = 1$.

As a simple example of a quantum walk on a dynamic graph, consider the case of two disjoint K_1 graphs switched to a bipartite K_2 . The dynamic graph is expressed as $\mathcal{G} = \{(K_1 + K_1, t_0), (K_2, t_1)\}$, where t_0 and t_1 denote the transition times. Taking the initial quantum state as a superposition over the nodal basis, Fig. 1.3 plots the time-dependent probability for each basis state with respect to the propagation time. Initially under the $K_1 + K_1$, the probability remains constant until the transition time t_1 , after which the Hamiltonian switches to K_2 and creates an edge between vertices. This leads to the oscillations in probability as expected by Eq. (1.2.11). Figure 1.4 is an example of two K_2 graphs allowed to propagate on

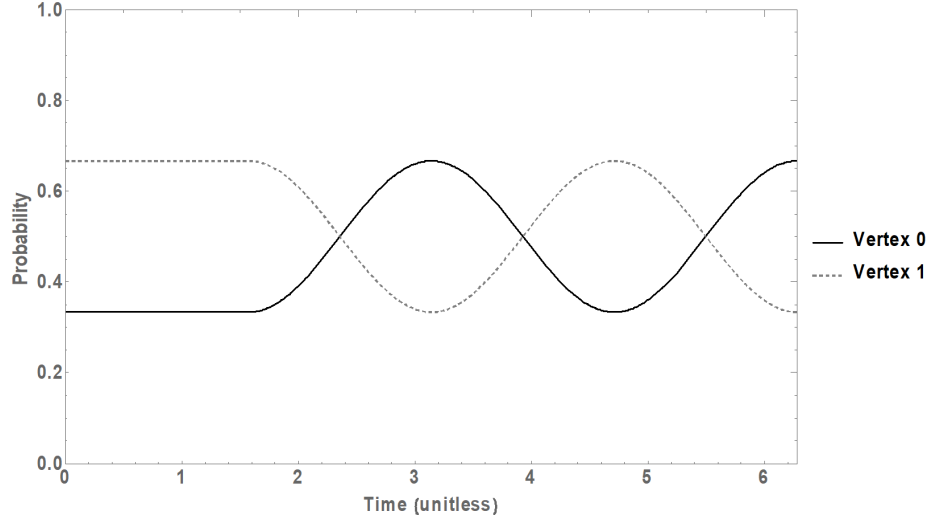


Figure 1.3: The time-dependent probability densities of two vertices, 0 and 1, as the state propagates under $K_1 + K_1$ for $t = \frac{\pi}{2}$ units of time before switching to K_2 and propagating for an additional time $t = \frac{3\pi}{2}$. In this example, the initial state $\sqrt{\frac{1}{3}}|0\rangle + \sqrt{\frac{2}{3}}|1\rangle$.

their own and then connected as a C_4 and allowed to propagate again.

1.5 Quantum Walks for Elementary Gates

The formalism of quantum walks on dynamic graphs may be used to realize one- and two-qubit gates within the quantum circuit model by identifying the quantum walk on a graph of $|V| = N = 2^n$ vertices with a corresponding n -qubit circuit. Let the vertex label $v \in V$ map to the computational basis state $|v_1, v_2, \dots, v_n\rangle$ with v_i the i -th coefficient in the binary expansion of the n -bit, non-negative integer v . We demonstrate several explicit examples of how few-qubit quantum gates can be realized using perfect state transfer limited to K_1 , K_2 , and C_4 graphs. We limit our CTQWs to those on K_1 , K_2 , and C_4 because the periods are all multiples of π and achieve perfect state transfer at times $\frac{k\pi}{2}$ for $k \in \mathbb{N}$. In fact, we use the $K_1^{(i)}$ graph exclusively to add a phase factor to the i^{th} qubit. We add the phase factors for sake

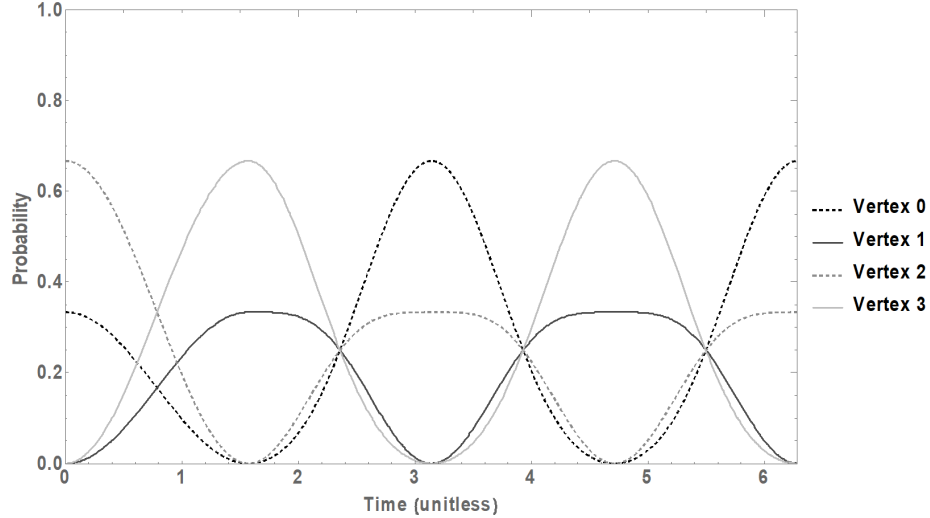


Figure 1.4: The time-dependent probability density of four vertices, 0, 1, 2, and 3, as the state propagates under $K_2 + K_2$ for time $t = \frac{\pi}{2}$ followed by C_4 for time $t = \frac{3\pi}{2}$. In this example, the initial state is $\sqrt{\frac{1}{3}}|00\rangle + \sqrt{\frac{2}{3}}|10\rangle$.

of completeness in some of the CTQWs, but for implementation purposes, the phase factor may be omitted if desired by removing the appropriate CTQWs. We show that in some instances, such as the Z gate, the realization of gate logic within the quantum walk model requires additional vertices whereas other gates, such as CNOT and CCNOT, are straightforward to realize.

The realization of elementary gates from the circuit model provides a constructive approach to demonstrate the completeness of quantum walks on dynamics graphs. While the quantum walk formalism can naturally represent any unitary of the form $\exp(iAt)$, we have imposed the restriction that the Hermitian matrix A must represent the connectivity of the dynamic graph and that these graphs should be limited to a small number of vertices. By demonstrating that a complete basis of elementary gates can be constructed under these restrictions, we can then invoke the Solovay-Kitaev theorem to establish universality. The Solovay-Kitaev theorem

establishes the feasibility of approximating an arbitrary unitary transformation when only a limited subset of such transformation may be accessed [24]. We demonstrate an explicit realization for a universal set of gates, including the Pauli, H , T and CNOT gates described below, from which it follows that sequences of these gates of length $O(\log^c(1/\epsilon))$ may approximate an arbitrary unitary within precision ϵ for constant $c \approx 3.97$ [24].

1.5.1 Single-qubit Gates

The Pauli gates provide a set of single-qubit operations represented in the computational basis as

$$X = \begin{pmatrix} 0 & 1 \\ 1 & 0 \end{pmatrix}, \quad Y = \begin{pmatrix} 0 & -i \\ i & 0 \end{pmatrix}, \quad Z = \begin{pmatrix} 1 & 0 \\ 0 & -1 \end{pmatrix}. \quad (1.5.1)$$

We can implement these gates exactly using perfect state transfer within a dynamic graph. For example, the X gate may be implemented on two graph vertices using a quantum walk on K_2 . For simplicity, we assume the vertices are labeled 0 and 1 and that the graph state is initially prepared as $c_0|0\rangle + c_1|1\rangle$. The walk under $K_2^{(0,1)}$ for a period of $\frac{3\pi}{2}$ prepares the state $i(c_1|0\rangle + c_0|1\rangle)$. The resulting global phase factor of i may be removed by evolving under $K_1^{(0)} + K_1^{(1)}$ for a second period of $\frac{\pi}{2}$, and we include these dynamics in our definition of the X gate. The dynamic graph for the X gate is defined as

$$\mathcal{G}_X = \left\{ \left(G_{K_2}^{(0,1)}, \frac{3\pi}{2} \right), \left(G_{K_1}^{(0)} + G_{K_1}^{(1)}, \frac{\pi}{2} \right) \right\}, \quad (1.5.2)$$

and Fig. 1.5 provides a graphical representation. When the target pair of vertices is embedded in a larger graph state, it is understood that all other nodes evolve disjointly from the above dynamic graph.



Figure 1.5: A dynamic graph representation of the X gate consists of two graphs and the associated propagation times. This sequence of CTQW executes the logical bit flip operation on the graph state.

The Z gate may be implemented using a K_1 and C_4 defined on five vertices. Notice that $|001\rangle$ must propagate as a singleton for π units of time to flip the sign of the coefficient, however, $|000\rangle$ needs to propagate as a C_4 in the same time frame in order to keep its original sign. We maintain a clear correspondence with the circuit model by using a graph on eight vertices which represent the full Hilbert space for three qubits. Three of these vertices will propagate as singletons for the entirety of the walk. For example, given the initial state $c_0|0\rangle + c_1|1\rangle$ for a graph of $|V| = 8$ vertices, the dynamic graph representing the Z gate is defined as

$$\mathcal{G}_Z = \{(G_{C_4}^{(0,2,4,6)} + G_{K_1}^{(1)} + G_{K_1}^{(3)} + G_{K_1}^{(5)} + G_{K_1}^{(7)}, \pi)\} \quad (1.5.3)$$

A graphical representation of the walk for the Z gate is shown in Fig. 1.6. Note these dynamic flips the signs of $|011\rangle$, $|101\rangle$, and $|111\rangle$ in addition to $|001\rangle$

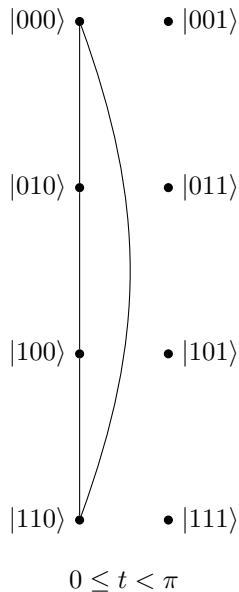


Figure 1.6: A graphical representation of the Z gate using CTQW on \mathcal{G}_Z .

A Y gate may be derived from the commutation relations for the Pauli operators and implemented by performing the X and Z gates in series. An additional phase shift of i is required and this may be recovered by evolving all vertices under disjoint singletons for $t = 3\pi/2$. Of course, reversing the order in which the X and Z gates are performed would change the necessary phase shift, $-iY$. Alternatively, the Y transformation may be implemented by propagating vertices $|000\rangle$ and $|001\rangle$ under K_2 for $\pi/2$ units of time, then allowing vertex $|001\rangle$ to propagate as a singleton for π units while simultaneously allowing $|000\rangle$ to propagate as a C_4 to three new vertices. The dynamic graph for the latter Y operation is given as

$$\mathcal{G}_Y = \left\{ \left(G_{K_2}^{(0,1)} + G_{K_1}^{(2)} + G_{K_1}^{(3)} + G_{K_1}^{(4)}, \frac{\pi}{2} \right), \left\{ \left(G_{K_1}^{(1)} + G_{C_4}^{(0,2,3,4)}, \pi \right) \right\} \right\}, \quad (1.5.4)$$

Completing the Pauli group, we note that the identity gate may be implemented using a number of different dynamic graphs. This includes assigning every vertex to propagate under the singleton graph for $t = 2\pi$, connecting pairs of vertices as K_2 graphs for $t = 2\pi$, or connecting four vertices as a C_4 and propagating for $t = \pi$.

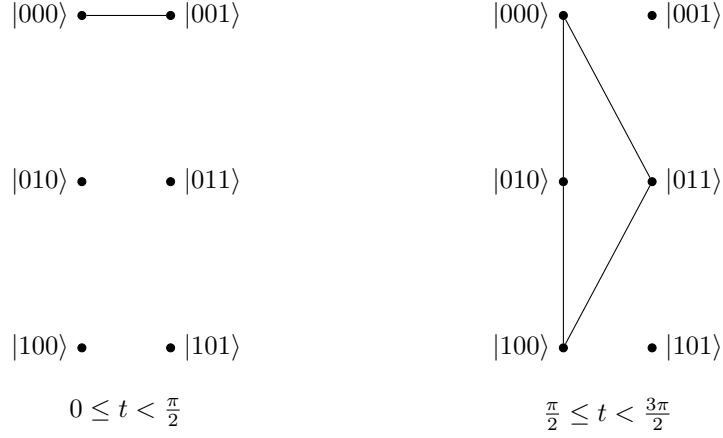


Figure 1.7: A graphical representation of the Y gate using CTQW on \mathcal{G}_Y .

The best choice for implementation is likely to be determined by other scheduling concerns.

The single-qubit Hadamard gate is defined in the computational basis as

$$H = \frac{1}{\sqrt{2}} \begin{pmatrix} 1 & 1 \\ 1 & -1 \end{pmatrix} \quad (1.5.5)$$

and may be implemented using a series of C_4 and K_2 graphs. The Hadamard gate may be performed with only five vertices, but we again use eight vertices to establish a clear correspondence with three qubits in the circuit model. Consider the initial state $c_0|0\rangle + c_1|1\rangle$ embedded in a Hilbert space represented by $|V| = 8$ nodes.

Figure 1.8 illustrates the dynamic graph for the H gate, defined as

$$\begin{aligned} \mathcal{G}_H = \{ & (G_{C_4}^{(0,2,4,6)} + G_{K_1}^{(1)} + G_{K_1}^{(3)} + G_{K_1}^{(5)} + G_{K_1}^{(7)}, 3\pi/2), \\ & (G_{K_2}^{(0,7)} + G_{K_2}^{(1,6)} + G_{K_2}^{(2,5)} + G_{K_2}^{(3,4)}, \pi/4), \\ & (G_{C_4}^{(0,2,4,6)} + G_{K_1}^{(1)} + G_{K_1}^{(3)} + G_{K_1}^{(5)} + G_{K_1}^{(7)}, 3\pi/2), \\ & (G_{K_2}^{(0,1)} + G_{K_2}^{(2,3)} + G_{K_2}^{(4,5)} + G_{K_2}^{(6,7)}, \pi/2), \\ & (G_{K_1}^{(0)} + G_{K_1}^{(1)} + G_{K_1}^{(2)} + G_{K_1}^{(3)} + G_{K_1}^{(4)} + G_{K_1}^{(5)} + G_{K_1}^{(6)} + G_{K_1}^{(7)}, 3\pi/2) \} \end{aligned} \quad (1.5.6)$$

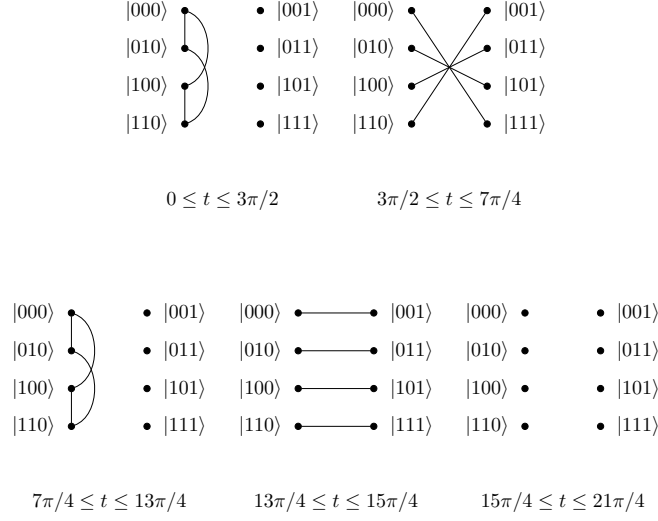


Figure 1.8: A graphical representation of the H gate using CTQW on \mathcal{G}_H .

We show in the Appendix that the CTQW defined by Eq. (1.5.6) implements the logical transformation for the Hadamard gate.

The T gate is defined as

$$T = \begin{pmatrix} 1 & 0 \\ 0 & e^{\frac{i\pi}{4}} \end{pmatrix} \quad (1.5.7)$$

and may be implemented using K_1 , K_2 , and C_4 graphs, along with the star graph on five vertices. A star graph is a connected graph G on n vertices such that exactly one vertex has degree $n - 1$ and all other vertices have degree one. Figure 1.9 illustrates the dynamic graph used for the T gate, which is written as

$$\begin{aligned} \mathcal{G}_T = & \{(G_{K_2}^{(0,2)} + G_{K_1}^{(1)} + G_{K_1}^{(3)} + G_{K_1}^{(4)} + G_{K_1}^{(5)} + G_{K_1}^{(6)} + G_{K_1}^{(7)}, \frac{\pi}{4}), \\ & (G_{C_4}^{(0,3,4,5)} + G_{K_1}^{(1)} + G_{K_1}^{(2)} + G_{K_1}^{(6)} + G_{K_1}^{(7)}, \frac{\pi}{2}), \\ & (G_{K_2}^{(2,4)} + G_{K_2}^{(3,5)} + G_{K_1}^{(0)} + G_{K_1}^{(0)} + G_{K_1}^{(1)} + G_{K_1}^{(6)} + G_{K_1}^{(7)}, \frac{\pi}{4}), \\ & (G_{C_4}^{(2,5,6,7)} + G_{K_1}^{(0)} + G_{K_1}^{(1)} + G_{K_1}^{(3)} + G_{K_1}^{(4)}, \frac{\pi}{2}), \\ & (G_{S_5}^{(0,2,3,4,5)} + G_{K_1}^{(1)} + G_{K_1}^{(6)} + G_{K_1}^{(7)}, \frac{7\pi}{4}), \\ & (G_{K_1}^{(0)} + G_{K_1}^{(1)} + G_{K_1}^{(2)} + G_{K_1}^{(3)} + G_{K_1}^{(4)} + G_{K_1}^{(5)} + G_{K_1}^{(6)} + G_{K_1}^{(7)}, \frac{\pi})\}. \end{aligned} \quad (1.5.8)$$

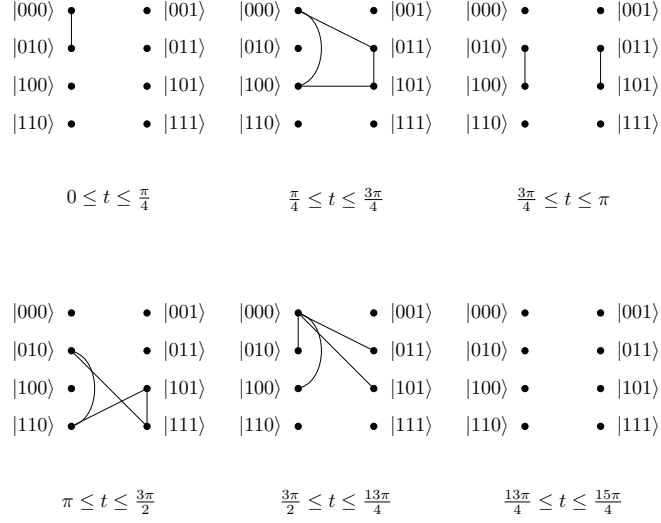


Figure 1.9: A graphical representation of the T gate using \mathcal{G}_T .

We show in the Appendix that the CTQW defined by Eq. (1.5.8) implements the logical transformation for the T gate.

1.5.2 Multi-qubit gates

Quantum walks on dynamics graphs may also be used to construct multi-qubits gates. For example, the two-qubit CNOT gate,

$$\text{CNOT} = \begin{pmatrix} 1 & 0 & 0 & 0 \\ 0 & 1 & 0 & 0 \\ 0 & 0 & 0 & 1 \\ 0 & 0 & 1 & 0 \end{pmatrix} \quad (1.5.9)$$

can be realized using a quantum walk on 4 vertices that span the space of the control and target qubits. Let vertices 0 and 1 propagate as singletons for time 2π while allowing vertices 2 and 3 to propagate under K_2 as shown in Fig. 1.10.

$$\mathcal{G}_{\text{CNOT}} = \left\{ \left(G_{K_1}^{(0)} + G_{K_1}^{(1)} + G_{K_1}^{(2)} + G_{K_1}^{(3)}, \frac{3\pi}{2} \right), \left(G_{K_1}^{(0)} + G_{K_1}^{(1)} + G_{K_2}^{(2,3)}, \frac{\pi}{2} \right) \right\} \quad (1.5.10)$$

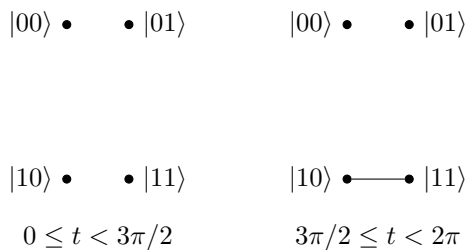


Figure 1.10: A graphical representation of the CNOT gate using CTQW on $\mathcal{G}_{\text{CNOT}}$.

The three-qubit CCNOT, or Toffoli, gate

$$\text{CNOT} = \begin{pmatrix} 1 & 0 & 0 & 0 & 0 & 0 & 0 & 0 \\ 0 & 1 & 0 & 0 & 0 & 0 & 0 & 0 \\ 0 & 0 & 1 & 0 & 0 & 0 & 0 & 0 \\ 0 & 0 & 0 & 1 & 0 & 0 & 0 & 0 \\ 0 & 0 & 0 & 0 & 1 & 0 & 0 & 0 \\ 0 & 0 & 0 & 0 & 0 & 1 & 0 & 0 \\ 0 & 0 & 0 & 0 & 0 & 0 & 0 & 1 \\ 0 & 0 & 0 & 0 & 0 & 0 & 1 & 0 \end{pmatrix} \quad (1.5.11)$$

is constructed similarly but now using $|V| = 8$ vertices that represent the two control qubits and one target qubit. The implementation of the Toffoli gate is identical to the *CNOT* gate but with four additional vertices allowed to propagate as singletons for 2π units of time. It is used in both the carry and sum subcircuits in the quantum adder circuit. It is also reversible, meaning the its effects may be reversed using other operations. Figure 1.11 illustrates the dynamic graph for the Toffoli gate.

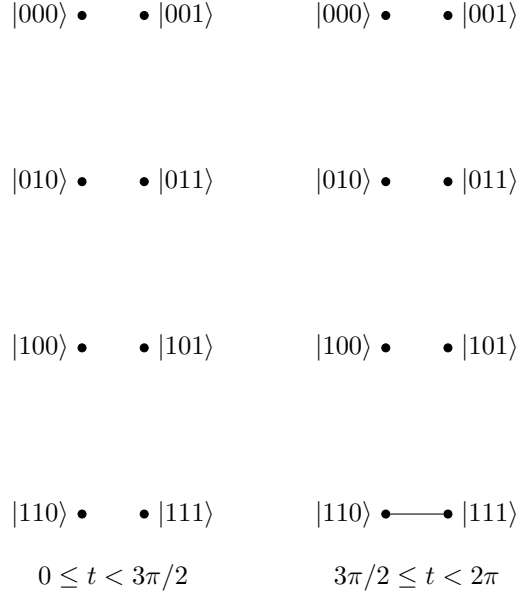


Figure 1.11: A graphical representation of the CCNOT (Toffoli) gate using CTQW on $\mathcal{G}_{\text{CCNOT}}$.

1.5.3 Measurement and Initialization

We model measurement of the quantum state on a graph G as a projection onto a subspace of the basis B_G . In establishing a correspondence with the qubit-encoded circuit model, we decompose the labels of the basis according to a binary expansion

$$|j\rangle = \sum_{i=1}^m j_i 2^{m-i} \quad (1.5.12)$$

with $j_i \in \{0, 1\}$ and $m = \log_2 |V|$. In this binary representation, a quantum state $|\psi_G\rangle \in B_G$ can be expressed as

$$|\psi_G\rangle = \sum_{j \in V} c_j |j_1, \dots, j_m\rangle, \quad (1.5.13)$$

and measuring the i -th qubit to have a fixed value $\bar{j}_i \in \{0, 1\}$ corresponds to projecting the state onto a subset of nodes in the graph, i.e.,

$$|\bar{j}_i\rangle\langle\bar{j}_i|\psi_G\rangle = \sum_{j \in V} c_j |j_1, \dots, \bar{j}_i, \dots, j_m\rangle \quad (1.5.14)$$

The probability to observe node the i^{th} qubit as \bar{j}_i is given as

$$\text{Prob}(j) = |\langle\bar{j}_i|\psi_G\rangle|^2 = \sum_{j \in V, j_i = \bar{j}} |c_j|^2 \leq 1 \quad (1.5.15)$$

We may use measurement as part of a deterministic initialization method, in which the projective outcome is transformed into the desired initial state. This requires conditional operations based on the decoded output from the measurement, from which the necessary series of single-qubit gates are applied to graph. For projections into the label basis, these feed-forward operations consist of products of the Pauli operators flip the label state to a fiducial starting label, e.g., the vertex 0.

1.6 Quantum Walks For Quantum Circuits

We complete our analysis by providing explicit examples of how quantum walks on dynamic graphs realize circuits within gate-model computing. These examples highlight the differences in the representation of the logic as well as the resources required to achieve the desired unitary transformations. In our examples, CTQWs are performed in series and the number of vertices needed to implement each circuit is equal to the largest of the number of vertices needed to perform the CTQW equivalent for each logic gate. For the sake of completeness, we also explicitly indicate singleton vertices that add global phase evolution to select vertices in order to clearly demonstrate where each gate is used in the implementation. Future optimizations may remove such singleton CTQWs that sum to 2π from actual

implementations.

1.6.1 Quantum Teleportation Circuit

In quantum teleportation, a qubit of information is transferred from one logical element to another as shown in Fig. 1.12. In the circuit model description, three qubits are initially prepared in the state $|000\rangle$. The first element is prepared in the state $|\psi_1\rangle$ by applying the necessary single-qubit transformation. The remaining elements are prepared in a two-qubit entangled state by applying the Hadamard gate to the second element followed by the CNOT gate acting on the second and third elements. A second CNOT gate entangles the first and second qubits. A final Hadamard gate is applied to the first, after which measurements performed on elements 1 and 2 generate binary values b_1 and b_2 , respectively. The effect of these measurements is to project element 3 into the state $X_3^{b_1} Z_3^{b_2} |\psi_3\rangle$, which may be transformed to the original state of element 1 with knowledge of (b_1, b_2) .

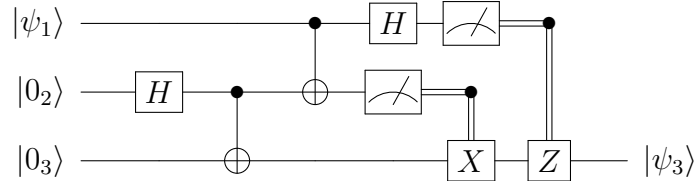


Figure 1.12: The circuit model representation of quantum teleportation uses three qubits and a series of elementary gates.

The implementation of quantum teleportation using CTQW on a dynamic graph is shown in Fig. 1.13, and it begins with a graph on eight vertices. Initialization of these vertices is realized through a projective measurement and, depending on the measurement outcome, a sequence of X operations to populate the 0 vertex. We then approximate an arbitrary unitary operation to prepare the input superposition state $|\psi\rangle = \sqrt{1-a}|0\rangle + \sqrt{a}|1\rangle$ for $a \in \mathcal{C}$ where $|a| = 1$. The number of vertices needed to represent an arbitrary $|\psi\rangle$ depends on the desired state, but this single-qubit unitary can be constructed using the universal basis described above. A

Hadamard transform is then applied to vertices 0 and 7 using Eq. (1.5.6) followed by a pair of CNOT transforms using Eq. (1.5.10) acting on vertices $\{2, 3, 6, 7\}$ and $\{0, 1, 2, 3\}$, respectively. The output from this series of CTQWs prepares the graph state

$$|\psi\rangle = \frac{1}{2} \left(-\sqrt{1-a}|0\rangle + \sqrt{1-a}|1\rangle + \sqrt{1-a}|2\rangle - \sqrt{1-a}|3\rangle - \sqrt{a}|4\rangle - \sqrt{a}|5\rangle + \sqrt{a}|6\rangle + \sqrt{a}|7\rangle \right) \quad (1.6.1)$$

and a partial projective measurements on the first two bits of the label representation generates the four possible teleported states.

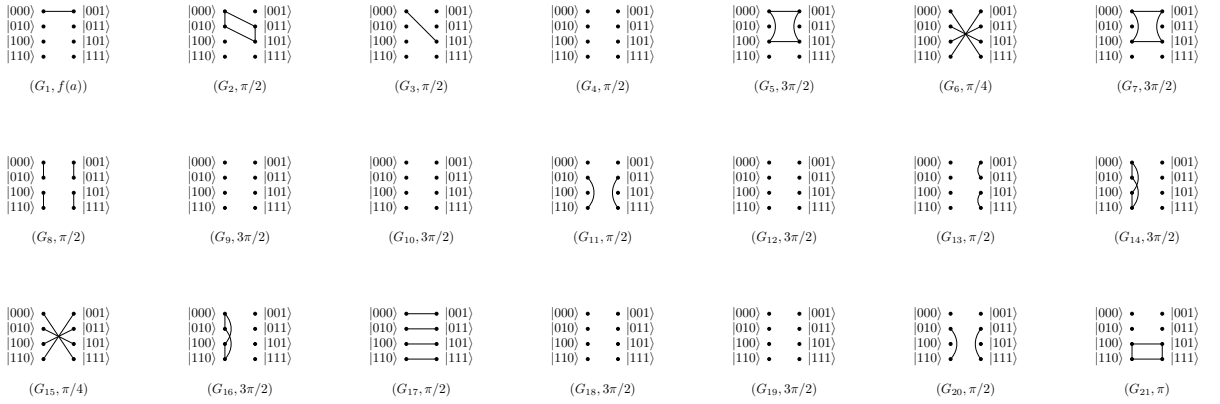


Figure 1.13: In this graphical representation of quantum teleportation, each graph is labeled as (G_ℓ, τ_ℓ) with τ_ℓ the propagation time in the ℓ -th graph. The time $f(a) = \arcsin(\sqrt{a})$ is the state specific time required to rotate $|000\rangle$ to $\sqrt{1-a}|000\rangle + \sqrt{a}|001\rangle$. From left to right, the first four graphs rotate the state while the next five graphs correspond to the H gate on the second qubit. The following four graphs represent a pair of CNOT gates. The next five graphs correspond with an H gate on the first qubit. Assuming a measurement outcome $(b_1 = 1, b_2 = 1)$, the remaining graphs implement the X and Z gates needed to complete teleportation.

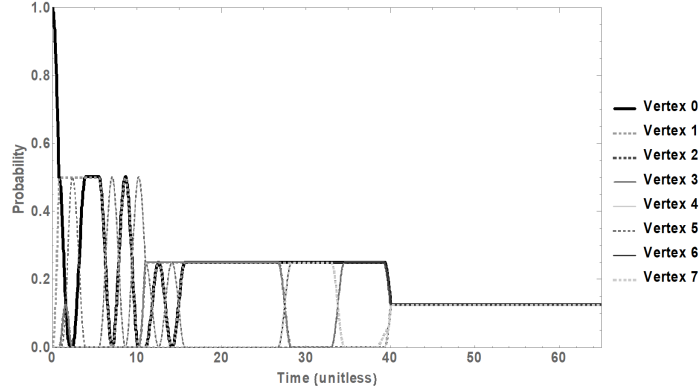


Figure 1.14: The population dynamics for state preparation and quantum teleportation using CTQW on the dynamic graph shown in Fig. 1.13. This example corresponds to the case of measurement outcomes $b_1 = 1$ and $b_2 = 1$ for qubits 1 and 2, respectively, and completes the protocol by applying the necessary recovery operations, X and Z .

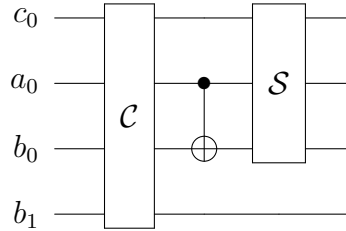


Figure 1.15: A quantum circuit for addition of two 1-bit numbers, where the carry circuit \mathcal{C} and the sum circuit \mathcal{S} are defined in Figs. 1.16 and 1.17. Note that since we only have one carry operation, it is our last carry, and thus is not reversed.

1.6.2 Quantum Adder

As a second example, we consider a quantum addition circuit for summing two positive integers such that the input $|a, b\rangle \rightarrow |a, a \oplus b\rangle$ [59]. This variant of in-place addition takes two inputs encoded in registers a and b with the binary representations $a = a_{n-1}a_{n-2}\dots a_1a_0$ and $b = b_{n-1}b_{n-2}\dots b_1b_0$. An additional bit $b_{n+1} = 0$ is added to register b to give a size $n + 1$. A third workspace register c of size $n - 1$ is used in this implementation to store carry values with initialization

$c_i = 0 \forall i$, while the final carry value is stored in the bit b_{n+1} . The circuit is composed from two subcircuits for carry and sum operations denoted as \mathcal{C} and \mathcal{S} , respectively, and the subcircuits for \mathcal{C} and \mathcal{S} are specified in Figs. 1.16 and 1.17, respectively. The carry operation uses a Toffoli gate with the second and third qubit as controls and the fourth qubit as the target. This is followed by a CNOT gate on the second and third qubits before another Toffoli gate on the first, second, and fourth qubits. The reverse carry \mathcal{RC} circuit undoes the carry computation by applying the gates in the reverse order. The last carry bit in the computation is not reversed but stored as b_{n+1} . The sum subcircuit denoted as \mathcal{S} in Fig. 1.17 takes three qubits as input, in which a CNOT is applied to the second and third qubits followed by a Toffoli gate performed with the first two qubits being the controls and the third qubit as the target. In Fig. 1.15, we show the demonstrated instance of one-bit inputs, i.e., $n = 1$, for which the reverse carry subcircuit is unnecessary. For this example, carry bits are also unnecessary but we include the single carry bit c_0 to confirm generality.

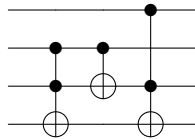


Figure 1.16: The carry subcircuit \mathcal{C} used in Fig. 1.15

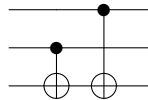


Figure 1.17: The sum subcircuit \mathcal{S} used in Fig. 1.15

We reduce the gate sequences in the quantum addition circuit into the dynamic graph shown in Fig. 1.18. Our reduction uses the CTQWs for CNOT and CCNOT gates described in Sec. 1.5 and sequentially orders them according to the gate specification in Figs. 1.15, 1.16, and 1.17. In order to verify the correctness of the

reduction, we have used numerical simulation to determine the quantum state generated by the CTQW on the dynamic graph shown in Fig. 1.18. Numerical simulation of the CTQW requires a memory space that is exponential in the number of qubits, i.e, 2^{3n+1} . Implementing the quantum adder circuit for $n = 1$ requires a dynamic graph on sixteen vertices.

We show results from a specific simulation with $|a_0\rangle = |1\rangle$ and $|b_0\rangle = \frac{1}{\sqrt{2}}(|0\rangle + |1\rangle)$ in Fig. 1.19. We plot the time-dependent population of the vertices that represent the joint state of the computational registers. The carry register is initialized to $|c_0\rangle = |0\rangle$ and the resulting computational output is

$|b_1, b_0, a_0, c_0\rangle = \frac{1}{\sqrt{2}}(|0, 0, 1, 0\rangle + |1, 1, 1, 0\rangle)$, where the a_0 and c_0 registers remain in their initial states, and the sum $a_0 + b_0$ is stored in the b_0 and b_1 . As shown in

Fig. 1.19, our CTQW simulations verify that the dynamic graph yields the expected output states, which corresponds to a uniform superposition of the vertex labels 6 and 10.

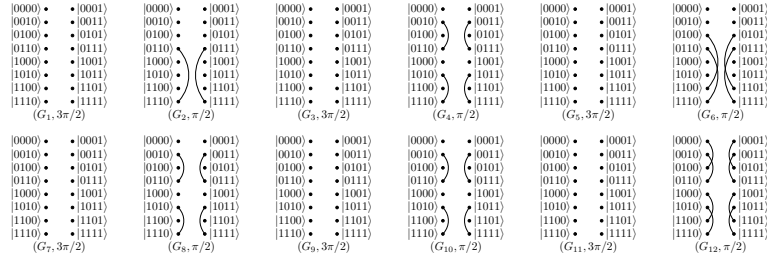


Figure 1.18: In this graphical representation of a one-bit quantum adder circuit, each graph is labeled as (G_ℓ, τ_ℓ) with τ_ℓ the propagation time in the ℓ -th graph.

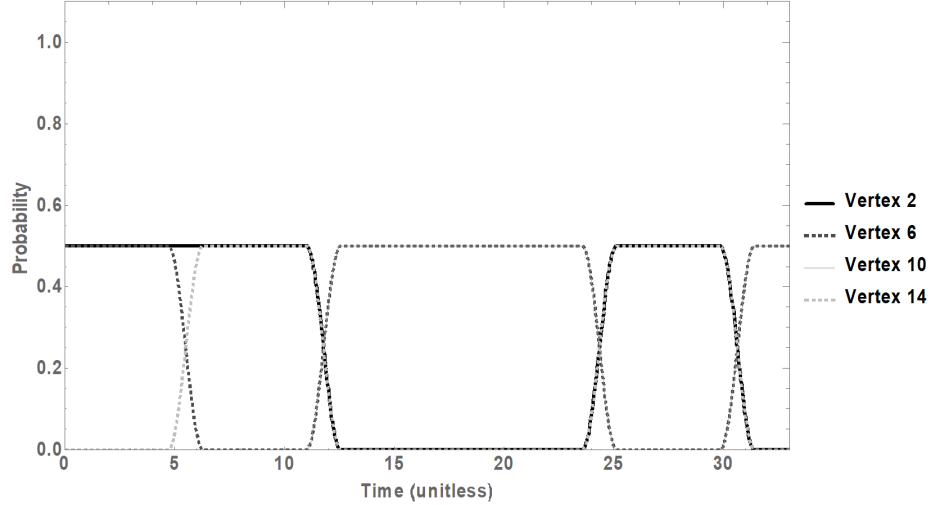


Figure 1.19: The population dynamics of the CTQW for quantum addition of inputs $|a\rangle = |1\rangle$ and $|b\rangle = \frac{1}{\sqrt{2}}|0, 0\rangle + \frac{1}{\sqrt{2}}|0, 1\rangle$. Numerical simulations of the CTQW on the dynamic graph shown in Fig. 1.18 calculates exactly the amplitudes of each vertex and the final state is $|b_1, b_0, a_0, c_0\rangle = \frac{1}{\sqrt{2}}(|0, 1, 1, 0\rangle + |1, 0, 1, 0\rangle)$, which corresponds to a uniform superposition of the vertices 6 and 10.

1.7 Discussion

Continuous-time quantum walks offer a versatile paradigm for quantum computing, in which the edges between vertices in a graph serve to model the connectivity between basis states. We have defined a dynamic graph as a time-ordered sequence of changing connectivity through which a the state of a continuous quantum walk can be tailored to perform computation and, in particular, we have provided constructions of continuous-time quantum walks on dynamic graphs that implement a diverse set of gates taken from the quantum circuit computational model. Our realizations of the single-qubit Pauli, Hadamard, and T gates, and the CNOT and Toffoli gates, as well as measurement and initialization, form a complete set of primitive operations that can be composed to approximate an arbitrary unitary operator. We were able to implement these gates with a complete basis set of at

most eight sparsely connected nodes, allowing the small graph motif to extend across any algorithm. We have presented implementations of the bit-wise addition operation and quantum teleportation to demonstrate composition of quantum walks and shown how some reduction in the composite dynamic graph can be realized by eliminating redundancies.

An important distinction in our formulation of continuous-time quantum walks is the condition that the Hamiltonian represent the connectivity of the underlying basis states. Although we permit variations in this Hamiltonian, the restriction has several side-effects on the computational model. For example, our design for some single-qubit gates taken from the circuit model require graphs with more than two vertices. These additional vertices are effectively ancilla used to store temporarily intermediate states of the walk. This unique representation may afford opportunities for optimizing quantum logic by better understanding the transformation of an input state to its output form. Similarly, multi-qubit gates such as CNOT and Toffoli are trivial to implement by using the starkly different periods for perfect state transfer. Algorithmic methods that take advantage of these otherwise idle vertices may provide more compact representations of logical transformations.

We have restricted designs of the current quantum walks to small and relatively simple graphs, e.g, K_2 and C_4 . These designs are appealing because they require less complex interactions between the physical elements, but the ability to realize these designs will depend on technological constraints as well as algorithmic requirements. In particular, perfect state transfer has been implemented recently in a photonic processor [15]. Chapman et al. used a linear array of evanescently coupled waveguides to realize nearest-neighbor coupling and transfer the polarized state of one photon to another. The underlying tight-binding Hamiltonian provides an approximation to the connectivity graph underlying a continuous-time quantum walk defined within the space of the single-photon Fock states. The approximation

is controlled by the spectra of the coupled waveguides, which must be non-uniform in their geometry for (almost) perfect state transfer using a linear coupled chain [20, 19]. The geometrical constraints imposed by linear chains have been overcome by a recent demonstration of continuous-time quantum walks in two-dimensional waveguide arrays [57]. Tang et al. demonstrated control of the coupling between waveguide in a two-dimensional array by fabricating specific distance between the channels. We anticipate that these capabilities may be applied to vary the coupling along the waveguide length and, consequently, develop a physical realization of a dynamic graph. These adaptations may require relaxations of our model, including modifying the sharp transitions induced by the rectangle function with more gradual transitions. As a second possible implementation, we note that the Mølmer-Sørensen gate commonly used in ion trap technology enables highly tunable connectivity between multiple qubits for a specific Hamiltonian [48, 55], and it would be interesting to apply our principles of continuous-time quantum walks on dynamics graphs to these systems as well.

Acknowledgments

This work was supported in part by the U.S. Department of Energy, Office of Science, Office of Workforce Development for Teachers and Scientists (WDTS) under the Science Undergraduate Laboratory Internships Program (SULI) as well as the Department of Energy, Office of Science Early Career Research Program and the Mathematical Sciences Graduate Internship program of the National Science Foundation.

1.8 Appendix

We demonstrate that the dynamic graph representing Eq. (1.5.6) implements the Hadamard transform by showing explicitly the graph state prepared under the

sequence of CTQWs. We first note that the CTQW on each element G_ℓ in a dynamic graph can be evaluated numerically for the designated propagation time t_ℓ . For \mathcal{G}_H , we have

$$U_{G_0} = \begin{pmatrix} 0 & 0 & 0 & 0 & 0 & 0 & -1 & 0 \\ 0 & i & 0 & 0 & 0 & 0 & 0 & 0 \\ 0 & 0 & 0 & 0 & -1 & 0 & 0 & 0 \\ 0 & 0 & 0 & i & 0 & 0 & 0 & 0 \\ 0 & 0 & -1 & 0 & 0 & 0 & 0 & 0 \\ 0 & 0 & 0 & 0 & 0 & i & 0 & 0 \\ -1 & 0 & 0 & 0 & 0 & 0 & 0 & 0 \\ 0 & 0 & 0 & 0 & 0 & 0 & 0 & i \end{pmatrix}$$

$$U_{G_1} = \begin{pmatrix} \frac{1}{\sqrt{2}} & 0 & 0 & 0 & 0 & 0 & 0 & \frac{-i}{\sqrt{2}} \\ 0 & \frac{1}{\sqrt{2}} & 0 & 0 & 0 & 0 & \frac{-i}{\sqrt{2}} & 0 \\ 0 & 0 & \frac{1}{\sqrt{2}} & 0 & 0 & \frac{-i}{\sqrt{2}} & 0 & 0 \\ 0 & 0 & 0 & \frac{1}{\sqrt{2}} & \frac{-i}{\sqrt{2}} & 0 & 0 & 0 \\ 0 & 0 & 0 & \frac{-i}{\sqrt{2}} & \frac{1}{\sqrt{2}} & 0 & 0 & 0 \\ 0 & 0 & \frac{-i}{\sqrt{2}} & 0 & 0 & \frac{1}{\sqrt{2}} & 0 & 0 \\ 0 & \frac{-i}{\sqrt{2}} & 0 & 0 & 0 & 0 & \frac{1}{\sqrt{2}} & 0 \\ \frac{-i}{\sqrt{2}} & 0 & 0 & 0 & 0 & 0 & 0 & \frac{1}{\sqrt{2}} \end{pmatrix}$$

$$U_{G_2} = \begin{pmatrix} 0 & 0 & 0 & 0 & 0 & 0 & -1 & 0 \\ 0 & -i & 0 & 0 & 0 & 0 & 0 & 0 \\ 0 & 0 & 0 & 0 & -1 & 0 & 0 & 0 \\ 0 & 0 & 0 & -i & 0 & 0 & 0 & 0 \\ 0 & 0 & -1 & 0 & 0 & 0 & 0 & 0 \\ 0 & 0 & 0 & 0 & 0 & -i & 0 & 0 \\ 0 & 0 & 0 & 0 & 0 & 0 & 0 & -1 \\ -i & 0 & 0 & 0 & 0 & 0 & 0 & 0 \end{pmatrix}$$

$$U_{G_3} = \begin{pmatrix} 0 & -i & 0 & 0 & 0 & 0 & 0 & 0 \\ -i & 0 & 0 & 0 & 0 & 0 & 0 & 0 \\ 0 & 0 & 0 & -i & 0 & 0 & 0 & 0 \\ 0 & 0 & -i & 0 & 0 & 0 & 0 & 0 \\ 0 & 0 & 0 & 0 & 0 & -i & 0 & 0 \\ 0 & 0 & 0 & 0 & -i & 0 & 0 & 0 \\ 0 & 0 & 0 & 0 & 0 & 0 & 0 & -i \\ 0 & 0 & 0 & 0 & 0 & 0 & -i & 0 \end{pmatrix}$$

$$U_{G_4} = \begin{pmatrix} i & 0 & 0 & 0 & 0 & 0 & 0 & 0 \\ 0 & i & 0 & 0 & 0 & 0 & 0 & 0 \\ 0 & 0 & i & 0 & 0 & 0 & 0 & 0 \\ 0 & 0 & 0 & i & 0 & 0 & 0 & 0 \\ 0 & 0 & 0 & 0 & i & 0 & 0 & 0 \\ 0 & 0 & 0 & 0 & 0 & i & 0 & 0 \\ 0 & 0 & 0 & 0 & 0 & 0 & i & 0 \\ 0 & 0 & 0 & 0 & 0 & 0 & 0 & i \end{pmatrix}$$

By multiplying the resulting matrices in order, we construct an explicit numerical representation for the CTQW under the dynamic graph \mathcal{G}_H as

$$U_{\mathcal{G}_H} = \begin{pmatrix} \frac{1}{\sqrt{2}} & \frac{1}{\sqrt{2}} & 0 & 0 & 0 & 0 & 0 & 0 \\ \frac{1}{\sqrt{2}} & \frac{-1}{\sqrt{2}} & 0 & 0 & 0 & 0 & 0 & 0 \\ 0 & 0 & \frac{1}{\sqrt{2}} & \frac{1}{\sqrt{2}} & 0 & 0 & 0 & 0 \\ 0 & 0 & \frac{1}{\sqrt{2}} & \frac{-1}{\sqrt{2}} & 0 & 0 & 0 & 0 \\ 0 & 0 & 0 & 0 & \frac{1}{\sqrt{2}} & \frac{1}{\sqrt{2}} & 0 & 0 \\ 0 & 0 & 0 & 0 & \frac{1}{\sqrt{2}} & \frac{-1}{\sqrt{2}} & 0 & 0 \\ 0 & 0 & 0 & 0 & 0 & 0 & \frac{1}{\sqrt{2}} & \frac{1}{\sqrt{2}} \\ 0 & 0 & 0 & 0 & 0 & 0 & \frac{1}{\sqrt{2}} & \frac{-1}{\sqrt{2}} \end{pmatrix}$$

It is then apparent from this numerical representation that the CTQW for \mathcal{G}_H is equivalent to applying the circuit-model operator $H_1 \otimes H_2 \otimes H_3$ on the three-qubit Hilbert space.

We provide a similar proof that the dynamic graph representing Eq. (1.5.8) implements the T gate by showing explicitly the graph state prepared under the

sequence of CTQWs. We first note that

$$U_{G_0} = \begin{pmatrix} \frac{1}{\sqrt{2}} & 0 & \frac{-i}{\sqrt{2}} & 0 & 0 & 0 & 0 & 0 \\ 0 & e^{\frac{-i\pi}{4}} & 0 & 0 & 0 & 0 & 0 & 0 \\ \frac{-i}{\sqrt{2}} & 0 & \frac{1}{\sqrt{2}} & 0 & 0 & 0 & 0 & 0 \\ 0 & 0 & 0 & e^{\frac{-i\pi}{4}} & 0 & 0 & 0 & 0 \\ 0 & 0 & 0 & 0 & e^{\frac{-i\pi}{4}} & 0 & 0 & 0 \\ 0 & 0 & 0 & 0 & 0 & e^{\frac{-i\pi}{4}} & 0 & 0 \\ 0 & 0 & 0 & 0 & 0 & 0 & e^{\frac{-i\pi}{4}} & 0 \\ 0 & 0 & 0 & 0 & 0 & 0 & 0 & e^{\frac{-i\pi}{4}} \end{pmatrix}$$

$$U_{G_1} = \begin{pmatrix} 0 & 0 & 0 & 0 & 0 & -1 & 0 & 0 \\ 0 & -i & 0 & 0 & 0 & 0 & 0 & 0 \\ 0 & 0 & -i & 0 & 0 & 0 & 0 & 0 \\ 0 & 0 & 0 & 0 & -1 & 0 & 0 & 0 \\ 0 & 0 & 0 & -1 & 0 & 0 & 0 & 0 \\ -1 & 0 & 0 & 0 & 0 & 0 & 0 & 0 \\ 0 & 0 & 0 & 0 & 0 & 0 & -i & 0 \\ 0 & 0 & 0 & 0 & 0 & 0 & 0 & -i \end{pmatrix}$$

$$U_{G_2} = \begin{pmatrix} e^{-\frac{i\pi}{4}} & 0 & 0 & 0 & 0 & 0 & 0 & 0 \\ 0 & e^{-\frac{i\pi}{4}} & 0 & 0 & 0 & 0 & 0 & 0 \\ 0 & 0 & \frac{1}{\sqrt{2}} & 0 & \frac{-i}{\sqrt{2}} & 0 & 0 & 0 \\ 0 & 0 & 0 & \frac{1}{\sqrt{2}} & 0 & \frac{-i}{\sqrt{2}} & 0 & 0 \\ 0 & 0 & \frac{-i}{\sqrt{2}} & 0 & \frac{1}{\sqrt{2}} & 0 & 0 & 0 \\ 0 & 0 & 0 & \frac{-i}{\sqrt{2}} & 0 & \frac{1}{\sqrt{2}} & 0 & 0 \\ 0 & 0 & 0 & 0 & 0 & 0 & e^{-\frac{i\pi}{4}} & 0 \\ 0 & 0 & 0 & 0 & 0 & 0 & 0 & e^{-\frac{i\pi}{4}} \end{pmatrix}$$

$$U_{G_3} = \begin{pmatrix} -i & 0 & 0 & 0 & 0 & 0 & 0 & 0 \\ 0 & -i & 0 & 0 & 0 & 0 & 0 & 0 \\ 0 & 0 & 0 & 0 & 0 & -1 & 0 & 0 \\ 0 & 0 & 0 & -i & 0 & 0 & 0 & 0 \\ 0 & 0 & 0 & 0 & -i & 0 & 0 & 0 \\ 0 & 0 & -1 & 0 & 0 & 0 & 0 & 0 \\ 0 & 0 & 0 & 0 & 0 & 0 & 0 & -1 \\ 0 & 0 & 0 & 0 & 0 & 0 & -1 & 0 \end{pmatrix}$$

$$U_{G_4} = \begin{pmatrix} 0 & 0 & \frac{i}{2} & \frac{i}{2} & \frac{i}{2} & \frac{i}{2} & 0 & 0 \\ 0 & e^{\frac{i\pi}{4}} & 0 & 0 & 0 & 0 & 0 & 0 \\ \frac{i}{2} & 0 & \frac{3}{4} & \frac{-1}{4} & \frac{-1}{4} & \frac{-1}{4} & 0 & 0 \\ \frac{i}{2} & 0 & \frac{-1}{4} & \frac{3}{4} & \frac{-1}{4} & \frac{-1}{4} & 0 & 0 \\ \frac{i}{2} & 0 & \frac{-1}{4} & \frac{-1}{4} & \frac{3}{4} & \frac{-1}{4} & 0 & 0 \\ \frac{i}{2} & 0 & \frac{-1}{4} & \frac{-1}{4} & \frac{-1}{4} & \frac{3}{4} & 0 & 0 \\ 0 & 0 & 0 & 0 & 0 & 0 & e^{\frac{i\pi}{4}} & 0 \\ 0 & 0 & 0 & 0 & 0 & 0 & 0 & e^{\frac{i\pi}{4}} \end{pmatrix}$$

$$U_{G_5} = \begin{pmatrix} -i & 0 & 0 & 0 & 0 & 0 & 0 & 0 \\ 0 & -i & 0 & 0 & 0 & 0 & 0 & 0 \\ 0 & 0 & -i & 0 & 0 & 0 & 0 & 0 \\ 0 & 0 & 0 & -i & 0 & 0 & 0 & 0 \\ 0 & 0 & 0 & 0 & -i & 0 & 0 & 0 \\ 0 & 0 & 0 & 0 & 0 & -i & 0 & 0 \\ 0 & 0 & 0 & 0 & 0 & 0 & -i & 0 \\ 0 & 0 & 0 & 0 & 0 & 0 & 0 & -i \end{pmatrix}$$

Thus, as \mathcal{G}_T is the product of the above matrices, we have that

$$U_{\mathcal{G}_T} = \begin{pmatrix} 1 & 0 & 0 & 0 & 0 & 0 & 0 & 0 \\ 0 & e^{\frac{i\pi}{4}} & 0 & 0 & 0 & 0 & 0 & 0 \\ 0 & 0 & \frac{-1}{2} & 0 & \frac{-e^{\frac{-i\pi}{4}}}{\sqrt{2}} & \frac{1}{2} & 0 & 0 \\ 0 & 0 & \frac{-1}{2} & 0 & \frac{e^{\frac{-i\pi}{4}}}{\sqrt{2}} & \frac{1}{2} & 0 & 0 \\ 0 & 0 & \frac{1}{2} & \frac{e^{\frac{-i\pi}{4}}}{\sqrt{2}} & 0 & \frac{1}{2} & 0 & 0 \\ 0 & 0 & \frac{1}{2} & \frac{-e^{\frac{-i\pi}{4}}}{\sqrt{2}} & 0 & \frac{1}{2} & 0 & 0 \\ 0 & 0 & 0 & 0 & 0 & 0 & 0 & e^{-\frac{i\pi}{4}} \\ 0 & 0 & 0 & 0 & 0 & 0 & e^{-\frac{i\pi}{4}} & 0 \end{pmatrix}$$

CHAPTER 2

BROADCAST DOMINATION NUMBER OF SOME REGULAR GRAPHS

2.1 Introduction

Let $G = (V(G), E(G))$ be a graph with vertices $V(G)$ and edges $E(G)$. The *domination number* of a graph G is the cardinality of the smallest dominating set of the graph, which is the smallest set S such that every vertex in $V(G) \setminus S$ is adjacent to a vertex of S .

In 2014, Blessing, Insko, Johnson, and Mauretour generalized this notion to (t, r) *broadcast domination* [9]. In broadcast domination, there is a collection of vertices called towers, \mathcal{T} , that transmit a signal $t \in \mathbb{N}$ in the following manner. If $u \in \mathcal{T}$, and $v \in G$, then the signal at v from u is denoted $f_u(v)$ and is $f_u(v) = \max\{0, t - d(u, v)\}$, where $d(u, v)$ is the distance between u and v . The set \mathcal{T} is said to be (t, r) *broadcast dominating* if each tower transmits a signal t and for all $v \in G$, $\sum_{u \in \mathcal{T}} f_u(v) \geq r$. The (t, r) broadcast domination number of G , $\gamma_{t,r}(G)$, is the minimum cardinality of a (t, r) broadcasting set \mathcal{T} .

The (t, r) broadcasting domination number has been studied for two-dimensional grids, paths, triangular grids, matchstick graphs, and n -dimensional grids [9, 23, 26, 38, 54]. Asymptotic bounds of the $(t, 2)$ broadcast domination number on finite grids has been studied [52], as well.

To describe the (t, r) broadcast domination number of \mathbb{Z}^2 , we consider the *density* of a set $\mathcal{T} \subset \mathbb{Z}^2$ defined as $\limsup_{n \rightarrow \infty} \frac{|\mathcal{T} \cap [-n, n]^2|}{(2n+1)^2}$. Accordingly, $\delta_{t,r}(\mathbb{Z}^2)$ is the minimal density of a (t, r) broadcasting set in \mathbb{Z}^2 . In 2019, Drews, Harris, and Randolph [26] showed that $\delta_{t,3}(\mathbb{Z}^2) \leq \delta_{t-1,1}(\mathbb{Z}^2) = \frac{1}{2t^2 - 6t + 5}$ for grid graphs \mathbb{Z}^2 and conjectured $\delta_{t,3}(\mathbb{Z}^2) = \delta_{t-1,1}(\mathbb{Z}^2)$ for $t > 2$. We prove this conjecture for $t > 17$.

Theorem 1. For $t > 17$, $\delta_{t,3}(\mathbb{Z}^2) = \delta_{t-1,1}(\mathbb{Z}^2)$

Following the proof of Theorem 1, in Section 2.3, we explore other statements in this direction and suggest some conjectures.

Additionally, we extend the previous result on the (t, r) -broadcast domination number of paths [23] to powers of paths:

Theorem 2. *Let $n \geq 1$ and $t \geq r \geq 1$. Then $\gamma_{t,r}(P_n^{(k)}) = \lceil \frac{n+k(r-1)}{2kt-k(r+1)+1} \rceil$.*

Crepeau et. al. found $\gamma_{t,r}(C_n) \leq \lceil \frac{n+r-1}{2t-r} \rceil$ and asked if this bound could be improved [23]. We answer their question by giving the exact value for the (t, r) broadcast domination number for all powers of cycles:

Theorem 3. *Let $n \geq 1$ and $t \geq r \geq 1$. Then*

$$\gamma_{t,r}(C_n^{(k)}) = \begin{cases} 1 & \text{if } n \leq 2(t-r)k + 1 \\ 2 & \text{if } 2(t-r)k + 1 < n \leq (2t-r-1)k + 1 \\ \lceil \frac{n}{(2t-r-1)k+1} \rceil & \text{if } n > (2t-r-1)k + 1 \end{cases}$$

2.2 Proof of Theorem 1

First consider the following $(t, 1)$ broadcasting set of vertices with minimal density $\mathcal{T}_0 = \{ma + nb : m, n \in \mathbb{Z}\}$ where $a = (t-1, t-2)$ and $b = (t-2, 1-t)$. Part of this configuration is shown in Figure 2.1.

We consider for every tower the usable transmission which is the sum over the amount transmitted to all the vertices, not exceeding r . For a tower at vertex v that is $signal(v) := \sum_{u: d(u,v) \leq t-1} \min\{r, t-d(u,v)\}$.

Note that the previously described \mathcal{T}_0 is also a configuration that provides a $(t+1, 3)$ broadcast. We find that four vertices within distance $t-2$ of any tower receive signal 4 rather than the required 3. In Figure 2.1, the bold vertices are the one with extra signal. To formalise the notion of extra signal, let $excess(v) := signal(v) - r$ be the *excess signal* received by a vertex v in a given

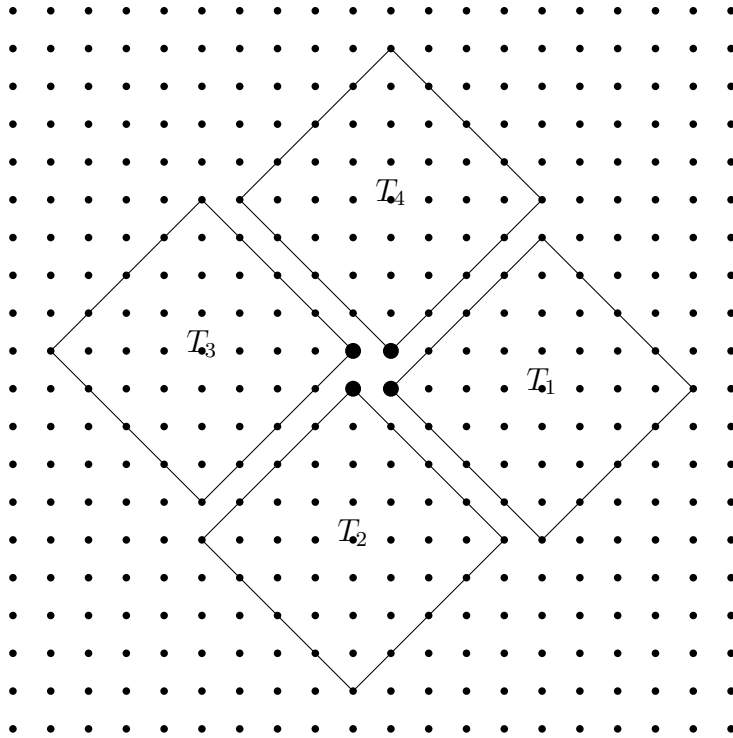


Figure 2.1: An example of a $(5, 1)$ broadcasting set. When considered as a $(6, 3)$ broadcasting set, the four large vertices in the middle receive excess signal.

(t, r) -broadcasting set of towers. We would like to attribute the amount of excess to a given tower T . Note that the average attributable excess exactly determines the broadcast domination number on vertex transitive graphs.

Our goal is to show $\delta_{t,3}(\mathbb{Z}^2) \geq \delta_{t-1,1}(\mathbb{Z}^2)$. In the starting configuration, we have exactly 4 excess attributed to each tower. We want to show that the excess attributed to each tower must be at least 4 in any $(t + 1, 3)$ broadcasting configuration, so that the configuration \mathcal{T}_0 minimises the excess.

Henceforth fix some $(t, 3)$ broadcasting set of towers. We will prove the following lemma.

Lemma 2.2.1. *For any tower at (x, y) , there is at least four excess within the vertices $(x, y) + [t - 4, t + 2] \times [-4, 4]$.*

Proof. Without loss of generality consider a tower T , that will be fixed throughout the argument, at $(-t + 2, 0)$. We shall consider the following three main cases, along

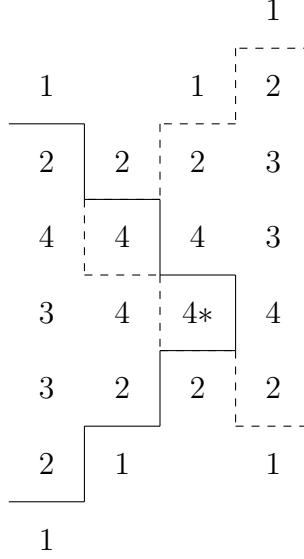


Figure 2.2: The signal received from T and T' in Subcase 2.2.1.2, where second tower T' is located at $(t - 3, 1)$. The line (dashed line resp.) denote the boundary of those vertices receiving at least 2 signal from T (T'' resp.). For a minimal $(t - 1, 1)$ broadcasting set, these regions partition the plane. The $*$ marks the origin.

with their subcases. Figures that help visualize the cases are found below.

Case 2.2.1.1. *There is another tower T' with $|T'|_1 \leq t - 2$.*

Subcase 2.2.1.2. *T' is not on the x -axis.*

Without loss of generality assume T' is above the x -axis, then T' is closer to $(0, 1)$ than to $(0, 0)$, so $t - |T' - (0, 1)|_1 \geq 3$ and similarly $t - |T' - (-1, 1)|_1 \geq 2$ and $t - |T' - (-1, 0)|_1 \geq 1$. Hence, we find that the excess on $(0, 0)$, $(0, 1)$, $(-1, 0)$ and $(-1, 1)$ alone is already more than four, as seen in Figure 2.2.

Subcase 2.2.1.3. *T' is at $(x, 0)$ for $x \leq t - 3$.*

If T' is at $(x, 0)$ for $x \leq t - 3$, the vertices $(-1, 0)$ and $(0, 0)$ both have excess at least 2, as seen in Figure 2.3.

Subcase 2.2.1.4. *T' is at $(t - 2, 0)$.*

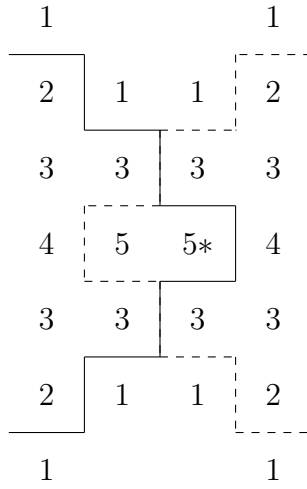


Figure 2.3: The signal received from T and T' in Subcase 2.2.1.3, where second tower $T' = (t - 3, 0)$.

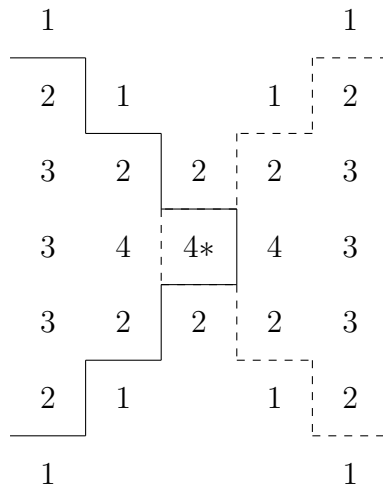


Figure 2.4: The signal received from T and T' in Subcase 2.2.1.4, where the second tower is at $T' = (t - 2, 0)$.

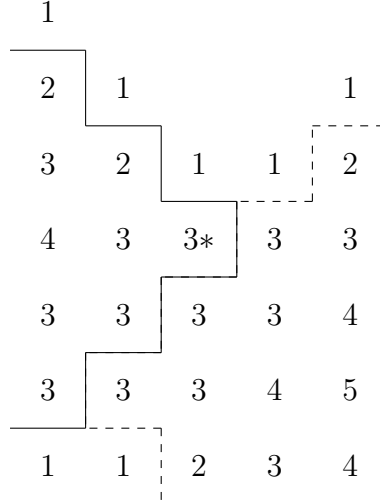


Figure 2.5: The signal received from T and T' in Case 2.2.1.5 for the specific example $t = 5$ where second tower $T' = (2, 4)$.

Note that $(-1, 0)$, $(0, 0)$ and $(1, 0)$ all receive at least one excess from T and T' combined. $(-1, 1)$, $(0, 1)$ and $(1, 1)$ receive 2 signal from T and T' combined, so they need another tower to supply at least one signal. If this is the same tower for two of these, one must get excess signal. On the other hand consider they receive one signal from three different towers. Either $(-2, 1)$, $(2, 1)$ or $(0, 0)$ must receive excess signal from these towers, or $(0, 2)$ receives at least signal 4 from the three towers combined, as seen in Figure 2.4

This concludes Case 2.2.1.1.

We now distinguish two possible configurations for the tower T' giving additional signal to vertex $(0, 0)$. Note that this tower has distance exactly $t - 1$ to the origin. Consider whether $T' \in \{(0, t - 1), (1, t - 2), (0, 1 - t), (1, 2 - t)\}$ or not. Note that up to reflection, if $T' \notin \{(0, t - 1), (1, t - 2), (0, 1 - t), (1, 2 - t)\}$, we are in the realm of Figure 2.5.

Case 2.2.1.5. $T' \notin \{(0, t - 1), (1, t - 2), (0, 1 - t), (1, 2 - t)\}$

Reflecting if necessary, assume T' is somewhere on $y = x - (t - 1)$.

Note that in this case both $(0, 1)$ and $(1, 1)$ receive 1 signal from T and T'

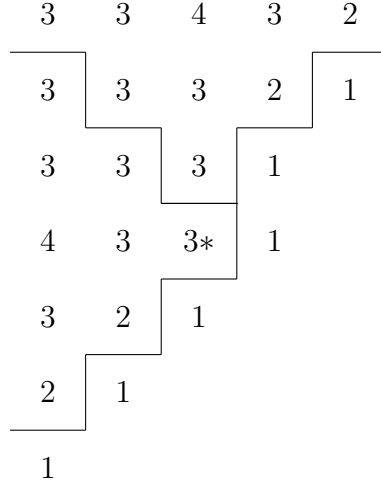


Figure 2.6: The signal received from T and T' in Case 4.3, where second tower $T' = (1, t - 2)$.

combined. Hence, they both need signal from an additional tower.

Subcase 2.2.1.6. *One additional tower covers both $(0, 1)$ and $(1, 1)$.*

This tower will transmit at least a combined signal of three to $(0, 0)$ and $(1, 0)$, causing a total excess of at least 4 on these four vertices combined.

Subcase 2.2.1.7. *$(0, 1)$ and $(1, 1)$ receive additional signal from two distinct towers.*

Consider the tower T'' giving additional signal to $(-1, 1)$. If that tower gives signal at least 2 to $(-2, 1)$ or $(-1, 0)$, we immediately find the excess. As we additionally know there is no tower at $(0, t - 1)$, we find that it must be at $(-1, t)$.

Note that more specifically we know that $(0, 1)$ must receive signal from two additional towers. A tower that gives signal 1 to $(0, 1)$ must give at least 1 signal to one of $(-1, 2)$ and $(1, 0)$ and to one of $(-2, 3)$ and $(2, -1)$. All of those points already receive 3 signal, so the two additional towers for $(0, 1)$ give rise to at least 4 excess on these vertices.

Case 2.2.1.8. $T' \in \{(0, t - 1), (1, t - 2), (0, 1 - t), (1, 2 - t)\}$

Without loss of generality $T' = (1, 2 - t)$. Note that $(-1, 1)$ receives only signal 2 from T and T' , so receives additional signal from another tower T'' . By Case 2.2.1.1, we only need to consider towers at distance $t - 1$ from $(-1, 1)$. There are only two significant cases. If T'' has x -coordinate at least 1, then the excess signal on $(0, 0)$, $(1, 0)$ and $(1, -1)$ is at least 4 already. Hence, T'' is either $(0, t - 1)$ or $T(-1, t)$.

Subcase 2.2.1.9. $T'' = (0, t - 1)$

Note that $(1, 1)$ and $(1, 2)$ only receive 2 signal from towers T , T' and T'' . If these two were reached by the same tower say T''' , then one of the two must receive signal 2 from T''' . If that is $(1, 1)$, note that $(0, 0)$, $(0, 1)$, $(1, 0)$ and $(1, 1)$ all receive excess at least 1. If it is $(1, 2)$, note that $(0, 0)$, $(0, 2)$, $(1, 2)$ and $(1, 3)$ all receive excess at least 1, as seen in Figure 2.6.

Subcase 2.2.1.10. $T'' = (-1, t)$

This case is completely analogous to Subcase 2.2.1.7.

On the other hand, suppose the points $(1, 1)$ and $(1, 2)$ receive signal 1 from two distinct towers. If either of these towers transmits 2 signal to $(0, 1)$, $(0, 2)$, $(1, 3)$ or $(1, 0)$, the excess is immediately more than 4. The towers transmit 2 to $(1, 1)$ and $(1, 2)$ respectively, then $(2, 2)$ receives 1 excess signal and $(3, 1)$ receives 2 excess signal. □

The next goal is to show that for large t , we have excess at least four times the number of towers.

Lemma 2.2.2. *Let $t > 17$. For any $(t, 3)$ broadcasting set \mathcal{T} there is at least $4|\mathcal{T}|$ excess.*

Proof. We devise a way to attribute excess to towers. First to all towers T with no other towers within $T + [-6, 6] \times [-8, 8]$, assign 4 excess from the rectangle

$T + [t - 4, t + 2] \times [-4, 4]$. Note that this excess exists by Lemma 2.2.1 and that these rectangles are disjoint.

Let R_i be a $[-6, 6] \times [-8, 8]$ rectangle around a tower T_i . If a tower T_j lies in R_i , place an edge between T_i and T_j . Suppose T' lies in the rectangle around T , so the edge TT' exists. We find that all the vertices in $R' = \frac{T+T'}{2} + [-4, 2] \times [-4, 4]$ receive at least 3 excess from T and T' . Moreover, R' intersects at most four regions of the form $T'' + [t - 4, t + 2] \times [-4, 4]$ with $T'' \in \mathcal{T}$ as considered in Lemma 2.2.1.

Therefore, at least $6 \cdot 8 - 4 \cdot 4 = 32$ excess remains available in R' . This is cumulative in the sense that if regions of the form R' overlap for different edges in the graph, then still at least 32 excess is available per edge. As the number of edges is at least half the number of vertices in any nontrivial component, we find that for every vertex, at least 16 excess can be assigned to that vertex. Hence, we find at least $4|\mathcal{T}|$ excess. □

We are now ready to prove Theorem 1.

Proof. Let $G_{2n+1, 2n+1}$ be the $2n + 1$ by $2n + 1$ grid. We then need at least $3(2n + 1)^2$ signal to be transmitted. By Lemma 2.2.2, a $(t, 3)$ -broadcasting set \mathcal{T} of towers can transmit at most $|\mathcal{T}|3(t - 1)^2$ signal effectively. Therefore $|\mathcal{T}| \geq \frac{3(2n+1)^2}{3(t-1)^2}$, so we find

$$\begin{aligned} \delta_{t,3}(\mathbb{Z}^2) &\geq \lim_{n \rightarrow \infty} \frac{\left(\frac{3(2n+1)^2}{3(t-1)^2}\right)}{(2n+1)^2} \\ &= \frac{1}{(t-1)^2} \\ &= \delta_{t-1,1}(\mathbb{Z}^2) \end{aligned}$$

□

2.3 Generalizations of the (t, r) broadcast number for grids

The proof of Theorem 1 suggests that the result may be extended to any odd value of r . Note first the following simple, though seemingly unobserved fact;

Proposition 4. *For all $t, k \geq 1$;*

$$\delta_{t,1}(\mathbb{Z}^2) \geq \delta_{t+k,1+2k}(\mathbb{Z}^2)$$

Proof. It suffices to show a $(t, 1)$ broadcasting set of towers \mathcal{T} is also $(t + k, 1 + 2k)$ broadcasting. Consider a vertex $v \in \mathbb{Z}^2$. As \mathcal{T} is $(t, 1)$ -broadcasting, $\exists T \in \mathcal{T}$ with $d(T, v) < t$. Find a vertex $u \in \mathbb{Z}^2$ with $d(T, u) = d(T, v) + d(u, v) = t$, which is possible in the plane. Again, as \mathcal{T} is $(t, 1)$ broadcasting, there is a $T' \in \mathcal{T}$ with $d(T', u) < t$. Now note that if all towers transmitted $t + k$ of signal, then v receives $t + k - d(T, v) = k + d(u, v)$ signal from tower T and $t + k - d(T', v) \geq t + k - d(u, v) - d(T', u) \geq k + 1 - d(u, v)$ from tower T' . In total v thus receives signal at least $k + d(u, v) + k + 1 - d(u, v) = 2k + 1$. Hence, \mathcal{T} is also $(t + k, 1 + 2k)$ broadcasting. \square

Similarly we have

Proposition 5. *For all $t, k \geq 1$;*

$$\delta_{t,2}(\mathbb{Z}^2) \geq \delta_{t+k,2+2k}(\mathbb{Z}^2)$$

Proof. As before, consider $\mathcal{T} \subset \mathbb{Z}^2$ to be $(t, 2)$ -broadcasting and $v \in \mathbb{Z}^2$. We will show that if the towers in \mathcal{T} transmitted $t + k$ signal, then all vertices would receive at least $2 + 2k$ signal. If there is a $T \in \mathcal{T}$ with $d(T, v) \leq t - 2$ the proof of the previous lemma suffices completely analogously. If there is no such T , there must be $T, T' \in \mathcal{T}$ with $d(T, v) = d(T', v) = t - 1$. That implies that v receives signal $k + 1$ from both towers and thus $2k + 2$ in total. \square

In [9], Blessing et al. conjectured that in general this inequality is sharp, i.e. that $\delta_{t+1,r+2}(\mathbb{Z}^2) = \delta_{t,r}(\mathbb{Z}^2)$. However, Drews, Harris, and Randolph in [26], showed by computing these quantities that, in fact, $\delta_{t+1,r+2}(\mathbb{Z}^2) < \delta_{t,r}(\mathbb{Z}^2)$ for several values of t and r . Consequently, they formulated a stronger conjecture on the value of $\delta_{t,r}(\mathbb{Z}^2)$ for $r \leq 10$. We believe the improved bounds suggested in [26] are an artifact of the small values of t used in the simulation run by Drews, Harris, and Randolph, as results for $t \leq 15$ were reported in the paper. We propose the following weakening of the conjecture proposed by Blessing, et al.

Conjecture 2.3.1. *For all $r \geq 2$, there exists t_0 such that for all $t \geq t_0$;*

$$\delta_{t+1,r+2}(\mathbb{Z}^2) = \delta_{t,r}(\mathbb{Z}^2).$$

In the hopes of proving this result along the line of the proof of Theorem 1, we compute the average amount of excess per tower in an optimally $(t, 1)$ broadcasting configuration when viewed as a $(t + k, 2k + 1)$ broadcasting configuration. The task of showing that one cannot achieve a configuration with a smaller average amount of excess per tower remains open, but a proof along the same lines as Lemma 2.2.1 seems reasonable. Our attempts have resulted in impenetrable casework, and more ideas to improve elegance would be needed.

Lemma 2.3.2. *Let $t > k$. The average excess per tower in an optimally $(t, 1)$ broadcasting configuration when viewed as a $(t + k, 2k + 1)$ broadcasting configuration is $\frac{1}{6}k(k + 1)(2k + 1)$.*

Proof. Consider four towers around the origin at

$T_1 = (t - 1, 0), T_2 = (-1, -(t - 1)), T_3 = (-t, 1)$ and $T_4 = (0, t)$ and call the square

formed by these towers S . This configuration provides a $(t, 1)$ - broadcast. To

complete the proof, it suffices to show that the starting configuration also provides a $(t + k, 1 + 2k)$ -broadcast.

We shall divide S into two regions. Let S' be the square with corner vertices $(k-1, -(k-1)), (-k, -(k-1)), (-k, k)$, and $(k-1, k)$, along with all points on the boundary, and in the interior of this region. As $t > k$, S' is contained inside S , since $k < t$, $-(k-1) > -(t-1)$, $k-1 < t-1$ and $-k > -t$.

Claim 2.3.3. *The vertices inside S that have signal at least r and no excess are the vertices that do not lie in S' and are in S .*

Proof. Consider the regions defined by the lines $x + y = k$, $x + y = -k - 1$, $x - y = k$ and $x - y = -k - 1$. Note that by symmetry we need only check that there is no excess above the line $x + y = k$. Above the line $x + y = k$, no vertex receives any signal from T_2 and T_3 . Consider a vertex (x, y) in this region. If this vertex is above $x - y = k$ or below $x - y = -k - 1$, it will receive signal from only one tower. This will be signal at least $2k + 1$ but will have no excess as it lies in the broadcast zone of exactly one tower. Otherwise, this vertex will receive signal $t + k - (t - 1 - x + y)$ from T_1 and $t + k - (x + t - y)$ from T_4 , which amounts to a total signal of $2k + 1$. \square

In the proof of the next claim, we find that each vertex in S' has excess and calculate how much. This process shows that each vertex in S' has signal greater than r .

Claim 2.3.4. *The excess of S' is $\frac{1}{6}k(k+1)(2k+1)$.*

Proof. In fact we note that for every $0 \leq i \leq k-1$, a vertex on the intersection between $x + y = i$ and S' receives an excess of $2k - 2i - 1$. We proceed by induction on i . For $i = 0$, note that $(0, 0)$ receives $(t - (t' - 1)) + (t - t') + (t - (t' + 1)) + (t - t') = 4k$ signal, which corresponds to $2k - 1$ excess. For a vertex v with $i \geq 1$, note that at least one of $v - e_1$ and $v - e_2$ was in the intersection between S' and $x + y = i - 1$. Fix one of these to be v' . Now the distances to three towers increases, while to one tower it decreases.

In particular, if $v = v' + e_1$, then $d(v, T_2) = d(v', T_2) - 1$, $d(v, T_3) = d(v', T_3) - 1$, $d(v, T_4) = d(v', T_4) - 1$, and $d(v, T_1) = d(v', T_1) - 1$. On the other hand, if $v = v' + e_2$, then $d(v, T_1) = d(v', T_1) - 1$, $d(v, T_3) = d(v', T_3) - 1$, $d(v, T_4) = d(v', T_4) - 1$, and $d(v, T_2) = d(v', T_2) - 1$.

Either way the signal received by v is 2 less than by v' finishing the induction.

The number of vertices on the intersection between S' and $x + y = i$ is $i + 1$, so we find total excess: $\sum_{i=0}^{k-1} (i + 1)(2k - 2i - 1) = \frac{1}{6}k(k + 1)(2k + 1)$ \square

Thus, each vertex on the infinite grid with a tiling of this pattern has signal at least r . This concludes the proof of Theorem 2.3.2. \square

2.4 Proof of Theorem 2

Proof. We will consider the power of a path, $G = P_n^{(k)}$ on vertex set $\{0, \dots, n - 1\}$ with $v_i v_j$ an edge if and only if $|i - j| \leq k$. For the lower bound we consider the potentially useful amount of signal transmitted by a tower. Note that from the signal submitted to a vertex at distance at most $t - r$ from a tower, only r can be used to exceed the signal threshold. Hence, the total amount of potentially useful signal transmitted by a tower is at most

$(2k(t - r) + 1)r + 2k((r - 1) + (r - 2) + \dots + 1) = ((2t - r - 1)k + 1)r$. Moreover, as the vertex v_0 receives signal at least r , there must be a tower at v_i for some $i \leq (t - r)k$. This tower wastes $k((r - 1) + (r - 2) + \dots + 1) = kr(r - 1)/2$ of its potentially useful amount of transmitted signal. Similarly, v_n receives signal at least r . We may conclude that the total amount of transmitted signal needed is at least $nr + kr(r - 1)$. This gives the lower bound $\left\lceil \frac{n + k(r - 1)}{(2t - r - 1)k + 1} \right\rceil$.

For the upper bound consider $\mathcal{T} = \{v_i : 0 \leq i \leq n - 1, i \equiv (t - r)k \pmod{(2t - r - 1)k + 1}\}$ if $(n - 1) \pmod{(2t - r - 1)k + 1}$ is between $(t - r)k$ and $2(t - r)k + 1$. Otherwise, let $\mathcal{T} = \{v_i : 0 \leq i \leq n - 1, i \equiv (t - r)k$

$\text{mod } (2t - r - 1)k + 1 \} \cup \{v_{n-1}\}$.

Note that vertices v_i with $i \leq (t - r)k$ all receive enough signal from the tower at $v_{(t-r)k}$. By construction, the last tower is at distance at most $(t - r)$ away from the vertex v_{n-1} , so all the vertices not between two towers receive enough signal.

Now consider a vertex v_i between two towers, say

$i = l((2t - r - 1)k + 1) + (t - r)k + p$ where $0 \leq p < (2t - r - 1)k + 1$ and both $v_{l((2t-r-1)k+1)+(t-r)k}$ and $v_{\min\{n, (l+1)((2t-r-1)k+1)+(t-r)k\}}$ are in \mathcal{T} . Then

$$\begin{aligned}
d(v_i, v_{l((2t-r-1)k+1)+(t-r)k}) + d(v_i, v_{\min\{(l+1)((2t-r-1)k+1)+(t-r)k, n\}}) \\
&\leq \left\lceil \frac{p}{k} \right\rceil + \left\lceil \frac{(2t - r - 1)k + 1 - p}{k} \right\rceil \\
&= (2t - r - 1) + \left\lceil \frac{p}{k} \right\rceil + \left\lceil \frac{1 - p}{k} \right\rceil \\
&\leq (2t - r - 1) + 1 \\
&= 2t - r
\end{aligned}$$

Thus, the broadcast received by vertex v_i is

$$\begin{aligned}
&\max\{t - d(v_i, v_{l((2t-r-1)k+1)+(t-r)k}), 0\} + \max\{t - d(v_i, v_{\min\{(l+1)((2t-r-1)k+1)+(t-r)k, n\}}), 0\} \\
&\geq 2t - (d(v_i, v_{l((2t-r-1)k+1)+(t-r)k}) + d(v_i, v_{\min\{(l+1)((2t-r-1)k+1)+(t-r)k, n\}})) \\
&\geq 2t - (2t - r) = r
\end{aligned}$$

Thence, all vertices receive sufficient signal. □

When $k = 1$, we are left with a path, and obtain $\gamma_{t,r}(P_n) = \left\lceil \frac{n+r-1}{2t-r} \right\rceil$, agreeing with the result by Crepeau, et al.

2.5 Proof of Theorem 3

Proof. If $n \leq 2(t-r)k+1$, then any vertex is at most distance $(t-r)$ from any other vertex, so a tower at any vertex is (t,r) -broadcasting. If, on the other hand, $n > 2(t-r)k+1$ we find that for all $0 \leq i < n$, $d(v_i, v_{i+(t-r)k+1}) = (t-r) + 1$. Hence, no one tower can be (t,r) -broadcasting. For $n \leq (2t-r-1)k+1$, $\mathcal{T} = \{0, \lfloor \frac{n}{2} \rfloor\}$ is (t,r) -broadcasting.

First we will show the upper bound. When $2(t-r)k+1 < n$, consider the set $\mathcal{T} = \{v_i : i \equiv 0 \pmod{(2t-r-1)k+1}\} \cap \{v_0, \dots, v_n\}$. Evidently, $|\mathcal{T}| = \lceil \frac{n}{(2t-r-1)k+1} \rceil$. Moreover, we will show that these towers are (t,r) -broadcasting. Consider vertex v_i . Choose l and p such that $p \in \{0, \dots, (2t-r-1)k\}$ and $i = l((2t-r-1)k+1) + p$. Note that the two towers closest to v_i are $v_{l((2t-r-1)k+1)}$ and $v_{\min\{(l+1)((2t-r-1)k+1), n\}}$. We find that the sum of the distance between each tower and v_i is

$$\begin{aligned} d(v_i, v_{l((2t-r-1)k+1)}) + d(v_i, v_{\min\{(l+1)((2t-r-1)k+1), n\}}) &\leq \left\lceil \frac{p}{k} \right\rceil + \left\lceil \frac{(2t-r-1)k+1-p}{k} \right\rceil \\ &= (2t-r-1) + \left\lceil \frac{p}{k} \right\rceil + \left\lceil \frac{1-p}{k} \right\rceil \\ &\leq (2t-r-1) + 1 \\ &= 2t-r \end{aligned}$$

Thus, the broadcast received by vertex v_i is

$$\begin{aligned} &\max\{t-d(v_i, v_{l((2t-r-1)k+1)}), 0\} + \max\{t-d(v_i, v_{\min\{(l+1)((2t-r-1)k+1), n\}}), 0\} \\ &\geq 2t - (d(v_i, v_{l((2t-r-1)k+1)}) + d(v_i, v_{\min\{(l+1)((2t-r-1)k+1), n\}})) \\ &\geq 2t - (2t-r) = r \end{aligned}$$

Note that from the signal submitted to a vertex at distance at most $t-r$ from a tower, only r is used to exceed the signal threshold. Hence, the total amount of

potentially useful signal submitted by a tower is at most

$(2k(t-r)+1)r + 2k((r-1)+(r-2)+\dots+1) = ((2t-r-1)k+1)r$. The total signal needed to saturate all the vertices is at least nr . Hence,

$$\gamma_{t,r}(C_n^{(k)}) \geq \left\lceil \frac{nr}{r((2t-r-1)k+1)} \right\rceil = \left\lceil \frac{n}{(2t-r-1)k+1} \right\rceil. \quad \square$$

2.6 Concluding Remarks

A natural next direction would be to consider n -dimensional generalizations.

Analogously to the 2 dimensional definitions, let the density of a set $\mathcal{T} \subset \mathbb{Z}^n$ be defined to be $\limsup_{m \rightarrow \infty} \frac{|\mathcal{T} \cap [-m,m]^n|}{(2m+1)^n}$ and let $\delta_{t,r}(\mathbb{Z}^n)$ be the minimal density of a (t,r) broadcasting set $\mathcal{T} \subset \mathbb{Z}^n$.

Question 2.6.1. *Is there a relationship between $\delta_{t,r}(\mathbb{Z}^n)$ and $\delta_{t-1,r-2}(\mathbb{Z}^n)$ for some t , and r ?*

In complete parallel to Propositions 4 and 5, we have that $\delta_{t+k,1+2k}(\mathbb{Z}^n) \leq \delta_{t,1}(\mathbb{Z}^n)$ and $\delta_{t+k,2+2k}(\mathbb{Z}^n) \leq \delta_{t,2}(\mathbb{Z}^n)$ by an analogous proof. Note that in dimensions $n > 2$, unlike in dimensions one and two, l_1 -balls of constant radius do not partition \mathbb{Z}^n , so even the exact value of $\delta_{t,1}(\mathbb{Z}^n)$ can be hard to obtain. In 3 dimensions this amounts to efficiently covering space with octahedrons.

In another direction, the continuous generalization of Conjecture 2.3.1 might provide a lot of insight. We say a set of towers $\mathcal{T} \subset \mathbb{R}^2$ is (t,r) broadcasting if all points in points $v \in \mathbb{R}^2$ satisfy that

$$\sum_{T \in \mathcal{T}} \max\{t - d(T, v), 0\} \geq r$$

where d is some metric on \mathbb{R}^2 . It is natural to look for the minimal density $\limsup_{x \rightarrow \infty} \frac{\text{card}(\mathcal{T} \cap [-x,x]^2)}{4x^2}$ of a (t,r) -broadcasting set. For d the Euclidean ℓ_2 distance, this problem is intimately related to efficient sphere packing. To stay as close to the discrete context as possible, let d be the ℓ_1 distance. Let $\delta'_{t,r}(\mathbb{R}^2)$ be the

smallest density of a (t, r) broadcasting set in \mathbb{R}^2 . Note that in this definition being (t, r) broadcasting and being $(1, \frac{r}{t})$ broadcasting are equivalent. In fact for $\alpha > 0$, $\delta'_{t,r}(\mathbb{R}^2) = \delta'_{\alpha t, \alpha r}(\mathbb{R}^2)$. Analogously to Conjecture 2.3.1, we believe

Conjecture 2.6.2. *There exists $\gamma_0 > 0$ such that for all $\gamma \leq \gamma_0$,*

$$\delta'_{1,\gamma}(\mathbb{R}^2) = \lim_{\epsilon \rightarrow 0} \delta'_{1-\gamma/2,\epsilon}(\mathbb{R}^2) = \frac{1}{4(1-\frac{\gamma}{2})^2}$$

The right equality follows from the fact that the set $\mathcal{T}_\epsilon = \{ma + nb : m, n \in \mathbb{Z}\}$ with $a = (1 - \frac{\gamma}{2} - \epsilon, 1 - \frac{\gamma}{2} - \epsilon)$ and $b = (1 - \frac{\gamma}{2} - \epsilon, \frac{\gamma}{2} + \epsilon - 1)$ is $(1 - \gamma/2, \epsilon)$ broadcasting and has asymptotic density $\frac{1}{4(1-\frac{\gamma}{2}-\epsilon)^2}$, which tends to $\frac{1}{4(1-\frac{\gamma}{2})^2}$ as $\epsilon \rightarrow 0$. Moreover, the set \mathcal{T}_0 immediately shows $\delta'_{1,\gamma} \leq \frac{1}{4(1-\frac{\gamma}{2})^2}$.

When viewing the discrete setting as an approximation of the continuous setting, Conjecture 2.6.2 would indicate that the minimal t_0 as a function of r in Conjecture 2.3.1 would be at most linear, i.e. $t_0 = O(r)$.

CHAPTER 3

CAPTURE TIMES IN BRIDGE-BURNING COPS AND ROBBERS

3.1 Introduction

Cops and Robbers is a well-studied game on a graph G in which there are two players. One player controls the cops, and the other controls the robber. Each cop and robber occupies a vertex of G and takes turns moving between vertices of the graph, with the cop choosing its initial positions first. The goal of the cops is to capture the robber, which occurs when a cop occupies the same vertex as a robber, and the robber's goal is to continually evade the cop. The game is played in *rounds*, where a round consists of the cops moving, or choosing not to move, and the robber moving, or choosing not to move.

Several variants of the game have been introduced over the years, including where the robbers can move more quickly than the cops [6, 32], with imperfect information [21], and where there is more than one cop [3]. Recently, Kinnersley and Peterson [44] introduced the variant *bridge-burning cops and robbers*. In the bridge-burning version, the cops and robber may only move to vertices adjacent to the one they currently occupy, however each time the robber moves from vertex u to vertex v , the edge uv is erased from the graph. Using the notation introduced in [44], let $c_b(G)$ be the bridge burning cop number, which is the minimum number of cops required to catch the robber on the graph G in the bridge-burning game. Kinnersley and Peterson studied the game on numerous graphs including paths P_n , cycles C_n , complete bipartite graphs $K_{m,n}$, hypercubes Q_n , and two dimensional finite grids $G_{m,n}$ [44].

A related notion to $c_b(G)$ is the capture time of G , denoted $\text{capt}_b(G)$. The bridge-burning capture time is the minimum number of rounds it takes for the cop to capture the robber. The capture time of cops and robbers was introduced in 2009

by Bonato, Golovach, Hahn, and Kratochvíl [13] and has been studied on trees [61] and planar graphs [50]. Kinnersley and Peterson [44] showed that if one cop can capture the robber on a graph G , then $\text{capt}_b(G) = O(n^3)$ and conjectured that there exists a graph G such that $c_b(G) = 1$ and $\text{capt}_b(G) = \Omega(n^3)$. We generalise their result by showing that $\text{capt}_b(G) = O(n^{c_b(G)+2})$ and prove the matching lower bound analogous to the one in their conjecture for $c_b(G) \geq 3$.

Theorem 6. *There exists a universal constant $C > 0$ such that the following holds. For every $k \geq 3$ and n sufficiently large, there exists a graph G_n such that $v(G_n) = n$, $c_b(G_n) = k$, and*

$$C \frac{n^{k+2}}{k^{k+2}} \leq \text{capt}_b(G_n).$$

In fact, in Proposition 10 we show that for all G on n vertices $\text{capt}_b(G) \leq \frac{n^{c_b(G)+2}}{2^{c_b(G)}!}$, which shows that even the asymptotics in $c_b(G)$ are fairly tight.

In Section 3.2, we present some preliminary and additional results and in Section 3.3 we proof Theorem 6.

3.2 Capture times

In this paper, we will show that the graph G on n vertices with cop number $k \geq 3$ which maximizes the capture time satisfies

$$C \frac{n^{k+2}}{k^{k+2}} \leq \max\{\text{capt}_b(G) : c_b(G) = k\} \leq C' \frac{n^{k+2}}{k!}$$

for some universal constants C and C' .

First, we show that the capture time of $K_{n,n}$ is $\Theta(n^2)$. Our proof significantly simplifies the proof given in [44, Theorem 5.2]. In order to prove this, we need the following slight strengthening of a theorem from Kinnersley and Peterson [44,

Theorem 2.2].

Lemma 7. *If $\exists X \subset V(G)$, such that $G[X]$ is a clique and $X \cup \Gamma(X) = V(G)$, then $c_b(G) = 1$ and $\text{capt}_b(G) = O(n^2)$, where $\Gamma(X)$ is the neighbourhood of X .*

Proof. Place the cop on any vertex in X . Subsequently, always move the cop to a vertex in X adjacent to the position of the robber. Note that the robber can never move onto a vertex in X and, moreover, can never remove an edge incident to X . Hence, $X \cup \Gamma(X) = V(G)$ remains constant throughout the game. After each round, the cop is adjacent to the robber, so the robber must move in every round. Given that the robber removes one edge in every round, eventually he must move into X , as all the other possible edges have been removed. As there are $O(n^2)$ edges, this must happen within $O(n^2)$ moves. \square

This lemma provides the cop number and an upper bound in the following proposition.

Proposition 8. *$K_{n,n}$ has capture time $\Theta(n^2)$*

Proof. As any two adjacent vertices in $K_{n,n}$ satisfy the conditions in Lemma 7, we find that $c_b(K_{n,n}) = 1$ and $\text{capt}_b(G) = O(n^2)$.

On the other hand, we consider the following strategy for the robber to delay capture. First, we find an Euler cycle of $K_{\lfloor \frac{n}{2} \rfloor, \lfloor \frac{n}{2} \rfloor}$ (or $K_{\lfloor \frac{n}{2} \rfloor - 1, \lfloor \frac{n}{2} \rfloor - 1}$ if $\lfloor \frac{n}{2} \rfloor$ is odd). Next, we traverse the following route through $K_{n,n}$; to each vertex in $K_{\lfloor \frac{n}{2} \rfloor, \lfloor \frac{n}{2} \rfloor}$, assign a distinct pair of vertices in $K_{n,n}$ such that the pairs of vertices from the same part of $K_{\lfloor \frac{n}{2} \rfloor, \lfloor \frac{n}{2} \rfloor}$ are in the same part of $K_{n,n}$. Now, the robber follows the Euler cycle through $K_{n,n}$ in the sense that every time he is forced to move, he goes to an element in the corresponding pair which is available. As the cop is only able to occupy one vertex of a given pair, there is no way for the cop to obstruct the robber's path. This route has length $\Omega(n^2)$. \square

In fact Lemma 7 implies the following result for random graphs $\mathcal{G}(n, p)$.

Corollary 9. *Let $G \in \mathcal{G}(n, p)$. Then w.h.p. $c_b(G) = 1$ and $\text{capt}_b(G) = O(n^2)$.*

Proof. By Lemma 7 it suffices to show that G contains a dominating clique w.h.p. This follows from a second moment argument included in Lemma 12 in the Appendix. □

For general graphs, we find the following generalization of a result from [44] which showed this proposition in the case $c_b(G) = 1$.

Proposition 10. *Let G be a graph on n vertices, then $\text{capt}_b(G) \leq \frac{n^{c_b(G)+2}}{2^{c_b(G)}!}$.*

Proof. Note that as the robber removes an edge with every move, the robber can make at most $e(G) \leq \binom{n}{2}$ moves before getting caught. Between two moves of the robber, the cops move around. Without the robber moving, there is no point in the cops returning twice to the exact same configuration. As there are at most $\binom{n}{c_b(G)} \leq \frac{n^{c_b(G)}}{c_b(G)!}$ configurations of the cops on the vertices, it can take at most $\frac{n^{c_b(G)+2}}{2^{c_b(G)}!}$ moves before the robber is caught. □

The remainder of the paper is dedicated to proving Theorem 6.

3.3 Proof of Theorem 6

We first prove the result for $k = 3$ and then extend the construction to larger k . We claim the following graph G has $c_b(G) = 3$ and $\text{capt}_b(G) = \Theta(n^5)$.

$$\begin{aligned}
V(G) = & \{p_i, q_i : i \in [3n]\} \cup \{x_1, x_2\} \cup \{d_x, h_x\} \\
& \cup X \cup Y \\
& \cup \{d_{X,1}, d_{X,2}, d_{Y,1}, d_{Y,2}, h_{X,1}, h_{X,2}, h_{Y,1}, h_{Y,2}\} \\
& \cup \{a_i : i \in [3n]\} \cup \{d_a, h_a\} \\
& \cup \{d_{a,v,1}, d_{a,2}, h_{a,1}, h_{a,2}\} \\
& \cup \{b_i : i \in [3n]\} \\
& \cup \{d_{b,1}, d_{b,2}, h_{b,1}, h_{b,2}\} \\
& \cup \{d_{a,i,1}, d_{a,i,2}, h_{a,i,1}, h_{a,i,2} : i \in [3]\} \\
& \cup \{d_{b,i,1}, d_{b,i,2}, h_{b,i,1}, h_{b,i,2} : i \in [3]\}
\end{aligned}$$

with $|X| = |Y| = 3n$.

$$\begin{aligned}
E(G) = & \{p_i p_{i+1}, q_i q_{i+1} : i \in [3n - 1]\} \cup \{p_1 x_1, q_1 x_1, p_n x_2, q_n x_2\} \\
& \cup \{p_i d_x, q_i d_x, x_1 d_x, x_2 d_x : i \in [3n]\} \\
& \cup \{x_1 v : v \in X\} \cup \{x_2 v : v \in Y\} \cup \{uv : u \in X, v \in Y\} \\
& \cup \{p_i d, q_i d, x_1 d, x_2 d : i \in [3n], d \in \{d_{X,1}, d_{X,2}, d_{Y,1}, d_{Y,2}\}\} \\
& \cup \{v d_{X,1}, v d_{X,2} : v \in X\} \cup \{v d_{Y,1}, v d_{Y,2} : v \in Y\} \\
& \cup \{a_i a_{i+1} : i \in [3n]\} \\
& \cup \{a_i d_a : i \in [3n]\} \\
& \cup \{a_i d_{a,1}, a_i d_{a,2} : i \in [3n]\} \\
& \cup \{v d_{a,1}, v d_{a,2} : v \in X \cup Y\} \\
& \cup \{a_i x_1 : i \in [3n]\} \\
& \cup \{b_i b_{i+1} : i \in [3n]\} \\
& \cup \{b_i d_b : i \in [3n]\} \\
& \cup \{b_i d_{b,1}, b_i d_{b,2} : i \in [3n]\} \\
& \cup \{v d_{b,1}, v d_{b,2} : v \in X \cup Y\} \\
& \cup \{b_i x_2 : i \in [3n]\} \\
& \cup \{v d_{a,i,1}, v d_{a,i,2} : v \in X \cup Y, i \in [3]\} \\
& \cup \{x_1 d_{a,i,1}, x_1 d_{a,i,2}, x_2 d_{a,i,1}, x_2 d_{a,i,2} : i \in [3]\} \\
& \cup \{p_j d_{a,i,1}, p_j d_{a,i,2}, q_j d_{a,i,1}, q_j d_{a,i,2} : j \not\equiv i \pmod{3}\} \\
& \cup \{a_{(i-1)n+j} d_{a,i,1}, a_{(i-1)n+j} d_{a,i,2} : j \in [n], i \in [3]\} \\
& \cup \{v d_{b,i,1}, v d_{b,i,2} : v \in X \cup Y, i \in [3]\} \\
& \cup \{a_j d_{b,i,1}, a_j d_{b,i,2} : j \not\equiv i \pmod{3}\} \\
& \cup \{b_{(i-1)n+j} d_{b,i,1}, b_{(i-1)n+j} d_{b,i,2} : j \in [n], i \in [3]\} \\
& \cup \{h_i d_i : \text{all } i, \text{ such that } d_i \in V(G)\}
\end{aligned}$$

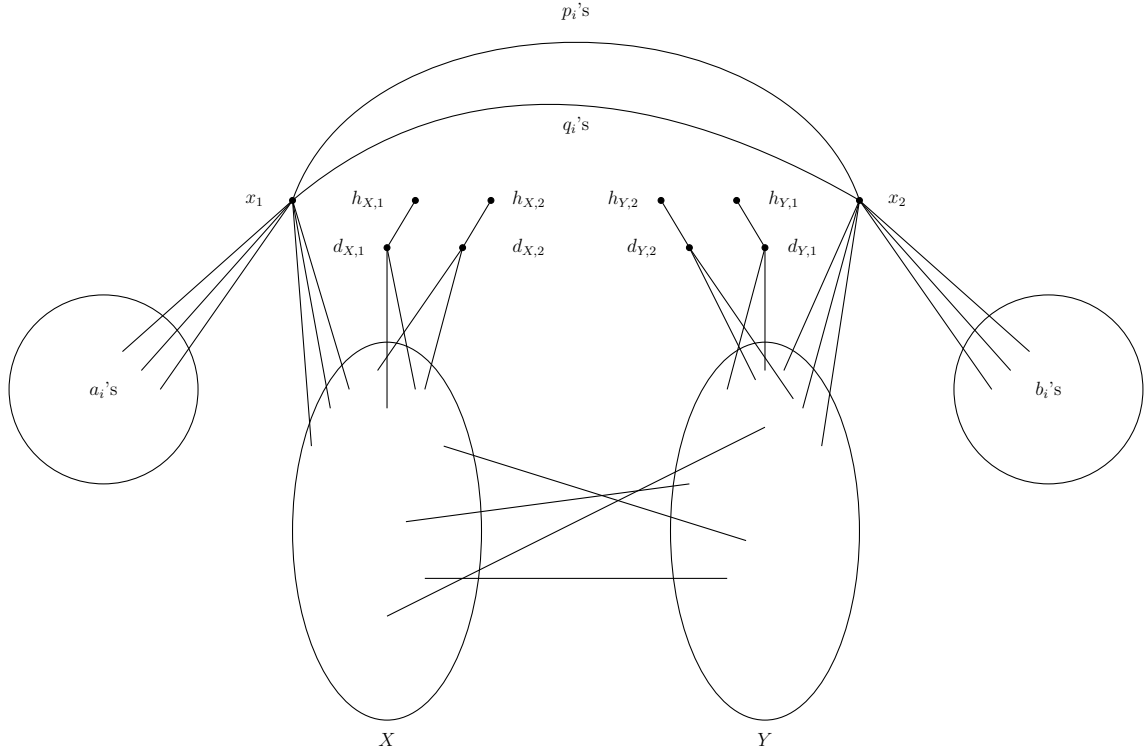


Figure 3.1: The graph G described in the proof of Theorem 6. Most of the doors and holes are omitted though all the other vertices and edges are displayed.

For an illustration of G , see Figure 3.1.

This graph G consists of three cycles, $\{a_i\}_i$, $\{b_i\}_i$ and $\{x_i, p_i, q_i\}_i$, a complete bipartite graph on the sets X and Y and a great number of *doors*, d_i 's, and *holes*, h_i 's, which are degree one vertices with their neighbours. There are two special vertices, x_1 and x_2 , in one of the cycles each of which is complete to one of the parts of the bipartite graph and to one of the cycles. Those are the only edges between non-door and hole vertices in the graph. The doors and holes restrict the freedom of the cops; if the robber manages to move to an unguarded door, he will move to the corresponding hole in the next move, isolating himself from the rest of the graph and thus winning the game.

Clearly, G has $O(n)$ vertices. We first aim to establish that $c_b(G) = 3$, starting with the lower bound.

Lemma 3.3.1. $c_b(G) \geq 3$. Moreover, if $c_b(G) = 3$, then one cop starts in $\{a_i\}_i$, one cop starts in $\{b_i\}_i$ and one cop starts in $\{x_i, p_i, q_i\}_i$.

Proof. To see that $c_b(G) \geq 3$, note that we initially need a cop next to, or on, every door. In particular, doors d_a, d_b and d_x . Since $\Gamma(d_a) = \{a_i\}_i$, $\Gamma(d_b) = \{b_i\}_i$ and $\Gamma(d_x) = \{x_i, p_i, q_i\}_i$, there is no vertex next to or on more than one of these, so we need at least three cops. \square

To see that three cops suffice to catch the robber, consider the following strategy for the cops. Start one cop on a_1 , say Alex, one on b_1 , say Blake, and one on x_1 , say Charlie. We will refer to this starting position as the *standard position*. Note that these three vertices cover all the doors. Each of the cops will stay on their respective cycles unless the robber moves onto a vertex adjacent to them, in which case they catch him.

Lemma 3.3.2. *If the cops start in the standard position, then every cop can reach any vertex in their cycle, while guarding all doors at each of the intermediate steps. Moreover, if the robber starts and remains in $X \cup Y$ and the cops start in standard position and remain in their cycles always guarding all the doors, then it takes Charlie $\Omega(n^3)$ moves to get from x_1 to x_2 and from x_2 to x_1 .*

Proof. We will show that every cop can move to a neighbouring vertex in at most $O(n^2)$ steps. Recall that each cycle has diameter $O(n)$.

We first consider Blake's moves. Blake can move freely between the vertices in $\{b_{kn+j} : j \in [n]\}$ for any fixed $k \in \{0, 1, 2\}$, as each of these vertices has the same neighbourhood outside $\{b_i\}_i$. When changing k , Blake's neighbourhood in $\{d_{b,i,j}\}_{i,j}$ changes, so in order to keep guarding all the doors, Alex must move in parallel to cover Blake's old neighbourhood. This, in turn, affects Alex's neighbourhood in $\{d_{a,i,j}\}_{i,j}$, which would then have to be compensated by Charlie. Thus, Blake can move anywhere in $\{b_i\}_i$ in $O(n)$ steps.

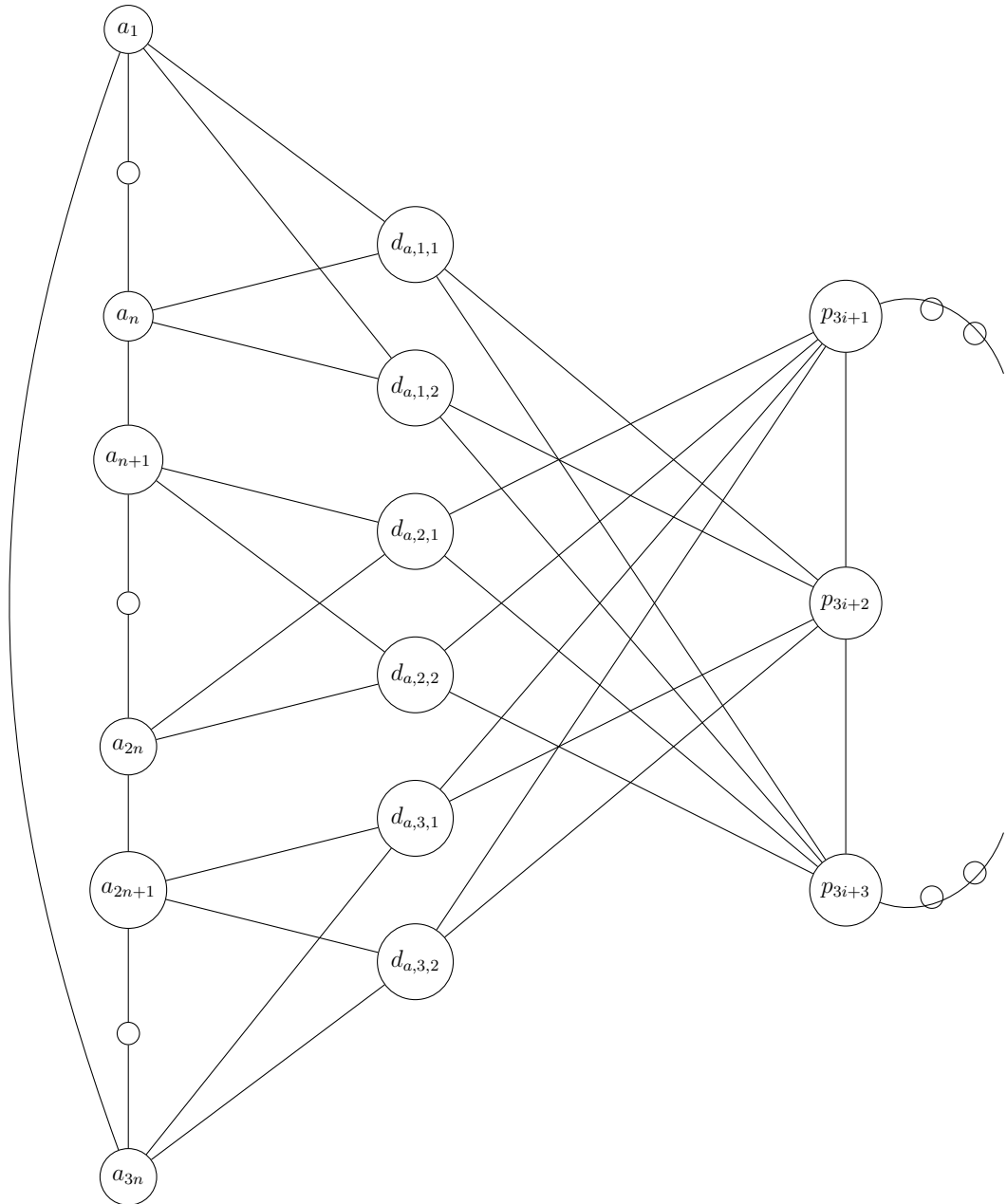


Figure 3.2: The graph described in the proof of Lemma 3.3.2. The central vertices are doors, and the other vertices form cycles $\{a_i\}_i$ and $\{p_i, q_i, x_i\}$ patrolled by Alex and Charlie respectively which watch the doors.

For Alex, the concerns are very similar. Two adjacent vertices in $\{a_i\}_i$ have different neighbourhoods in $\{d_{b,i,j}\}_{i,j}$, so for every consecutive step Alex takes, Blake has to take n steps. Hence, Alex can move anywhere in $O(n^2)$ steps. Moreover, to move to a vertex at distance $\Omega(n)$ in the cycle $\{a_i\}$ takes $\Omega(n^2)$ moves.

Finally, every move by Charlie requires $O(n)$ steps of Alex, which in turn requires $O(n^2)$ steps by Blake. Hence, Charlie can move anywhere in $O(n^3)$. Moreover, to move from x_1 to x_2 and back takes $\Omega(n^3)$ moves. □

We need to exclude the case that the robber doesn't start in $X \cup Y$.

Lemma 3.3.3. *If the cops start in the standard position and the robber starts on any vertex that is not in $X \cup Y$, then the robber is caught in $O(n^3)$ moves.*

Proof. If the robber starts on a door or hole or x_1 or x_2 , then the cops can immediately catch or corner him.

Alternatively, suppose the robber starts in one of the cycles. If the cops stay in their cycles, they can move along the cycles while guarding all the doors as shown in the previous lemmas. This implies that the robber cannot leave the cycle he starts in. It is easy to catch a robber on a cycle in $O(n)$ moves. Every step by the cop can require up to $O(n^2)$ moves by the other cops, so the cops need $O(n^3)$ moves to catch the robber. □

Now that we may assume the robber starts in $X \cup Y$, we are ready to show that Alex, Blake and Charlie will succeed in catching the robber.

Lemma 3.3.4. $c_b(G) = 3$

Proof. Lemma 3.3.1 shows we need at least three cops, so we only need provide a bound from above.

Consider the cops starting in the standard position. If the robber starts outside $X \cup Y$, then the cops can catch the robber according to Lemma 3.3.3. Hence, we

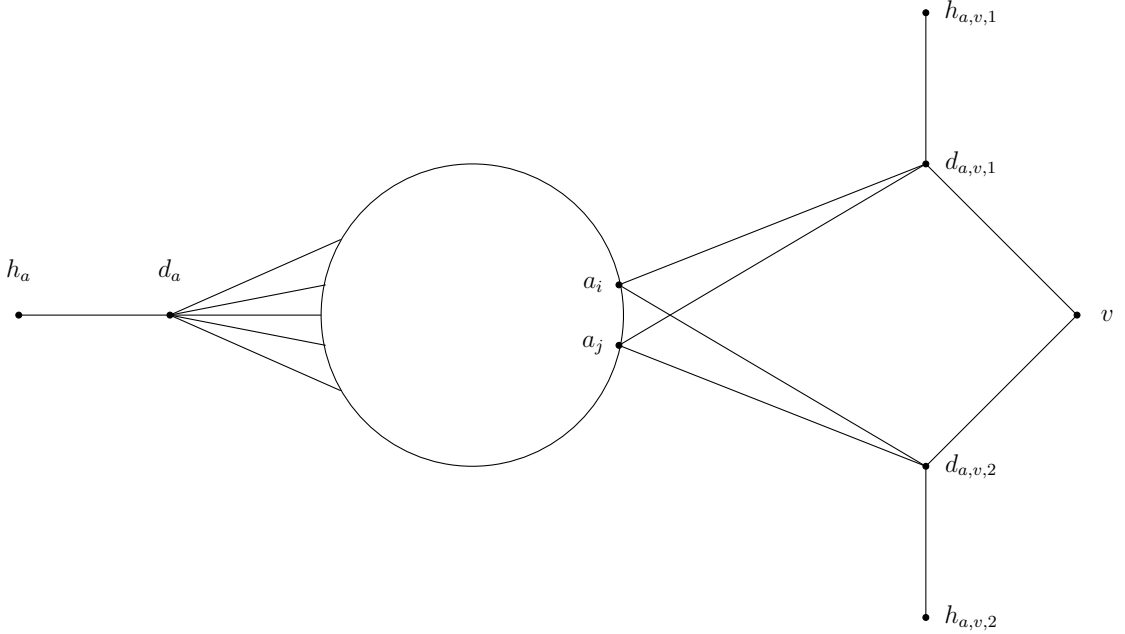


Figure 3.3: The graph described in Lemma 3.3.5, where v is a vertex in $X \cup Y$.

may assume the robber starts in $X \cup Y$.

The cops will move in such a way that all doors are guarded at all times. Moreover, Alex and Blake will stay on $\{a_i\}_i$ and $\{b_i\}_i$ respectively at all times. Hence, if at any point the robber leaves the set $X \cup Y$, either to a door or to one of x_1, x_2 , then the cops can immediately seize him. Hence, the robber has to stay inside $X \cup Y$.

Finally, to show that the cops can actually capture the robber, it suffices to show that they can force the robber to keep moving, as he can make at most $|X| \cdot |Y|$ moves staying on the vertices of $X \cup Y$. To this end, Charlie will move between x_1 and x_2 , which by Lemma 3.3.2 is possible while ensuring the cops guard all the doors at every intermediate step. As x_1 is complete to X and x_2 is complete to Y , this forces the robber to keep moving. Hence, the cops will eventually capture the robber. □

To find the lower bound on the capture time, we need to be sure that the cops do not have a better strategy.

Lemma 3.3.5. *If the cops start in the standard position and the robber starts in $X \cup Y$, then the cops need to stay on their respective cycles for as long as the robber stays in $X \cup Y$, unless they can capture the robber directly.*

Proof. For Charlie, let the robber be on $v \in X$, without loss of generality. If Charlie leaves the cycle still guarding $d_{X,1}$ and $d_{X,2}$, then Charlie must have moved into X . However, that would imply the cop was previously on x_1 , so Charlie could have caught the robber immediately. Hence, Charlie cannot leave the cycle without allowing the robber to escape.

For Alex (resp. Blake), note that if the robber is on $v \in X \cup Y$, then leaving their cycles would mean leaving either $d_{a,v,1}$ or $d_{a,v,2}$ (resp. $d_{b,v,1}$ or $d_{b,v,2}$) unguarded, providing an escape route for the robber, as seen in Figure 3.3.

□

Lemma 3.3.6. $\text{capt}_b(G) = \Omega(n^5)$

Proof. By Lemma 3.3.1, the cops must start in standard position or equivalent. The robber will follow the following strategy. He will fix a walk of length $\Omega(n^2)$ through the induced complete bipartite graph on vertex set $X \cup Y$, which he can trivially do. He will proceed to follow this walk as slowly as possible, i.e. only proceeding to the next vertex when a cop is adjacent to him.

The robber will only move through $X \cup Y$, so by Lemma 3.3.5 the cops are confined to their cycles. Only Charlie can be adjacent to $X \cup Y$ without leaving his cycle, so it is up to Charlie to walk up and down between x_1 and x_2 to force the robber to move. By Lemma 3.3.2, it thus takes the cops $\Omega(n^3)$ moves to make the robber move once. Hence, the robber manages to stay out of the cops hands for $\Omega(n^5)$ moves. □

The construction slowing down Charlie can be extended in a natural way to higher cop numbers. Consider the following construction for cop number k . For $k \geq 3$, let

G_k be the graph constructed as follows.

$$\begin{aligned}
V(G_k) &= V(G) \cup \{u_i^j : i \in [3n], j \in [k-3]\} \cup \{d_{u^j}, h_{u^j} : j \in [k-3]\} \\
&\quad \cup \{d_{u^j, i, l}, h_{u^j, i, l} : i \in [3], l \in [2], j \in [k-3]\} \\
E(G_k) &= E(G) \cup \{u_i^j u_{i+1}^j : i \in [3n], j \in [k-3]\} \\
&\quad \cup \{u_i^j d_{u^j} : i \in [3n], j \in [k-3]\} \\
&\quad \cup \{v d_{u^j, i, l} : v \in X \cup Y, i \in [3], l \in [2], j \in [k-3]\} \\
&\quad \cup \{u_l^{j-1} d_{u^j, i, k} : l \not\equiv i \pmod{3}, k \in [2], j \in [k-3]\} \\
&\quad \cup \{u_{(i-1)n+l}^j d_{u^j, i, k} : l \in [n], i \in [3], k \in [2], j \in [k-3]\}
\end{aligned}$$

where $u_i^0 = b_i$. The $\{u_i^j\}_i$ form cycles, which are similar to cycles $\{a_i\}_i$ and $\{b_i\}_i$.

The doors $\{d_{u^j, i, l}\}_{i, l}$ are connected to respective cycles in the same fashion $\{a_i\}_i$ and $\{b_i\}_i$ are connected to the doors $\{d_{b, i, l}\}_{i, l}$.

Proposition 11. $c_b(G_k) = k$ and $\text{capt}_b(G_k) \geq Cv(G_k)^{k+2} k^{-(k+2)}$ for some universal constant C .

Sketch of proof. As in Lemma 3.3.1, each of the doors d_x, d_a, d_b and d_{u^j} (with $j \in [k-3]$) must be guarded initially, so $c_b(G_k) \geq k$. Moreover, if $c_b(G_k) = k$, then one cop must start in each of the cycles; $\{p_i, q_i, x_i\}_i, \{a_i\}_i, \{b_i\}_i = \{u_i^0\}_i$ and $\{u_i^j\}_i$ for $j \in [k-3]$. As in lemma 3.3.3, if the robber starts in one of the cycles, he will be captured quickly. If the robber starts in the bipartite graph $X \cup Y$, the cops can prevent him from leaving it. Moreover, by Charlie moving between x_1 and x_2 the robber can be forced to use up all the edges between X and Y and thus be forced out of the bipartite graph, leading to his immediate capture. Hence, $c_b(G_k) \leq k$.

The robber will follow the same strategy as before; assuming for convenience that n is even, he plans an Eulerian walk through complete bipartite graph $X \cup Y$ and only proceeds with the walk when Charlie is directly adjacent to him. Note that this

walk has length $(3n)^2$. As in Lemma 3.3.5, the cops are restricted to their cycles as long as the robber stays in $X \cup Y$. As in Lemma 3.3.2, for Charlie to move once from x_1 to x_2 and back, the cops must make $2(3n)^k + o(n)$ moves. Thus, the robber can avoid the cops for at least $(3n)^{k+2}$ rounds.

Note that the graph has $(k+2)3n + 18k$ vertices. Hence,

$$\begin{aligned} \text{capt}_b(G_k) &\geq (3n)^{k+2} \\ &= \left(\frac{v(G_k) - 18k}{k+2} \right)^{k+2} \\ &\geq \left(\frac{v(G_k)}{k} \right)^{k+2} \left(\frac{1 - \frac{6}{n}}{1 + 2/k} \right)^{k+2} \\ &\geq C \left(\frac{v(G_k)}{k} \right)^{k+2} \end{aligned}$$

for some constant C . □

This completes the sketch of the proof of Theorem 6.

3.4 Appendix

By Lemma 7, it suffices to show that whp $G \in \mathcal{G}(n, p)$ contains a dominating clique.

We shall abbreviate $\log_{\frac{1}{1-p}}(x)$ to $\log(x)$.

Lemma 12. *Let $G \in \mathcal{G}(n, p)$ with $p \in (0, 1]$ constant, then with high probability, $\exists X \subset V(G)$ such that $G[X]$ is a complete graph and $X \cup \Gamma(X) = V(G)$.*

Proof. We use a second moment argument to show the result. Fix some small $\epsilon \in (0, \frac{1}{2})$ and let $k = (1 + \epsilon) \log(n)$.

Let S be the number of sets $X \subset V(G)$ such that $|X| = k$, X induces a clique and $X \cup \Gamma(X) = V(G)$. Note that the events that X is a clique and that

$X \cup \Gamma(X) = V(G)$ are dependent on disjoint edges.

$$\mathbb{E}[S] = \binom{n}{k} p^{\binom{k}{2}} (1 - (1-p)^k)^{n-k}$$

To compute the second moment of S , let A and B be two k -sets of vertices. We will use the law of total expectation to condition on the size of $A \cap B$. Note that the probability that A and B both satisfy the conditions is at most the probability that they are both independent sets.

$$\begin{aligned} \mathbb{E}[S^2] &\leq \sum_{i=0}^k \binom{n}{k-i, i, k-i} p^{2\binom{k}{2} - \binom{i}{2}} \\ &\leq \left(\binom{n}{k} p^{\binom{k}{2}} \right)^2 \left[1 + \sum_{i=1}^k \frac{\binom{n}{k-i, i, k-i}}{\binom{n}{k}^2} p^{-\binom{i}{2}} \right] \end{aligned}$$

Each of these last terms is bounded as:

$$\frac{\binom{n}{k-i, i, k-i}}{\binom{n}{k}^2} p^{-\binom{i}{2}} \leq \frac{k^{2i} p^{-\binom{i}{2}}}{n^i},$$

so for the entire sum we find

$$\sum_{i=1}^k \frac{\binom{n}{k-i, i, k-i}}{\binom{n}{k}^2} p^{-\binom{i}{2}} \leq \max_{i \in [k]} \left\{ \frac{k^{2i+1} p^{-\binom{i}{2}}}{n^i} \right\} = o(1),$$

and thus

$$\mathbb{E}[S^2] \leq \left(\binom{n}{k} p^{\binom{k}{2}} \right)^2 (1 + o(1)).$$

Now we find by Chebyshev's inequality:

$$\mathbb{P}(S > 0) \geq \frac{\left[\binom{n}{k} p^{\binom{k}{2}} (1 - (1-p)^k)^{n-k} \right]^2}{\left(\binom{n}{k} p^{\binom{k}{2}} \right)^2 (1 + o(1))} \rightarrow 1$$

Hence, the probability that there is a dominating clique tends to one.

□

CHAPTER 4

UNIFORM BOUNDS FOR NON-NEGATIVITY OF THE DIFFUSION GAME

4.1 Introduction

In 1986, J. Spencer [56] proposed the following solitaire game. Let N chips be arranged in a pile. At each time step, $\lfloor \frac{N}{2} \rfloor$ chips are moved one unit to the right of the pile, and $\lfloor \frac{N}{2} \rfloor$ chips are moved one unit to the left, with one chip remaining in the original pile if N is odd. In subsequent steps, we repeat this process simultaneously on each of the resulting piles.

This solitaire game inspired the chip-firing game, introduced by Björner, Lovász and Shor [8]. The chip-firing game is played on a simple, connected graph G on the vertex set $[n] = \{1, 2, \dots, n\}$. In the game, each vertex $v \in [n]$ is assigned an amount of chips, w_v . The vertex v is allowed to fire if $w_v \geq d_v$, where d_v denotes the degree of vertex v . When vertex v is fired, we remove d_v chips from it, and add one chip to each neighboring vertex. Only one vertex may be fired at a time, but Björner et al. found that the order of firings does not affect the length of the game. The game ends when all vertices have fewer chips than neighbors. The chip-firing game has several applications in computer science, mathematics, and physics [7, 35, 37, 39].

The diffusion game was first introduced by Duffy, Lidbetter, Messinger and Nowakowski [28] and is a variant of the chip-firing game. In the diffusion game, let G be a graph on the vertex set $[n]$. At time $t = 0$ each vertex $v \in [n]$ is assigned an initial integer label $w_v(0)$. We then update all labels at discrete integer time steps according to the rule

$$w_v(t+1) = w_v(t) + |u \in \Gamma(v) : w_u(t) > w_v(t)| - |u \in \Gamma(v) : w_u(t) < w_v(t)|.$$

Intuitively, this corresponds to moving one chip along each edge whose vertices have differing numbers of chips, with the vertex with more chips giving a chip to the vertex with fewer.

For each $t \geq 0$, let $w_G(t)$ denote the vector $(w_1(t), w_2(t), \dots, w_n(t))$. We say that $w_G(t) \geq k$ if $w_v(t) \geq k \forall v \in [n]$, and similarly for $w_G(t) \leq k$.

Long and Narayanan [47] proved that the diffusion game is eventually periodic with period one or two. That is, there exists $T \in \mathbb{N}$ and $k \in \{1, 2\}$ such that for all $t \geq T$, $w_G(t) = w_G(t + k)$.

Our main result answers one of the questions posed by Long and Narayanan in their paper:

Theorem 4.1.1. *Let $n \geq 2$. If $w_G(0) \geq f(n) = n - 2$, then at all times $t \geq 0$ we have $w_G(t) \geq 0$.*

Indeed, this is the best possible such result, as for each $n \geq 2$, the star on n vertices with $n - 3$ chips on each leaf and $n - 2$ chips on the central vertex will, after one time step, have -1 chips on the central vertex.

We also consider similar bounds based upon the maximum degree d of the graph.

We show the following:

Theorem 4.1.2. *Let $g(d)$ be the least possible bound on the minimum number of chips on a vertex such that non-negativity of the labels is guaranteed.*

- i If $d \leq 1$, then $g(d) = 0$*
- ii If $d = 2$, then $g(d) = 1$*
- iii If $d = 3$, then $g(d) \geq 3$*
- iv If $d \geq 4$, then $g(d) = \infty$*

For $d = 3$, we know only that $g(3) \geq 3$; it may be that this inequality is tight.

4.2 Order-based Bounds

We will proceed by defining the *weak diffusion game*, a more general, non-deterministic variant of the original diffusion game. We then reduce the problem to considering a specific initial state, and show that subsequent states can be represented by a digraph encoding, which need not be unique.

The following weaker result can be obtained by a conceptually simpler version of our main proof. This version differs from the one presented in two ways: the digraph encoding used does not require edge weights, and we need only reduce to the initial state $(n-1, n-1, \dots, n-1)$. One may wish to consider this variation as a stepping stone to understanding the full proof of Theorem 4.1.1.

Theorem 4.2.1. *Let G be a graph with n vertices. If $w_G(0) \geq n-1$, then at all times $t \geq 0$ we have $w_G(t) \geq 0$.*

4.2.1 The Weak Diffusion Game

We begin by making two modifications to the diffusion process.

First, rather than transferring chips along edges of a predetermined constant graph, we instead may choose at each time step whether or not to allow a chip to transfer between each pair of vertices. That is, at each time step, for each pair of vertices u and v with $w_u(t) > w_v(t)$, we are allowed to choose whether or not a chip is transferred from vertex u to vertex v (with these transfers being the only transfers allowed). So the original diffusion process is now one of many possible evolutions of the labels w_G .

Second, we permit also the transfer of chips between vertices having equal numbers of chips.

These modifications give us a process we shall call the *weak diffusion game*. We can represent our choices of when to move chips by the values $d_{uv}(t)$ ($u, v \in [n]$, $u \neq v$,

$t \in \mathbb{N}$), which satisfy:

$$\begin{aligned} d_{uv}(t) &\in \{-1, 0, 1\} \\ d_{uv}(t) &= -d_{vu}(t) \\ d_{uv}(t)(w_u(t-1) - w_v(t-1)) &\geq 0 \end{aligned}$$

The labels then evolve according to:

$$w_v(t) = w_v(t-1) + \sum_{u \neq v} d_{uv}(t)$$

We can now state the following theorem

Theorem 4.2.2. *Let G be a graph with n vertices. Suppose that w_G is a possible evolution of the weak diffusion game. Then, given any initial state $w'_G(0) \leq w_G(0)$, there exists an evolution of the weak diffusion game w'_G with this initial state, and a sequence of permutations P_t , such that for each $t \geq 0$ and $u \in [n]$, we have $w'_{P_t(u)}(t) \leq w_u(t)$. That is, if we remove some chips from the initial state of some evolution then, up to a permutation of the vertex labels at each time step, we can then remove chips from later states to obtain another valid evolution without ever needing to add chips to a vertex.*

Proof. It will suffice to prove this for a removal of one chip from the initial state; the full result then follows by induction on the number of chips removed.

Furthermore, it will suffice to show this for one time step; the result will then follow by induction on t .

Without loss of generality, we may assume that the graph of the weak diffusion game represented by $d_{uv}(1)$ is acyclic (since transfers forming a cycle have no net effect on the distribution of chips). We may then assume that the vertices are labeled such that if $1 \leq u < v \leq n$, then $w_u(0) \geq w_v(0)$ and $d_{uv}(1) \neq -1$. Now

suppose $w'_G(0)$ is obtained from $w_G(0)$ by removing one chip from vertex k . Let $k' = \max\{i \in [n] | w_i(0) = w_k(0)\}$, set the permutation $P_1 = P = (kk')$, and set $d'_{P(u)P(v)}(1) = d_{uv}(1)$. Applying the transfers represented by $d'(1)$ gives us $w'_G(1)$ satisfying $w'_{P_1(u)}(1) \leq w_u(1)$, as required. \square

4.2.2 Proof of Theorem 4.1.1

We begin by providing a link between bounds in the weak diffusion game and bounds in the original diffusion game, reducing the problem to establishing non-negativity of the weak diffusion game with specific initial conditions. We then produce an encoding of the game in a sequence of weighted directed graphs, leading to non-negativity as an immediate consequence.

Lemma 4.2.3. *Let G be a graph with n vertices, let $k \geq 0$ and let w_G be an evolution of the original diffusion process with $w_G(0) \geq k$. Suppose that, for some $t \geq 0$, we have $w_G(t) \not\geq 0$. Then there exists an evolution w'_G of the weak diffusion game with $w'_G(0) = (k + 1, k, k, \dots, k)$ up to relabeling, and $w'_G(t) \not\geq 0$.*

Proof. Note that w_G is automatically a valid evolution of the weak diffusion game. Furthermore, we cannot have $w_v(0) = k \forall v$, as otherwise w_G would be constant, contradicting $w_u(t) < 0$. The lemma then follows from Theorem 4.2.2 with an initial relabeling of the vertices. \square

It now suffices to show that the weak diffusion game with initial state $w_G(0) = (n - 1, n - 2, \dots, n - 2)$ must remain non-negative.

Definition 4.2.4. *Let G be an n -vertex graph, and let w_G be an evolution of the weak diffusion game on G with mean label $\mu = \sum_v w_v(0)/n$. A digraph encoding of a state $w_G(t)$ is a weighted directed graph with edge weights $\lambda_{uv}(t)$ for each*

$u, v \in [n]$, satisfying:

$$\lambda_{uv}(t) \in [-1, 1] \cap \mathbb{Z}/n$$

$$\lambda_{uv}(t) = -\lambda_{vu}(t)$$

$$w_v(t) = \mu + \sum_u \lambda_{uv}(t)$$

Some digraph encodings lead more naturally to a representation of the subsequent state. This property is captured in the following definition:

Definition 4.2.5. *Let w_G be as above. We say that an encoding of the state $w_G(t)$ is good if $\lambda_{uv}(t) \leq 0$ whenever $w_u(t) \geq w_v(t)$. Otherwise, we say that the encoding is bad.*

Note that the existence of a digraph encoding for a state $w_G(t)$ bounds the number of chips on each vertex between $\mu - (n - 1)$ and $\mu + (n - 1)$. We aim to show that a digraph encoding exists for every state of our evolution w_G . The following lemma will facilitate this:

Lemma 4.2.6. *Let w_G be as above. If $w_G(t)$ has a digraph encoding, then it has a good digraph encoding.*

Proof. Of the many possible digraph encodings for $w_G(t)$, consider an encoding of least absolute sum—that is, an encoding $\lambda_{uv}(t)$ in which $\sum_{u < v} |\lambda_{uv}(t)|$ is minimized. We show that this is necessarily a good encoding.

For a contradiction, suppose instead that this encoding is bad. Then there exist u, v such that $w_u(t) \geq w_v(t)$, but $\lambda_{uv}(t) > 0$. We then have:

$$\begin{aligned} \sum_{w \neq u, v} (\lambda_{wu}(t) - \lambda_{wv}(t)) + \lambda_{vu}(t) - \lambda_{uv}(t) &= w_u(t) - w_v(t) \\ \sum_{w \neq u, v} (\lambda_{wu}(t) - \lambda_{wv}(t)) &> 0 \end{aligned}$$

So there exists w such that:

$$\lambda_{wu}(t) - \lambda_{wv}(t) > 0$$

Now let $a = \lambda_{uv}(t)$, $b = \lambda_{vw}(t)$ and $c = \lambda_{wu}(t)$. We have that $a > 0$ and $b + c > 0$. Note that we can add a constant k to each of these terms without affecting the encoded vertex labels. Since this was an encoding that minimized the absolute sum, we have that $|a + k| + |b + k| + |c + k|$ is minimized at $k = 0$ (subject to $a + k, b + k, c + k \in [-1, 1]$). Since at least two out of a , b and c are positive, and none of them are equal to -1 , it is clear that taking $k = -1/n$ reduces the sum of the absolute values without breaking any of the constraints. Thus there is a digraph encoding with smaller absolute sum, contradicting the minimality of the original encoding.

It follows that the original encoding was good, as desired. \square

We can now show the existence of encodings at all time steps:

Lemma 4.2.7. *Let w_G be as above. Whenever $w_G(t)$ has a digraph encoding, then $w_G(t + 1)$ has a digraph encoding.*

Proof. By the previous lemma, we may take a good encoding $\lambda_{uv}(t)$ of $w_G(t)$. Then $\lambda_{uv}(t + 1) = \lambda_{uv}(t) + d_{uv}(t + 1)$ gives an encoding of $w_G(t + 1)$. In particular, $\lambda_{uv}(t + 1) \in [-1, 1]$, since $d_{uv}(t + 1) > 0$ implies $w_u(t) \geq w_v(t)$, which in turn implies $\lambda_{uv}(t) \leq 0$. \square

Corollary 4.2.8. *Whenever $w_G(0)$ has a digraph encoding, then $w_G(t)$ has a digraph encoding for all $t \geq 0$.* \square

We can now complete our proof of Theorem 4.1.1. First, observe that

$w_G(0) = (n - 1, n - 2, \dots, n - 2)$ has a digraph encoding where $\mu = n - 2 + (1/n)$, $\lambda_{u,1}(0) = 1/n$ and $\lambda_{uv}(0) = 0$ for $u, v \neq 1$. Thus by Corollary 4.2.8, $w_G(t)$ has a

digraph encoding for all $t \geq 0$.

This means that for any v, t , we have

$$w_v(t) = \mu - \sum_{u \neq v} \lambda_{uv}(t) \geq \mu - (n - 1) = -1 + (1/n)$$

Since $w_v(t)$ is an integer, this implies $w_v(t) \geq 0$, as required. \square

4.2.3 Remarks

The proof of Theorem 4.1.1 applies also to directed graphs and to graphs which vary over time. We can further extend it to multigraphs; in this case, if m is the maximum number of edges between two vertices, and our initial state has at least $m(d - 1) - 1$ chips on each vertex, then no vertex ever attains a negative number of chips.

The idea of digraph encodings can also be used to give an alternative proof of Long and Narayanan's result that the diffusion game is eventually periodic (although this method does not bound the eventual period as strongly). Indeed, we extend the definition of a digraph encoding to allow edge weights to take any value in \mathbb{R} . Then we encode a state using the digraph whose edge-weight sequence, ordered from largest to smallest, is lexicographically smallest. These edge-weight sequences form a sequence over time, which is decreasing (in the above order) until all the weights have magnitude less than 1. This happens in finite time since every edge weight is in \mathbb{Z}/k for some $k = k(n)$, after which an ordinary digraph encoding exists for every state.

4.3 Bounds using the Maximum Degree

We now prove the bounds given in Theorem 4.1.2. Note that we may restrict our attention to infinite d -regular trees. Indeed, for any graph G with maximum degree

d , take a disjoint union of two copies of G , and add edges between corresponding vertices in the two copies to make the graph d -regular. Then consider the universal cover H of G – this is the d -regular infinite tree. We may assign labels to H according to the labels of the corresponding vertices of G ; these labels evolve in the same manner as the corresponding labels on G . Conversely, if any vertex v of a d -regular tree can attain a negative label in finite time T , then this will be achieved also with the same initial conditions restricted to the finite graph consisting of all vertices at distance at most T from v .

Proof of Theorem 4.1.2 1. *We consider each case in turn:*

i $d \leq 1$

The graph G is either a point or a single edge; in either case the result is trivial.

ii $d = 2$

First, note that $g(2) > 0$, as a path on three vertices starting with a single chip on the central vertex attains a negative chip value on the second diffusion step.

Next, consider diffusion on the infinite path with vertex set $V = \mathbb{Z}$, and assume that all labels are initially at least 1. Suppose for contradiction that some label subsequently becomes negative, and let T_0 be the earliest time at which any vertex has a negative label. We will use the following lemma:

Lemma 4.3.1. *Before time T_0 , no vertex can have label 0 on two consecutive time steps.*

Proof. Suppose for a contradiction that $w_v(T-1) = w_v(T) = 0$ for some $v \in V$ and $0 < T < T_0$. Take the least such T .

Then $T > 1$ since $w_v(0) > 0 \forall v$, and $w_{v-1}(T-1), w_{v+1}(T-1) \geq 0$, as $T-1 < T_0$.

It follows that $w_{v-1}(T-1) = w_{v+1}(T-1) = 0$, else the diffusion process would yield $w_v(T) > 0$.

Finally, $w_v(T - 2) = 0$, otherwise $w_{v-1}(T - 1)$, $w_v(T - 1)$ and $w_{v+1}(T - 1)$ could not all be 0.

This contradicts the minimality of T , yielding the desired result. \square

Now let T_1 be the least time such that there exists a vertex v_1 with:

$$(w_{v_1-1}(T_1), w_{v_1}(T_1), w_{v_1+1}(T_1)) = (0, 1, 1) \text{ or } (1, 1, 0)$$

If the patterns $(0, 1, 1)$ and $(1, 1, 0)$ do not exist, then we say that $T_1 = \infty$. We have the following lemma about the labels that precede a zero:

Lemma 4.3.2. *Let $T \leq T_0, T_1$, and $w_v(T) = 0$. Then $w_v(T - 1) = 2$.*

Proof. By the definition of T_0 , we have $w_v(T - 1) \geq 0$. Lemma 4.3.1 tells us that $w_v(T - 1) \neq 0$. We also have $w_v(T - 1) \neq 1$, else, by the definition of T_0 , we would need $w_{v-1}(T - 1)$ and $w_{v+1}(T - 1)$ to equal 0 and 1 in some order, contradicting the definition of T_1 . Since w_v can change by at most 2 at each step of the diffusion process, it follows that $w_v(T - 1) = 2$. \square

We now show that the pattern $(0, 1, 1)$ or $(1, 1, 0)$ exists before time T_0 .

Lemma 4.3.3. $T_1 < T_0$.

Proof. Suppose for a contradiction that the pattern $(0, 1, 1)$ or $(1, 1, 0)$ does not exist before time T_0 . We work backwards from time T_0 . By the definition of T_0 and v_0 , it follows that $w_{v_0-1}(T_0 - 1) = w_{v_0+1}(T_0 - 1) = 0$ and $w_{v_0}(T_0 - 1) = 1$.

Now consider time $T_0 - 2$. By Lemma 4.3.2, we have that

$w_{v_0-1}(T_0 - 2) = w_{v_0+1}(T_0 - 2) = 2$. But then the diffusion process cannot attain $w_{v_0}(T_1) = 1$.

Hence the pattern $(0, 1, 1)$ or $(1, 1, 0)$ does exist before time T_0 . \square

We shall finish by working backwards from time T_1 until we reach another

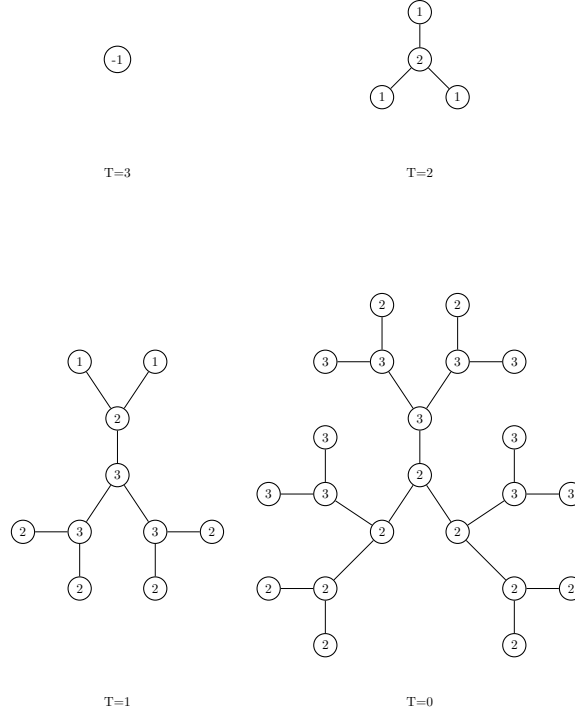


Figure 4.1: An example of an infinite 3 regular tree. This figure shows $d(3) \geq 3$.

contradiction. We assume that $(w_{v_1-1}(T_1), w_{v_1}(T_1), w_{v_1+1}(T_1)) = (0, 1, 1)$. Then by Lemma 4.3.2 we have that $w_{v_1-1}(T_1 - 1) = 2$. In order that the diffusion process gives us the stated values at time T_1 , we require that

$(w_{v_1}(T_1 - 1), w_{v_1+1}(T_1 - 1), w_{v_1+2}(T_1 - 1)) = (1, 0, 0)$ or $(0, 0, w)$, for some

$w \in \mathbb{N}$. In either case we have two adjacent 0's, which by Lemma 4.3.2 must each be preceded by a 2. However, adjacent 2's cannot become adjacent 0's under one step of the diffusion process.

Having derived a contradiction from our original assumption, we conclude that no vertex label can ever become negative.

iii $d = 3$

Figure 4.1 demonstrates that $f(3) \geq 3$. Note that the initial state uses only two different labels: 2 and 3.

iv $d = 4$

Consider the infinite d -regular tree, and fix some vertex v_0 . We assign labels to

each vertex according to its distance from v_0 ; in particular, at time t , we assign the label $w_i(t)$ to all vertices at distance i from v_0 .

Working backwards from a time T at which $w_i(T) = -1$, we can construct the following evolution:

t	T	$T - 1$	$T - 2$	\dots	0
$w_0(t)$	-1	$d - 1$	$2d - 1$	\dots	$Td - 1$
$w_1(t)$		$d - 2$	$2d - 4$	\dots	$Td - 2T$
$w_2(t)$			$2d - 5$	\dots	$Td - 2T - 1$
\vdots				\ddots	\vdots
$w_T(t)$					$Td - 3T + 1$

Thus $g(d) > Td - 3T + 1$ for all $T > 0$, so $g(d) = \infty$, as required.

4.4 Concluding Remarks

Our results on maximum degree bounds are incomplete; specifically, we leave the following unanswered:

Question 4.4.1. *What is $g(3)$? In particular, is it finite?*

More generally, when $g(d)$ was found to be infinite, we needed to use arbitrarily large ranges of initial labels in order to attain negative labels for a given minimum initial label.

This raises the following question, originally asked by Long and Narayanan in the equivalent context of infinite graphs of bounded degree:

Question 4.4.2. *Does there exist $g(d, k) < \infty$ such that for any graph G of maximum degree d , if the vertices of G are given initial labels in $[g(d, k), g(d, k) + k]$, then all vertex labels in this diffusion game remain non-negative?*

CHAPTER 5

ETERNAL GAME CHROMATIC NUMBER

5.1 Introduction

The *vertex colouring game* was introduced by Brams [34] in 1981; it was later rediscovered by Bodlaender [10]. In this game, two players, Alice and Bob, take turns choosing uncoloured vertices from a graph, G , and assigning a colour from a predefined set $\{1, \dots, k\}$, such that the resulting partial colouring of G is proper. Bob wins, if at some stage, he or Alice chooses a vertex that cannot be properly coloured. Alice wins if each chosen vertex can be properly coloured. The game chromatic number $\chi_g(G)$ is the smallest integer k such that if there are k colours, Alice has a winning strategy in the vertex colouring game. This number is well defined, as Alice can win if the number of colours is at least the number of vertices. The vertex colouring game has been well studied [25, 29, 36, 62]. In particular, Bohman, Frieze and Sudakov [11] studied the game chromatic number of random graphs $G_{n,p}$ and found that with high probability, $(1 - \epsilon) \frac{n}{\log(pn)} \leq \chi_g(G_{n,p}) \leq (2 + \epsilon) \frac{n}{\log(pn)}$, where all logarithms have base $\frac{1}{1-p}$. Keusch and Steger [43] improved the result to $\chi_g(G_{n,p}) = (1 + o(1)) \frac{n}{\log(pn)}$ with high probability, implying $\chi_g(G_{n,p}) = (2 + o(1)) \chi(G_{n,p})$ with high probability by a classic result of Bollobás [12]. Both of the results require lower bounds on p decaying with n slowly. Frieze, Haber and Lavrov [31] studied the game on sparse random graphs, finding that for $p = d/n$, $\chi(G_{n,p}) = \Theta(\frac{d}{\ln(d)})$, where $d \leq n^{-1/4}$ is at least a large constant.

This vertex colouring game requires Alice and Bob to colour the vertices once, attaching no value to the colouring that is produced at the end of the round. In a variant of the game called the *eternal vertex colouring game* recently introduced by Klostermeyer and Mendoza [45], the focus is shifted by continuing the game after a

colouring is produced.

In the eternal vertex colouring game, there is a fixed set of colours $\{1, \dots, k\}$. The game consists of rounds, such that in each round, every vertex is coloured exactly once. The first round proceeds precisely the same as the vertex colouring game, with Alice taking the first turn. During all further rounds, players keep choosing vertices alternately. After choosing a vertex, the player assigns a colour to the vertex which is distinct from its current colour such that the resulting colouring is proper. Each vertex retains its colour between rounds until it is recoloured. Bob wins if at any point the chosen vertex does not have a legal recolouring, while Alice wins if the game is continued indefinitely. The eternal game chromatic number $\chi_g^\infty(G)$ is the smallest number k such that Alice has a winning strategy. Note that if $k \geq \Delta(G) + 2$, there will always be a colour available for every vertex, so $\chi_g^\infty(G)$ is well-defined.

As Alice and Bob alternate their turns, the parity of the order of the graph determines whose turn it is at the beginning of the second round. For even order, Alice always has the first move, while for odd order Bob gets to play first in all even rounds.

This game has not been well studied, but Klostermeyer and Mendoza [45] obtained some basic results pertaining to paths, cycles, and balanced bipartite graphs.

In this paper, we determine $\chi_g^\infty(G_{n,p})$ for n odd by putting together the following two results.

Theorem 13. *For all $p \in (0, 1)$ constant, for odd n , with high probability,*

$$\chi_g^\infty(G_{n,p}) = (1 + o(1)) \frac{pn}{2}.$$

Theorem 14. For all $p \in (0, 1)$ constant, for even n , with high probability,

$$\chi_g^\infty(G_{n,p}) \leq (1 + o(1)) \frac{pn}{2}.$$

Moreover, when $p = \frac{1}{l}$ for some $l \in \mathbb{N}$,

$$\chi_g^\infty(G_{n,p}) = (1 + o(1)) \frac{pn}{2}.$$

The difference in the even and odd cases is because when n is odd, Bob moves first in the second round. Also, note that we made no efforts to optimize $o(n)$ terms. For the unresolved case when n is even and $p \notin \{\frac{1}{2}, \frac{1}{3}, \dots\}$, we conjecture the following.

Conjecture 5.1.1. $\forall p \in (0, 1) \setminus \{\frac{1}{2}, \frac{1}{3}, \dots\}, \exists \epsilon > 0$ such that with high probability,

$$\chi_g^\infty(G_{n,p}) \leq (1 - \epsilon) \frac{pn}{2}.$$

The structure of the paper is as follows. In Section 5.2, we prove the upper bound for $\chi_g^\infty(G_{n,p})$. In this proof, we make no distinction between odd and even values of n . In Section 5.3, we prove the corresponding lower bound for odd n . In Section 5.4, we prove a generalization of the result in Section 5.3, which we then use in Section 5.5 to get the lower bound for the case $p = 1/l$ for some $l \in \mathbb{N}$. Along the way, we use various structural results about the random graph $G_{n,p}$. As the proofs of these are usually quite easy but technical, we collect all of them in Section 5.7. Finally in Section 5.6, we provide answer to one of the questions posed in the paper of Klostermeyer and Mendoza.

Throughout the paper we will use the following conventions. We say that a result holds in $G_{n,p}$ with high probability (*whp*) if the probability that it holds tends to 1 as $n \rightarrow \infty$. The neighbourhood of a vertex v in a graph, G , denoted $\Gamma(v)$, will be

the vertices of G that v is connected to, as well as v itself. The partition of a set X will refer to a collection of disjoint non-empty subsets whose union is X .

5.2 Upper bound

In this section, we show the following proposition.

Proposition 15. *For any fixed $p, \epsilon \in (0, 1)$, whp $\chi_g^\infty(G_{n,p}) \leq (\frac{p}{2} + \epsilon)n$.*

To prove this, we formulate a deterministic strategy for Alice and prove that whp this strategy enables her to prevent Bob from winning when the game is played with $(\frac{p}{2} + \epsilon)n$ colours.

The biggest danger facing Alice is that at the end of some round, Bob would manage to introduce all the colours in the neighbourhood of at least one vertex. He could then win by choosing one of those vertices at the beginning of the next round. Thus, her strategy should be to ensure that at any point of each round, she has coloured roughly as many vertices in the neighbourhood of any single vertex as Bob has, and she should use few colours on them. If, at some point during a round, a vertex has many colours in its neighbourhood compared to other vertices, Alice might be forced to colour it so Bob cannot win by choosing it later that same round. Fortunately for Alice, the number of times she is forced to colour a vertex with many different coloured neighbours is so few that she can still follow her strategy.

Consider the following four properties of a graph $G_{n,p}$.

1. Every vertex of $G_{n,p}$ has degree at most $(p + \frac{\epsilon}{100})n$
2. There exists a constant $K = K(\epsilon, p)$ such that $G_{n,p}$ does not contain sets $A, B, S \subset V(G)$, with $|A \cap B| = 0$, $|A| = |B| \geq \frac{\epsilon}{200}n$, $|S| = K$, such that every $v \in S$ is connected to at least $\frac{\epsilon}{200}n$ more vertices in B than in A .
3. There exist constants $\beta = \beta(\epsilon, p)$, $\frac{\epsilon}{100} > \beta > 0$ and $C = C(\epsilon, p)$ such that the following holds: for any colouring of $G_{n,p}$ by $(\frac{p}{2} + \epsilon)n$ colours, the number of

vertices that have all but at most $2\beta n$ colours in their neighbourhood is at most $C \log n$.

4. There exist constants $\gamma = \gamma(\epsilon, p) > 0$ and $D = D(\epsilon, p)$ such that, in any colouring of $G_{n,p}$ by $(\frac{p}{2} + \epsilon)n$ colours, the number of vertices that have all but at most γn of the colours $1, 2, \dots, \frac{\epsilon}{200}n$ in their neighbourhood is at most $D \log n$.

We prove in the appendix that each of these holds whp in $G_{n,p}$. For the remainder of this paragraph, we will assume 1 through 4 hold for the graph $G_{n,p}$. Note that as we are assuming finitely many properties, each of which holds whp, then whp all of them hold simultaneously.

For a particular round of the game, let A_i and B_i denote the sets of vertices played by Alice and Bob respectively in the first i moves of that round. We shall define the vertices that threaten Alice's chance of winning as dangerous.

Definition 5.2.1. *For a fixed round of play, let D_i denote the set of dangerous vertices at i moves, denoted D_i . A vertex v belongs to D_i if for some number of moves $j \leq i$, Bob has played at least $\frac{\epsilon}{100}n$ times more in the neighbourhood of v than Alice has, i.e. $|N(v) \cap B_j| \geq |N(v) \cap A_j| + \frac{\epsilon}{100}n$.*

We additionally define vertices that Alice can colour to maintain some symmetry in the game as follows.

Definition 5.2.2. *Let S be a finite subset of vertices of a graph, G . For a vertex $v \notin S$, we say that a vertex w mirrors v with respect to S if $w \notin S$ and for any $t \in S$, G contains an edge vt if and only if it contains an edge wt .*

Let $C = \{1, 2, \dots, (\frac{p}{2} + \epsilon)n\}$ be the set of colours used in the game. We call a colour *large* if it is at least $\frac{\epsilon}{200}n$, and *small* otherwise.

Alice will use the following strategy at the i^{th} move of a round: from the list below, she chooses the first point that applies, and colours the corresponding vertex with

smallest colour available to that vertex. If there are multiple vertices for the same point on the list, she chooses one of these arbitrarily.

1. If there is a vertex v that misses less than βn colours in its neighborhood and such that v has not yet been coloured in the current round, she chooses v .
2. If Bob played a vertex w for his previous move, w is not dangerous, and there is a vertex v which mirrors w with respect to D_i , she chooses v .
3. She chooses an arbitrary vertex.

We shall prove that because 1, 2, 3, and 4 hold, selecting vertices in order of priority will ensure that Bob can never win the eternal vertex colouring game for sufficiently large n . To show Bob cannot win, we prove the following lemma.

Lemma 5.2.3. *For n sufficiently large, at the beginning of the k^{th} round of play for $k \geq 2$, the following two conditions hold:*

- *During the $(k - 1)^{\text{st}}$ round, there was no vertex v such that number of times Bob played in neighbourhood of v was more than $\frac{\epsilon}{50}n$ greater than number of times Alice played in neighbourhood of v .*
- *Alice used no more than $\frac{\epsilon}{100}n$ colours in $(k - 1)^{\text{st}}$ round.*

Then, by playing according to the above described strategy, Alice ensures the following:

- *Bob does not win during k^{th} round*
- *During k^{th} round, there is no vertex v such that number of times Bob played in neighbourhood of v is more than $\frac{\epsilon}{50}n$ greater than number of times Alice played in neighbourhood of v .*
- *Alice uses no more than $\frac{\epsilon}{100}n$ colours in the k^{th} round.*

Note that Lemma 5.2.3 implies that, if Alice plays according to the strategy described above, Bob can never win the eternal graph colouring game.

Proof. The first step is to establish that at beginning of the round, each vertex misses more than $2\beta(\epsilon, p)n$ colours in its neighbourhood, so that there is no immediate threat to Alice. In the first round, this is immediate, as no colour is used yet. When $k \geq 2$, Alice uses at most $\frac{\epsilon}{100}n$ colours in the neighbourhood of any vertex v . Bob played at most $\frac{\epsilon}{50}n$ more moves in the neighbourhood of v than Alice did, so by property 1, Bob played at most $(\frac{p}{2} + \frac{\epsilon}{200} + \frac{\epsilon}{100})n$ colours in the neighborhood of v . Hence, at least $\frac{39\epsilon}{40}n > 2\beta(\epsilon, p)n$ colours are missing from the neighbourhood of v . Now, if some vertex misses at most βn colours at any point during the round, then in particular at least one of the times $\beta n, 2\beta n, \dots, \lfloor \beta^{-1} \rfloor \beta n$, this vertex missed at most $2\beta n$ colours. By property 3, we conclude there are at most $C\beta^{-1} \log n = o(n)$ vertices that, at some point in this round, have missed at most βn colours. Recall that colouring vertices that miss at most βn colours is of the highest priority in Alice' strategy. If Bob were to create a vertex seeing all colours that was not yet played in this round, Alice must have spend the previous βn moves playing in other vertices missing at most βn colours in their neighbourhoods. However, this contradicts the fact that there were at most $C\beta^{-1} \log n < \beta n$ such vertices. Hence, Alice can colour all such vertices in time.

Next, note that Alice uses $o(n)$ (and in fact only constantly many) moves that are arbitrary. If Alice colours an arbitrary vertex, then either Bob played a dangerous vertex for his previous move or she cannot mirror Bob on the current set of dangerous vertices. By property 2, there are at most K vertices declared dangerous during the round, so Bob can play in a dangerous vertex no more than K times. On the other hand, consider if Bob did not play dangerous vertex and Alice cannot mirror his move on D , the set of dangerous vertices. If we partition the rest of the graph into $2^{|D|} \leq 2^K$ classes according to which vertices of D they are connected to, Bob must have just played last vertex from one of these classes. Hence, Alice must have played at most $K + 2^K = O(1)$ arbitrary moves in any particular round.

Following this strategy, Alice also ensures that Bob will play in the neighbourhood of any vertex at most $\frac{\epsilon}{50}n$ more than Alice does. Indeed, once Bob has played $\frac{\epsilon}{100}n$ more colours in the neighbourhood of any vertex, v , it is declared dangerous. She then plays in neighbourhood of v whenever Bob does, except $o(n)$ times when she plays a move of type 1 or an arbitrary vertex.

Finally, note that Alice uses large colours only if the vertex she wants to colour is connected to all the small colours. If at any point during the round a vertex is connected to all the small colours, then at least one of the times $\gamma n, 2\gamma n, \dots, \lfloor \gamma^{-1} \rfloor \gamma n$, this vertex must have been missing at most γn colours. By property 4, there could have only been at most $D\gamma^{-1} \log n = o(n)$ vertices that were connected to all small colours at some point in this round. Hence, as she can colour all other vertices with small colours, Alice uses at most $\frac{\epsilon}{200}n + D\gamma^{-1} \log n < \frac{\epsilon}{100}n$ colours during the round. □

5.3 Lower bound for odd n

In this section, we prove the lower bound for the eternal game chromatic number on a graph with an odd number of vertices.

Proposition 16. *For any $p, \epsilon \in (0, 1)$ fixed, whp $\chi_g^\infty(G_{2m+1,p}) \geq (\frac{p}{2} - \epsilon)(2m + 1)$.*

For convenience, we shall let $n = 2m + 1$. Fix any vertex v of the graph $G_{n,p}$.

We will show that whp, Bob can ensure that in the first round, all $(\frac{p}{2} - \epsilon)n$ colours are in the closed neighbourhood of v in $G_{n,p}$. Bob then wins in the first move of the second round, by choosing v .

Bob can introduce all colours in $N(v)$ by playing in $N(v)$ whenever Alice does, thus ensuring he plays in at least roughly half of the vertices in $N(v)$ while introducing a new colour every time. Some set of vertices X outside $N(v)$ might at some point be adjacent to all unplayed vertices of $N(v)$. If Alice were to play some colour not

appearing in $N(v)$ in all these vertices, this colour could no longer be introduced to $N(v)$. Fortunately for Bob, the number of such sets will be very limited, and thus Bob can take care of them in time.

Consider following two properties of a random graph.

1. Whp, every vertex of $G_{n,p}$ has degree at least $(p - \frac{\epsilon}{100})n$.
2. For all $\epsilon > 0$, and $p \in (0, 1)$, there exist positive constants $\delta = \delta(\epsilon, p)$, $K = K(\epsilon, p)$, such that in $G_{n,p}$
 - Whp, there exist no 3 vertices u, v, w such that the number of vertices in the neighbourhood of u , but not in the neighbourhood of v or w is at most δn
 - Whp, for any set S of size $\frac{\epsilon}{100}n$ in the graph, there exist at most K mutually disjoint pairs of vertices $\{a_i, b_i\}$ such that at most δn vertices of S are not in $N(a_i) \cup N(b_i)$

Henceforth, we assume our graph has both properties, and fix $\delta = \delta(\epsilon, p)$ and $K = K(\epsilon, p)$. In the appendix, we show that indeed whp $G_{n,p}$ has these properties.

Note that if at some stage there exists a colour c that does not appear in $N(v)$ and all vertices not yet played in $N(v)$ are adjacent to a vertex of colour c , then c will not appear in $N(v)$, which is contrary to Bob's goal.

We introduce the ideas of a *double block* and being α away from becoming a *double block* in order to describe a strategy Bob should take to achieve his goal of filling the neighbourhood of a vertex with several colours.

Definition 5.3.1. *A pair of vertices a and b is called a double block if at some stage in the round, all uncoloured vertices in $N(v)$ are in the neighbourhood of either a or b and neither a or b (if coloured) is coloured with a colour appearing in $N(v)$.*

Definition 5.3.2. *A pair of vertices a and b is said to be α away from becoming a*

double block, if all but at most α of the uncoloured vertices in $N(v)$ are in the neighbourhood of either a or b and neither a or b (if coloured) is coloured with a colour appearing in $N(v)$.

Bob will play according to the following strategy. From the list below, he picks the highest point that applies.

1. If there exists a colour that appears at least twice outside of $N(v)$ but not in $N(v)$, then Bob plays it in $N(v)$ if it is a valid colouring.
2. If at least $10K$ colours appear nowhere in the graph and there are at least $\frac{\epsilon}{100}n$ uncoloured vertices in the neighbourhood of v , then Bob does the blocking moves in the chronological order they were called for, if legally possible. Blocking moves are called for if a pair $\{a, b\}$ of unplayed vertices is δn away from becoming a double block. Blocking moves consist of the following steps. First colour vertex a a colour not yet appearing in the graph, say c_a . Second, unless Alice plays in vertex b or introduces c_a in $N(v)$, play c_a in $N(v)$ and repeat for vertex b . If Alice plays in vertex b with a colour c_b not appearing in $N(v)$, play c_b in $N(v)$, and finish by playing c_a in $N(v)$ on the next move.
3. If legally possible, Bob introduces colours appearing once outside of $N(v)$ into $N(v)$, in the order in which they were introduced to the game.
4. If legally possible, Bob introduces new colours to $N(v)$.
5. Otherwise Bob does anything.

Note that (2) might involve up to four moves for any pair close to becoming a double block. If in between these four moves a situation as in (1) arises, situation (1) takes priority.

Claim 5.3.3. *There are no more than $4K$ moves of type (2) used in the first round.*

Proof. Let U denote the set of vertices that are uncoloured in $N(v)$ when the last blocking moves were played. By the definition of type (2) moves, $|U| \geq \frac{\epsilon}{100}n$, so

property 2 gives the result. □

Let T be the first move after which precisely $10K - 1$ colours are missing in $G_{n,p}$ during the first round. We collect the following observations about T :

- T exists and at T , at least ϵn vertices in $N(v)$ are uncoloured

We shall show that $T \leq (p - 2\epsilon)n$. After Bob's first $(\frac{p}{2} - \epsilon)n$ moves, Alice has also played $(\frac{p}{2} - \epsilon)n$ moves. As $|N(v)| \geq (p - \frac{\epsilon}{100})n$, at this stage at least $\frac{199}{100}\epsilon n$ vertices in $N(v)$ are uncoloured. Bob spent at most $4K$ moves playing according to (2), and when he did not, he always introduced a new colour in $N(v)$, if he legally could.

Note that if there were still colours missing from $G_{n,p}$ and there were uncoloured vertices in $N(v)$, moves of type (4) were always legal. Hence, unless all colours appear in the graph, Bob played at least $(\frac{p}{2} - \epsilon)n - 4K$ colours in $N(v)$ and hence in $G_{n,p}$.

- At T , at most $18K$ colours are missing in $N(v)$

Between two consecutive moves of Bob before T , the number of colours appearing outside of $N(v)$ but not in $N(v)$ can increase by at most 2. In fact it only increases if Bob makes a move of type (2). Hence, there are at most $8K$ such colours at time T , and result follows.

- At T , Bob has played at most $8K$ (1) moves.

Let c be the number of colours appearing outside $N(v)$ and not in $N(v)$. Note that between two consecutive moves of Bob up to time T , c increases only if Bob plays a (2) move, in which case it increases by at most 2. On the other hand, note that Bob only plays (1) moves directly after Alice plays a colour already appearing outside $N(v)$. Hence, c decreases whenever Bob plays a (1) move. By 5.3.3, there were at most $4K$ (2) moves, so there were at most $8K$ (1) moves.

- No pair of vertices is closer than $\frac{\delta}{2}n$ to becoming a double-block at any point up to T

We know from 2 that at the beginning of the game, no pair is closer than δn to becoming a double block. Up to time T , whenever a pair gets closer than δn to becoming a double block, no (3)-(5) moves are played until this pair is eliminated. However, there are at most $12K$ (1) and (2) moves played until T . Hence, no pair can be closer than $\delta n - 12K \geq \frac{\delta}{2}n$ to becoming a double-block up to T .

- Every colour that does not appear in $N(v)$ at T appears at most once in $G_{n,p}$

Note that the only time before T that there is a colour appearing twice outside $N(v)$, but not inside, is directly after Alice has played this colour. In response, Bob immediately plays that same colour in $N(v)$, which is possible as no pair of vertices is a double block. Hence, if Bob made the last move before T , the statement follows. If the last move before T was by Alice, she must have introduced a new colour into the graph by the definition of T , which again implies the statement.

Next we claim:

Claim 5.3.4. *In the $18K$ moves of Bob following T , he will introduce all colours in $N(v)$.*

Proof. Moves of type (2) are no longer played after T by their definition. In the next $36K$ moves, $18K$ of which are made by Bob and the $18K$ by Alice, no complete double-block can be created, as all are at least $\frac{\delta}{2}n > 36K$ moves away. Since at T at least ϵn vertices of $N(v)$ are still uncoloured, during the next $36K < \epsilon n$ moves, there are ample uncoloured vertices in $N(v)$. Hence, Bob can and will introduce a new colour to $N(v)$ every move until all colours appear there, as he ceases the (2) moves. □

Thus we see that Bob will ensure that all colours appear in $N(v)$ during the first round and he will win in the first move of the second round by picking v .

5.4 Generalization of the lower bound for odd n

Proposition 16 doesn't trivially extend to even n , as it is not enough for Bob to let all colours appear in the neighbourhood of a fixed vertex because Alice could use her first move in the second round to remove one of the colours from this neighbourhood.

If Bob can manage to play all colours in the neighbourhood of two vertices, with no colour appearing uniquely in the intersection of the neighbourhoods, then Alice can not. This limits how Bob can colour the intersection of two neighbourhoods of vertices. By increasing the number of vertices that simultaneously see all colours, the size of this intersection can be reduced. Our aim is to show that if $p = 1/k$ for some $k \in \mathbb{N}$, then for any fixed l , Bob can choose l vertices and play all of $(p/2 - p^l/2 - \epsilon)n$ colours in the neighbourhoods of these vertices. The $p^l/2n$ correction term comes from the intersection of the neighbourhoods of these l vertices. As l can be taken arbitrarily large, this shows $\chi_g^\infty(G_n, p)$ for even n and $p = 1/k$.

In this section, we prove a generalization of Proposition 16, showing that if $V(G)$ is partitioned into constantly many parts and each of the parts is assigned a set of colours of size roughly half the size of the part, Bob can guarantee all these colours to appear in the parts by the end of the first round. This generalizes the notion that Bob could achieve this in the single set $N(v)$. In the next section, we will fix some set of vertices X of constant size and induce partition $\{A_I : I \subset [l]\}$, where $A_I = \{v \in V : N(v) \cap X = I\}$. We show in Lemma 19, that for the special case $p = \frac{1}{k}$, there exists an appropriate way of assigning colours to the A_I 's such that each vertex in X will see all colours after the first round.

Proposition 17. $\forall \epsilon, \eta, \gamma > 0, l \in \mathbb{N}$, and $p \in (0, 1)$, if $X_i \subset V$ ($i \in [l]$) are disjointly chosen independent sets of vertices of the graph $G_{n,p}$ with $|X_i| \geq \gamma n$ and

$Y_i \subset [(p/2 - \epsilon)n]$ with $|Y_i| \leq \frac{(1-\eta)|X_i|}{2}$, then whp Bob can guarantee that at the end of round all of the colours in Y_i appear in X_i .

To prove Proposition 17 we will use the following generalization of the structural result in 2.

Lemma 5.4.1. *For all $m \in \mathbb{N}$, $\alpha > 0$ and $p \in (0, 1)$, there exist positive constants $\delta = \delta(\alpha, p, m)$, $K = K(\alpha, p, m)$, such that*

- *For any set S of size at least αn in the graph, whp there exist no m -sets of vertices $\{a_1, \dots, a_m\}$ such that at most δn vertices of S are not in $\cup_j N(a_j)$*
- *Whp, for any set S of size at least αn in the graph, there exist at most K mutually disjoint m -sets of vertices $\{a_{i,1}, a_{i,2}, \dots, a_{i,m}\}$ such that at most δn vertices of S are not in $\cup_j N(a_{i,j})$*

In order to prove Proposition 17, we will define the concepts of an *end stage*, *m -block* and *α away from becoming an m -block*.

Definition 5.4.2. *Let T_i be the first move after which at most $10K$ of the colours in Y_i are missing from X_i , if this exists. After T_i , say X_i is in its end stage.*

Definition 5.4.3. *Given disjoint sets $X_i \subset V$, at some stage of the round we say a set $\{a_1, \dots, a_m\}$ is an m -block if for some i , X_i is not in its end stage, every uncoloured vertex in X_i is in the neighbourhood of some a_j , and no a_j is coloured in some colour also appearing in X_i .*

Definition 5.4.4. *Given disjoint sets $X_i \subset V$, at some stage of the round we say a set $\{a_1, \dots, a_m\}$ is α away from becoming a m -block if for some i , X_i is not in its end stage, all but α of the uncoloured vertices in X_i is in the neighbourhood of some a_j , and no a_j is coloured in some colour also appearing in X_i .*

Proof of Proposition 17. Let $C_l = \frac{12l}{\eta\gamma} + 4$ and let $\delta = \delta(\eta/4, p, 100C_l l)$ and

$K = K(\eta/4, p, 100C_l l)$ as in Lemma 5.4.1. Bob will play the move of the highest priority that he legally can according to the following list:

1. If for some $q \in [l]$, some colour c appears $C_l q$ times in the graph, but it is missing from more than $l - q$ of the X_i 's for which $c \in Y_i$, Bob plays it in any of X_i 's where it does not yet appear.
2. If for some i , X_i is in its end stage, Bob plays the missing colours into it, copying the colour Alice played if it was missing.
3. If there is $100C_l l$ block closer than δn moves away from becoming an m-block and at least $\eta/4n$ vertices in the corresponding X_i are uncoloured, Bob kills it. By killing it, we mean the following sequence of moves. Colour the first vertex of our $100C_l l$ -set by some colour that appears less than $C_l q$ times in the graph and is missing from at most $l - q$ of the relevant X_i 's. Then make sure in the next moves that this colour also appears in all of its designated X_i 's. Repeat this procedure for all vertices of our $100C_l l$ -set.
4. If for some $q \in [l]$, some colour appears $C_l q$ times in the graph, but it is still missing from more than $l - q + 1$ of X_i 's, Bob plays it in any of X_i 's where it does not yet appear.
5. Bob plays any colour in Y_i not yet used in X_i to that X_i , if possible in the same X_i as Alice played in the previous move.
6. Bob plays anything anywhere.

Note that (3) might involve up to $100C_l l(l + 1)$ moves. If in between these moves a situation as in (1) or (2) arises, those are resolved first.

Claim 5.4.5. *Let $C = 100C_l l^2(l + 1)$. There were no more than CK (3) moves called for.*

Proof. Let $U \subset X_i$ denote the set of vertices that are still uncoloured in X_i when the last blocking moves were called for, for this X_i . Lemma 5.4.1 says X_i called for at most $100C_l l(l + 1)K$ (3) moves. Hence, in total at most $100C_l l^2(l + 1)K = CK$ (3) moves are called for. □

Claim 5.4.6. *There were no more than $\frac{2l}{C_l}n$ moves of types (1),(2),(3) and (4) during the first round of the game.*

Proof. Note that at most $\frac{n}{C_l}$ colours appear at least C_l times in the graph.

Moreover, these colours prompt a (1) or (4) move at most l times. Finally, there are at most $10Kl$ (2) moves. Hence, there are at most $\frac{l}{C_l}n + 10Kl + CK \leq \frac{2l}{C_l}n$, given $n \geq \frac{C_l K}{l}(10l + C)$. \square

We collect the following observations about T_i :

- T_i exists and, at T_i , at least $\frac{\eta}{4}n$ vertices in X_i are still uncoloured

At the end of round one there were $|X_i|$ moves in X_i . Moreover, by Claim 5.4.6 there were at most $\frac{2l}{C_l}n$ (1)-(4) moves. After Bob's first $|Y_i| + \frac{2l}{C_l}n$ in X_i , he has played at most $\frac{2l}{C_l}n$ (1)-(4) moves. He also played in X_i after every move of Alice in that set, except the times when he played (1)-(4) moves. Thus, at least $\eta|X_i| - \frac{6l}{C_l}n \geq \frac{\eta\gamma}{2}n$ of the vertices in X_i are uncoloured. As $C_l \geq \frac{12l}{\eta\gamma}$, this gives the result.

- Let $C' = C + 10l$. At T_i , Bob has played at most $C'K$ (1) moves.

For a colour j , let q_j be the number such that colour j is missing from $l - q_j$ of its designated sets. Let r_j be the number of times j appears in the graph. If $r_j - q_j C_l > 0$, then Bob is forced to play a (1) move. If $r_j - (q_j - 1)C_l > 0$, then this induces a (4) move. Let $D = \sum_j \max\{r_j - (q_j - 1)C_l, 0\}$. Note that if $D > 0$, then Bob must play a (1),(2),(3) or (4) move. If D increases between consecutive moves of Bob, he must have played a (2) or (3) move. Moreover, D increases by at most 2 in that case. On the other hand, if Bob is prompted to play a (1) move, D decreases by at least $C_l - 1 > 2$. Hence, there are at most as many (1) moves as there are (2) and (3) moves, i.e. at most $C'K + 10Kl$ (1) moves.

- No pair of vertices is closer than $\frac{\delta}{2}n$ to becoming a $100C_l l$ block at any point up to T_i

By Lemma 5.4.1, at the beginning of the game no $100C_l l$ -set of vertices is closer

than δn to becoming a $100C_l l$ block. Whenever, up to time T_i , a $100C_l l$ -set gets closer than δn to becoming a $100C_l l$ block, no (4)-(6) moves are played until this pair is eliminated. However, there are at most $(2C + 10l)K$ (1) and (3) moves played until T_i . Hence, no $100C_l l$ -set gets closer than $\delta n - (2C + 10l)K \geq \frac{\delta}{2}n$ to becoming a $100C_l l$ block up to T_i .

- Every designated colour that does not appear in X_i at T_i appears at most $C_l l + 2$ times in our graph

By the definition of (1) moves, some colour c can never appear $C_l l + 2$ times in our graph, yet not appear in some of X_i 's with $c \in Y_i$.

Next we claim:

Claim 5.4.7. *In the $10Kl + C'K$ moves of Bob following T_i , he will introduce all colours in X_i .*

Proof. Note that while there are still colours missing from X_i in its end stage, Bob only plays (1) and (2) moves, both of which copy the colour Alice played. Hence, the colours missing from X_i can be played at most $2l$ times before being played into X_i . At that stage, the colour is played at most $C_l l + 2 + 2l < 100C_l l$ times and no $100C_l l$ -set is closer than $\frac{\delta}{2}n$ to becoming a $100C_l l$ block, so no $100C_l l$ block will be formed in the endstage of X_i . Hence, we can still play this colour in X_i . As we can introduce all the missing colours and we play at most $C'K$ (1) moves, we need at most $10Kl + C'K$ moves to introduce them all. □

Thus, since Bob can introduce all colours into X_i during the end game, the proof of Proposition 17 is complete. □

Having proven Proposition 17, we are ready to look at even n .

5.5 Even n

In this section, we shall prove that for particular values of p , we can achieve the same lower bound for even n as for odd n .

Proposition 18. *Let $p = 1/k$ for some $k \in \mathbb{N}$, and $\epsilon > 0$. Then whp*

$$\chi_g^\infty(G_{2m,p}) \geq (p/2 - \epsilon)2m.$$

For convenience write $n = 2m$. For given $p, \epsilon > 0$, fix $l \in \mathbb{N}$, such that $p^l < \epsilon/100$.

Lemma 19. *Let $X \subset V(G)$ be a set of l vertices and $p = 1/k$ for some $k \in \mathbb{N}$.*

There exists $\eta > 0$, and a function $f : \mathcal{P}(X) \mapsto \mathcal{P}((p/2 - p^l/2 - \epsilon)n)$, assigning to every subset $X' \subset X$, $p^{|X'|}(1-p)^{l-|X'|}(1-\eta)^{\frac{n}{2}}$ colours, such that

$$\bigcup_{X': x \in X' \subset X} f(X') = [(p/2 - p^l/2 - \epsilon)n] \text{ for every } x \in X.$$

To prove this lemma we will use the following auxiliary lemma.

Let $\mathcal{B}(X)$ be the set of all partitions of the set X .

Lemma 20. *Consider any $k \in \mathbb{N}$. Let $p = 1/k$ and $|X| = l$, then there exists $g : \mathcal{B}(X) \rightarrow [0, 1]$, such that for all $A \subset X$;*

$$\sum_{T: A \in T \in \mathcal{B}(X)} g(T) = p^{|A|}(1-p)^{l-|A|}$$

Proof. Define g as

$$g(T) = \begin{cases} k^{-l} \frac{(k-1)!}{(|T|-1)!} & \text{if } |T| \leq l \\ 0 & \text{else} \end{cases}$$

Fix $A \subset X$ and evaluate $\sum_{T: A \in T \in \mathcal{B}(X)} g(T)$. Consider ordered partitions of $X \setminus A$ into $k-1$ potentially empty sets. Each of these contributes exactly k^{-l} to this sum.

To see this, consider a particular ordered partition of $X \setminus A$ into $k-1$ potentially empty sets, with m non-empty sets. This corresponds to a partition T of $X \setminus A$ into m parts, which has weight $g(T) = k^{-l} \frac{(k-1)!}{(m-1)!}$. Note that to find ordered partitions

into $k - 1$ potentially empty sets corresponding to T , we need to pick the locations of the m sets among the $k - 1$ options. There are $\frac{(k-1)!}{(m-1)!}$ ways to do this. Hence, every ordered partition of $X \setminus A$ into $k - 1$ potentially empty sets contributes weight exactly k^{-l} to the sum.

Noting that there are exactly $(k - 1)^{l-|A|}$ ordered partitions of $X \setminus A$ into $k - 1$ potentially empty sets, we can evaluate the sum as

$$\sum_{T:A \in T \in \mathcal{B}(X)} g(T) = (k - 1)^{l-|A|} k^{-l} = \left(\frac{1}{k}\right)^{|A|} \left(\frac{k - 1}{k}\right)^{l-|A|} = p^{|A|} (1 - p)^{l-|A|}$$

□

Proof of Lemma 19. Let $g : \mathcal{B}(X) \rightarrow [0, 1]$ as in Lemma 20 and set

$\mathcal{B}'(X) = \mathcal{B}(X) \setminus \{X\}$. Note that $\sum_{T \in \mathcal{B}'(X)} g(T) = p(1 - p^{l-1})$. Consider any linear order on $\mathcal{B}'(X)$ and let

$$f' : \mathcal{B}'(X) \rightarrow \mathcal{P}((p/2 - p^l/2 - \epsilon)n), T \mapsto \left\{ \left\lfloor \sum_{T' < T} g(T') \right\rfloor \frac{(1 - \eta)n}{2} + 1, \dots, \left\lfloor \sum_{T' \leq T} g(T') \right\rfloor \frac{(1 - \eta)n}{2} \right\}$$

where η is such that $\left\lfloor \sum_{T \in \mathcal{B}'(X)} g(T) \right\rfloor \frac{(1 - \eta)n}{2} = (p/2 - p^l/2 - \epsilon)n$. Let

$$f : \mathcal{P}(X) \rightarrow \mathcal{P}((p/2 - p^l/2 - \epsilon)n); X' \mapsto \bigcup_{T \supset X'} f'(T)$$

Hence;

$$\begin{aligned} \bigcup_{X': x \in X' \subset X} f(X') &= \bigcup_{X': x \in X' \subset X} \bigcup_{T: T \supset X'} f'(T) \\ &= \bigcup_{T \in \mathcal{B}(X)} f'(T) \end{aligned}$$

□

Proof of Proposition 18. Fix $X \subset V$ with $|X| = l$. Sample all edges incident to X .

For $I \subset X$, let $X_I = \{v \in V \setminus X : N(v) \cap X = I\}$. Note that whp $|X_I| \geq p^{|I|}(1-p)^{l-|I|}(1-\eta/10)n$ for any $\xi > 0$. Use Lemma 19 to find $Y_I = f(I)$, such that $|Y_I| \leq \frac{(1-\eta/10)|X_I|}{2}$. Now sample all the other edges in the graph. By Lemma 17, whp Bob can guarantee that at the end of round one the colours in Y_I appears in X_I . By construction of Y_I , all vertices in X will see all colours and, moreover, there is no single vertex whose recolouring changes that. Regardless of Alice' first move in the second round, Bob can choose a vertex that sees all colours in his first move in the second round. Thus, the proposition follows. \square

Note that the condition $p = 1/k$ is essential. In fact, if $p \notin \{\frac{1}{2}, \frac{1}{3}, \dots\}$, then whp for any three vertices v_1, v_2 and v_3 , it is impossible to assign colours Y_I to $X_I = \{v : N(v) \cap \{v_1, v_2, v_3\} = I\}$, such that $|Y_I| \leq (1/2 + \eta)|X_I|$ and $\bigcup_{I:i \in I \subset [3]} Y_I = [(p/2 - \epsilon)n]$ for every $i \in [3]$. Crucially, Lemma 20 fails to hold. Hence, given that Alice can play in roughly half the vertices in $N(v)$ for all $v \in V$, at most two vertices at the end of every round can see all colours. Some must appear uniquely in the intersection, so Alice can recolour one of these in the first move of the second round. Hence, we cannot expect Bob to win at the beginning of round two. However, it is not immediately clear whether Bob cannot reintroduce the colour successfully. We believe this cannot be done, so we conjecture that for all $p \in (0, 1) \setminus \{\frac{1}{2}, \frac{1}{3}, \dots\}$, $\exists \epsilon > 0$ such that whp $\chi_g^\infty(G_{n,p}) \leq (1 - \epsilon)\frac{pn}{2}$, as stated in Conjecture 5.1.1.

5.6 Answer to a question of Klostermeyer and Mendoza

We conclude the paper by answering a question posed by Klostermeyer and Mendoza in their original paper.

They define other variants of the eternal chromatic game on graph. One of them is greedy colouring game, where Bob must colour whatever vertex he chooses with the

smallest colour possible. Let $\chi_g^{\infty 2}(G)$ be the smallest number k such that when this game is played with k colours on G , Alice is guaranteed to win. Further, they consider the variant of game when not only Bob, but also Alice, must use the smallest colour available for each vertex she chooses, and define $\chi_g^{\infty 3}(G)$ to be eternal number of the game played with these rules. Note that clearly $\chi_g^{\infty 2}(G) \leq \chi_g^{\infty 3}(G)$ since Alice can, if she wishes so, choose the smallest colour for each vertex she chooses in any variant of the game and analogously $\chi_g^{\infty 2}(G) \leq \chi_g^{\infty}(G)$.

Klostermeyer and Mendoza pose the following question about these new variants of the game.

Question 5.6.1. *Let G be a graph with subgraph or induced subgraph H . Is it necessarily true that $\chi_g^{\infty 2}(G) \geq \chi_g^{\infty 2}(H)$? Is it necessarily true that $\chi_g^{\infty 3}(G) \geq \chi_g^{\infty 3}(H)$?*

Indeed, it is not true. Consider the following example.

Proposition 21. *For $n \geq 2$, $\chi_g^{\infty 3}(K_{1,2n+1}) = 3$ and $\chi_g^{\infty 2}(K_{1,2n}) \geq 4$.*

Proof. For $\chi_g^{\infty 3}(K_{1,2n+1}) = 3$ note that Alice starts every round as the number of vertices is even. Every round she will first play in the central vertex which will become the unique element from [3] not yet appearing in the graph. All the other vertices will now become the former colour of the central vertex.

For $\chi_g^{\infty 3}(K_{1,2n}) \geq 4$. assume for a contradiction 3 colours suffice and note that Bob begins the second round. Let x for the central vertex. Then x is either adjacent to two different colours or $N(x)$ is monochromatic. In the former case, Bob plays in x and finds that there is no colour available, a contradiction.

In the latter case, Bob plays in $N(x)$, bringing the number of colours in $N(x)$ to two. Hence, Alice cannot play in x . She can also not bring down the number of colours in $N(x)$ as it contains at least three vertices. Thence, when Bob gets to play his second move in the second round, and plays x , he finds no colours available,

again a contradiction. □

Note that $H = K_{1,2n}$ is an (induced) subgraph of $G = K_{1,2n+1}$, and

$$\chi_g^{\infty 2}(G) \leq \chi_g^{\infty 3}(G) \leq \chi_g^{\infty 2}(H) \leq \chi_g^{\infty 3}(H)$$

This answers all the subquestions in the negative.

Finally, note that while there is no clear relationship between $\chi_g^{\infty 3}(G)$ and $\chi_g^{\infty}(G)$ for general graphs G , in our definition of strategy of Alice in Section 2, we let her always play the smallest colour available, and so in particular we show

$$\chi_g^{\infty 3}(G_{n,p}) \leq \left(\frac{p}{2} + o(1)\right)n \text{ whp.}$$

5.7 Appendix

In this appendix, we provide proofs of various structural results about $G_{n,p}$ that were used in earlier proofs. Some of them will be shown in a more general form. One of our main tools will be the following well-known form of Hoeffding's Inequality.

Lemma 5.7.1. *For any $\epsilon > 0$, $n \in \mathbb{N}$, and $p \in (0, 1)$,*

$$\mathbb{P}(\text{Bin}(n, p) \geq (p + \epsilon)n) \leq \exp(-2\epsilon^2 n) \text{ and } \mathbb{P}(\text{Bin}(n, p) \leq (p - \epsilon)n) \leq \exp(-2\epsilon^2 n).$$

Note that Hoeffding's inequality implies property 1 from Section 5.2 and property 1 from Section 5.3.

To prove 3 and 4 from Section 2, we first prove the following result.

Lemma 5.7.2. *For all $\alpha > 0$, $p \in (0, 1)$, there exist constants*

$K = K(\alpha, p)$, $\beta = \beta(\alpha, p) > 0$ such that whp the following holds. For any colouring of $G_{n,p}$ with αn colours, the number of vertices that have all but at most βn colours in their neighbourhood is at most $K \log n$.

Proof. Let $q = 1 - (1 - p)^{2/\alpha}$, $\beta = \frac{\alpha(1-q)}{8}$, and $K = \frac{4}{(1-q)^2}$. Without loss of generality, let $\frac{2}{\alpha} \in \mathbb{Z}$.

Note that in any colouring of $G_{n,p}$ by αn colours, we have $\frac{\alpha}{2}n$ colours appearing at most $\frac{2}{\alpha}$ times each.

Assume there exists a set S of $K \log n$ vertices missing at most βn colours each. For n satisfying $K \log n < \frac{\alpha}{4}n$, there exists a set C of $\frac{\alpha}{4}n$ colours appearing at most $\frac{2}{\alpha}$ times each such that no vertex in S has any colour from C . In particular, there must be mutually disjoint sets of vertices $S, T_1, \dots, T_{\frac{\alpha}{4}n}$, such that $|T_i| \leq \frac{2}{\alpha}$ for each i , $|S| = K \log n$ and each vertex in S is joined to at least $(\frac{\alpha}{4} - \beta)n$ sets T_i in our graph. Now, we consider the probability that such structure exists in $G_{n,p}$. For n sufficiently large, we find there are $\sum_{i=1}^{2/\alpha} \binom{n}{i} \leq 2 \binom{n}{2/\alpha}$ ways of choosing each of the sets T_i . So for such large n , we have at most

$$\begin{aligned} \binom{n}{K \log n} \left(2 \binom{n}{2/\alpha} \right)^{\frac{\alpha n}{4}} &\leq n^{K \log n} 2^{\frac{\alpha n}{4}} \left(\frac{e \alpha n}{2} \right)^{\frac{\alpha n}{4}} \\ &= \exp \left(K (\log n)^2 + \frac{\alpha n}{4} \log n + \frac{\alpha}{4} n \log (e \alpha) \right) \end{aligned}$$

ways to choose sets $S, T_1, \dots, T_{\alpha n/4}$. Now for any such fixed choice, the probability that these sets satisfy the conditions is at most

$$\mathbb{P} \left(\text{Bin} \left(\frac{\alpha n}{4}, q \right) \geq \left(q + \frac{1-q}{2} \right) \frac{\alpha n}{4} \right)^{K \log n} \leq \exp \left(-2 \left(\frac{1-q}{2} \right)^2 \frac{\alpha n}{4} K \log n \right)$$

The union bound then gives that the probability of finding appropriate

$S, T_1, \dots, T_{\alpha n/4}$ is at most

$$\begin{aligned}
& \exp \left(K(\log n)^2 + \frac{\alpha n}{4} \log n + \frac{\alpha}{4} n \log(e\alpha) - 2 \left(\frac{(1-q)}{2} \right)^2 \frac{\alpha n}{4} K \log n \right) \\
&= \exp \left(K(\log n)^2 + \frac{\alpha}{4} n \log(e\alpha) + \left(1 - K \frac{(1-q)^2}{2} \right) \frac{\alpha n}{4} \log n \right) \\
&= \exp \left(K(\log n)^2 + \frac{\alpha}{4} n \log(e\alpha) - \frac{\alpha n}{4} \log n \right) = o(1)
\end{aligned}$$

The result follows. \square

To conclude property 3, simply plug in $\alpha = (\frac{p}{2} + \epsilon)$, and note that if some value of $\beta > 0$ works, then any smaller one does too, so we can insist on β being not too large.

To conclude 4, plug in $\alpha = \frac{\epsilon}{200}$ and note that presence of other colours only helps us, as the result would still hold even if all the other vertices were also coloured in $\frac{\epsilon}{200}n$ small colours.

The following implies property 2 from Section 5.2.

Lemma 5.7.3. *Fix any ϵ , and δ greater than 0. Assume $K \in \mathbb{N}$ is fixed, such that $K > \frac{6\epsilon}{\delta^2}$. Whp, if $A, B \subset V(G)$ are disjoint subsets with $|A| = |B| \geq \epsilon n$, then there are less than K vertices connected to at least δn more vertices in B than in A .*

Proof. Assume for a contradiction $n \geq \frac{2K}{\epsilon}$ and there exist A, B , as stated in the lemma such that there are at least K vertices connected to at least δn more vertices in B than in A . Let S be a collection of K such vertices. Let $A' = A \setminus S$ and $B' = B \setminus S$. Note that $e(A', S) \leq e(A, S)$ and $e(B', S) \geq e(B, S) - K^2$, so that

$$e(B', S) - e(A', S) \geq e(B, S) - e(A, S) - K^2 \geq K\delta n - K^2 \geq K\delta n/2.$$

Hence, either $e(B', S) \geq (|B'| \cdot |S|p) + \delta K n/8$ or

$e(A', S) \leq (|B'| \cdot |S|p) - 3\delta K n/8 \leq (|A'| \cdot |S|p) - \delta K n/8$. The probability of the

former (the latter follows analogously) is given by;

$$\begin{aligned} \mathbb{P}(\text{Bin}(|B'| \cdot |S|, p) \geq (|B'|Kp) + \delta Kn/8) &\leq \exp\left(-2\left(\frac{\delta n}{8|B'|}\right)^2 |B'|K\right) \\ &\leq \exp\left(-\frac{\delta^2 nK}{2\epsilon}\right) \end{aligned}$$

We can choose sets A , B , and S in at most

$$\binom{n}{|A|}^2 \binom{n}{K} \leq 2^{3n}$$

ways. Thus, the probability that any such sets A , B and S exist is at most

$$2 \exp\left(-\frac{\delta^2}{2\epsilon} nK + 3n \log 2\right) \rightarrow 0$$

provided $K > \frac{6\epsilon}{\delta^2} > \frac{6\epsilon}{\delta^2} \log 2$. □

The proof of property 2 from section 5.3 follows from the fact that for $\delta(p)$ sufficiently small and positive, whp there exists no three vertices u, v, w such that the number of vertices in the neighbourhood of u , but not in the neighbourhood of v or w is at most δn by Hoeffding's Inequality. Property 2 follows directly from the following lemma, setting $m = 2$.

Lemma 5.4.1 follows in the same manner, this time using the particular m we need.

Lemma 5.7.4. *Fix $m \in \mathbb{N}$, $\gamma > 0$, $p \in (0, 1)$. Then for any $K > \frac{4}{\gamma(1-p)^{2m}}$, whp $G_{n,p}$ does not contain any collection of sets S, T_1, \dots, T_K such that T_1, \dots, T_K are all mutually disjoint, $|S| \geq \gamma n$, $|T_1| = \dots = |T_K| = m$ and for every T_i , all but at most $\frac{(1-p)^m}{4} \gamma n$ vertices of S are connected to at least one vertex in T_i .*

Proof. Provided $n > \frac{2Km}{\gamma}$, we can find $S' \subset S$ such that $|S'| = \frac{\gamma n}{2}$ and S' is disjoint from all of T_1, \dots, T_K . For any such fixed S', T_1, \dots, T_K , by Hoeffding's Inequality, the probability that for each T_i , all but at most $\frac{(1-p)^m}{4}\gamma n$ vertices of S' are connected to at least one vertex in T_i is at most

$$\begin{aligned} \mathbb{P}\left(\text{Bin}\left(\frac{\gamma}{2}n, (1-p)^m\right) \leq \frac{(1-p)^m}{2}\gamma n - \frac{(1-p)^m}{4}\gamma n\right)^K &\leq \exp\left(-2\frac{(1-p)^{2m}}{4}\frac{\gamma}{2}nK\right) \\ &= \exp\left(-\frac{(1-p)^{2m}\gamma Kn}{4}\right) \end{aligned}$$

There are at most

$$\begin{aligned} \binom{n}{m}^K \binom{n}{\gamma n/2} &\leq n^{mK} 2^n \\ &= \exp(mK \log n + n \log(2)) \end{aligned}$$

ways to choose such sets S', T_1, \dots, T_K . So, as long as $K > \frac{4}{\gamma(1-p)^{2m}} > \frac{4}{\gamma(1-p)^{2m}} \log(2)$, the result follows. \square

BIBLIOGRAPHY

- [1] S. Aaronson and A. Ambainis. Quantum search of spatial regions. In *Proc. 44th Ann. IEEE Symposium on Foundations of Computer Science*, pages 200–209. IEEE, 2003.
- [2] Y. Aharonov, L. Davidovich, and N. Zagury. Quantum random walks. *Physical Review A*, 48(2):1687, 1993.
- [3] M. Aigner and M. Fromme. A game of cops and robbers. *Discrete Applied Mathematics*, 8:1–12, 1984.
- [4] R. J. Angeles-Canul, R. M. Norton, M. Opperman, C. C. Paribello, M. C. Russell, and C. Tamon. Perfect state transfer, integral circulants, and join of graphs. *Quantum Information & Computation*, 10:325–342, 2010.
- [5] R. Bachman, E. Fredette, J. Fuller, M. Landry, M. Opperman, C. Tamon, and A. Tollefson. Perfect state transfer on quotient graphs. *Quantum Information & Computation*, 12:293–313, 2012.
- [6] P. Balister, B. Bollobás, B. Narayanan, and A. Shaw. Catching a fast robber on the grid. *Journal of Combinatorial Theory, Series A*, 152:341–352, 2017.
- [7] N. Biggs. Chip-firing and the critical group of a graph. *Journal of Algebraic Combinatorics*, 9(1):25–45, 1999.
- [8] A. Björner, L. Lovász, and P. Shor. Chip-firing games on graphs. *European Journal of Combinatorics*, 12(4):283–291, 1991.
- [9] D. Blessing, E. Insko, K. Johnson, and C. Mauretour. On (t, r) broadcast domination number of grids. *Discrete Applied Mathematics*, 187:19–40, 2015.
- [10] H. L. Bodlaender. On the complexity of some coloring games. In *Proceedings of the 16rd International Workshop on Graph-Theoretic Concepts in Computer Science*, WG '90, pages 30–40, Berlin, Heidelberg, 1991. Springer-Verlag.
- [11] T. Bohman, A. Frieze, and B. Sudakov. The game chromatic number of

- random graphs. *Random Structures & Algorithms*, 32:223–235, 2007.
- [12] B. Bollobás. The chromatic number of random graphs. *Combinatorica*, 8(1):49–55, 1988.
- [13] A. Bonato, P. Golovach, G. Hahn, and J. Kratochvíl. The capture time of a graph. *Discrete Mathematics*, 309(18):5588–5595, 2009.
- [14] S. Chakraborty, L. Novo, S. Di Giorgio, and Y. Omar. Optimal quantum spatial search on random temporal networks. *Phys. Rev. Lett.*, 119:220503, Nov 2017.
- [15] R. J. Chapman, M. Santandrea, Z. Huang, G. Corrielli, A. Crespi, M.-H. Yung, R. Osellame, and A. Peruzzo. Experimental perfect state transfer of an entangled photonic qubit. *Nature Communications*, 7:11339, 2016.
- [16] A. M. Childs. Universal computation by quantum walk. *Physical Review Letters*, 102:180501, May 2009.
- [17] A. M. Childs and J. Goldstone. Spatial search by quantum walk. *Physical Review A*, 70(2):022314, 2004.
- [18] A. M. Childs, D. Gosset, and Z. Webb. Universal computation by multiparticle quantum walk. *Science*, 339(6121):791–794, 2013.
- [19] M. Christandl, N. Datta, T. C. Dorlas, A. Ekert, A. Kay, and A. J. Landahl. Perfect transfer of arbitrary states in quantum spin networks. *Physical Review A*, 71(3):032312, 2005.
- [20] M. Christandl, N. Datta, A. Ekert, and A. J. Landahl. Perfect state transfer in quantum spin networks. *Phys. Rev. Lett.*, 92, 2004.
- [21] N. Clarke, D. Cox, C. Duffy, D. Dyer, S. Fitzpatrick, and M. Messinger. Limited visibility cops and robber. *Discrete Applied Mathematics*, 2019.
- [22] G. Coutinho and C. Godsil. Perfect state transfer in products and covers of graphs. *Linear and Multilinear Algebra*, 64(2):235–246, 2016.
- [23] N. Crepeau, P. E. Harris, S. Hays, M. Loving, J. Rennie, G. Rojas Kirby, and

- A. Vasquez. On (t, r) broadcast domination of certain grid graphs. 2019.
- [24] C. M. Dawson and M. A. Nielsen. The solovay-kitaev algorithm. *Quantum Info. Comput.*, 6(1):81–95, Jan. 2006.
- [25] T. Dinski and X. Zhu. A bound for the game chromatic number of graphs. *Discrete Math.*, 196(1-3):109–115, Feb. 1999.
- [26] B. F. Drews, P. E. Harris, and T. W. Randolph. Optimal (t, r) broadcasts on the infinite grid. *Discrete Applied Mathematics*, 255:183–197, 2019.
- [27] Y.-M. Du, L.-H. Lu, and Y.-Q. Li. A rout to protect quantum gates constructed via quantum walks from noises. *Scientific Reports*, 8(1):7117, 2018.
- [28] C. Duffy, T. Lidbetter, M. Messinger, and R. Nowakowski. A variation on chip-firing: the diffusion game. *Discrete Mathematics & Theoretical Computer Science*, 20(1), 2018.
- [29] U. Faigle, W. Kern, H. Kierstead, and W. Trotter. On the game chromatic number of some classes of graphs. *Ars combinatoria*, 35:143–150, 1993.
- [30] E. Farhi and S. Gutmann. Quantum computation and decision trees. *Physical Review A*, 58:915–928, Aug 1998.
- [31] A. Frieze, S. Haber, and M. Lavrov. On the game chromatic number of sparse random graphs. *SIAM J. Discrete Math.*, 27:768–790, 2011.
- [32] A. Frieze, M. Krivelevich, and P.-S. Loh. Variations on cops and robbers. *Journal of Graph Theory*, 69(4), 2012.
- [33] J. K. Gamble, M. Friesen, D. Zhou, R. Joynt, and S. Coppersmith. Two-particle quantum walks applied to the graph isomorphism problem. *Physical Review A*, 81(5):052313, 2010.
- [34] M. Gardner. Mathematical games. *Scientific American*, 244, 1981.
- [35] E. Goles and M. Margenstern. Universality of the chip-firing game. *Theoretical Computer Science*, 172(1-2):121–134, 1997.

- [36] D. Guan and X. Zhu. Game chromatic number of outerplanar graphs. *Journal of Graph Theory*, 30(1):67–70, 1999.
- [37] J. Guzmán and C. Klivans. Chip-firing and energy minimization on m -matrices. *Journal of Combinatorial Theory, Series A*, 132:14–31, 2015.
- [38] P. E. Harris, D. K. Luque, C. Reyes Flores, and N. Sepulveda. Broadcast domination of the triangular matchstick graphs and the triangular lattice. 2018.
- [39] T. Jiang, Z. Scully, and Y. X. Zhang. Motors and impossible firing patterns in the parallel chip-firing game. *SIAM Journal on Discrete Mathematics*, 29:615–630, 2015.
- [40] A. Kay. Perfect, efficient, state transfer and its application as a constructive tool. *International Journal of Quantum Information*, 8(04):641–676, 2010.
- [41] J. Kempe. Quantum random walks: an introductory overview. *Contemporary Physics*, 44(4):307–327, 2003.
- [42] V. M. Kendon and C. Tamon. Perfect state transfer in quantum walks on graphs. *Journal of Computational and Theoretical Nanoscience*, 8(3):422–433, 2011.
- [43] R. Keusch and A. Steger. The game chromatic number of dense random graphs. *Electronic Journal of Combinatorics*, 21, 06 2014.
- [44] W. B. Kinnersley and E. Peterson. Cops, robbers, and burning bridges. *arXiv preprint arXiv:1812.09955*, 2018.
- [45] W. Klostermeyer and H. Mendoza. The eternal game chromatic number of a rgraph. *arXiv preprint arXiv:1811.02332*, 2018.
- [46] S. Li and S. Boettcher. Renormalization group for a continuous-time quantum search in finite dimensions. *Physical Review A*, 95(3):032301, 2017.
- [47] J. Long and B. Narayanan. Diffusion on graphs is eventually periodic. *arXiv:1704.042953*, 2017.

- [48] K. Mølmer and A. Sørensen. Multiparticle entanglement of hot trapped ions. *Phys. Rev. Lett.*, 82(9), 1999.
- [49] P. Philipp, L. Tarrataca, and S. Boettcher. Continuous-time quantum search on balanced trees. *Physical Review A*, 93(3):032305, 2016.
- [50] P. Pisantechakool and X. Tan. On the capture time of cops and robbers game on a planar graph. 2016.
- [51] X. Qiang, T. Loke, A. Montanaro, K. Aungskunsiri, X. Zhou, J. L. O’Brien, J. B. Wang, and J. C. Matthews. Efficient quantum walk on a quantum processor. *Nature communications*, 7, 2016.
- [52] T. W. Randolph. Asymptotically optimal bounds for $(t, 2)$ broadcast domination on finite grids. 2018.
- [53] E. Sánchez-Burillo, J. Duch, J. Gómez-Gardenes, and D. Zueco. Quantum navigation and ranking in complex networks. *Scientific Reports*, 2, 2012.
- [54] T. Shlomi. Bounds on (t, r) broadcast domination of n -dimensional grids. 2019.
- [55] A. Sørensen and K. Mølmer. Entanglement and quantum computation with ions in thermal motion. *Phys. Rev. A*, 62(2):1835–1838, 2000.
- [56] J. Spencer. Balancing vectors in the max norm. *Combinatorica*, 6:55–66, 1986.
- [57] H. Tang et al. Experimental two-dimensional quantum walk on a photonic chip. *Science Advances*, 4(5):3174, 2018.
- [58] M. S. Underwood and D. L. Feder. Universal quantum computation by discontinuous quantum walk. *Physical Review A*, 82:042304, Oct 2010.
- [59] V. Vedral, A. Barenco, and A. Ekert. Quantum networks for elementary arithmetic operations. *Phys. Rev. A*, 54:147–153, Jul 1996.
- [60] S. E. Venegas-Andraca. Quantum walks: a comprehensive review. *Quantum Information Processing*, 11(5):1015–1106, Oct 2012.
- [61] B. Yang and W. Hamilton. The optimal capture time of the one-cop-moves

game. *Theoretical Computer Science*, 588:96–113, 2015.

- [62] X. Zhu. The game coloring number of planar graphs. *Journal of Combinatorial Theory, Series B*, 75(2):245–258, 1999.